

UNIVERSIDADE NOVA DE LISBOA  
FACULDADE DE CIÊNCIAS E TECNOLOGIA  
DEPARTAMENTO DE QUÍMICA



**Joana Isabel Sobral Romão**

**“Development of cyclodextrin-hydrogel polymeric systems  
in scCO<sub>2</sub> for drug delivery”**

Thesis for the Degree of  
*Master of Science* in Bioorganic  
Universidade Nova de Lisboa,  
Faculdade de Ciências e Tecnologia

**Supervisors:**

Professora Maria Manuel Marques  
Universidade Nova de Lisboa (UNL)  
Faculdade de Ciências e Tecnologias (FCT)

**Co-supervisors:**

Professora Teresa Casimiro (UNL-FCT)

**Jury:**

Professor João Aires de Sousa (UNL-FCT)  
Dr<sup>a</sup> Marta Corvo (UNL-FCT)  
Professora Maria Manuel Marques (UNL-FCT)

MONTE DE CAPARICA, July 2011

**UNIVERSIDADE NOVA DE LISBOA**  
**FACULDADE DE CIÊNCIAS E TECNOLOGIA**  
**DEPARTAMENTO DE QUÍMICA**



**Joana Isabel Sobral Romão**

**“Development of cyclodextrin-hydrogel polymeric systems  
in scCO<sub>2</sub> for drug delivery”**

Thesis for the Degree of  
*Master of Science* in Bioorganic  
Universidade Nova de Lisboa,  
Faculdade de Ciências e Tecnologia

**Supervisors:**

Professora Maria Manuel Marques  
Universidade Nova de Lisboa (UNL)  
Faculdade de Ciências e Tecnologias (FCT)

**Co-supervisors:**

Professora Teresa Casimiro (UNL-FCT)

**Jury:**

Professor João Aires de Sousa (UNL-FCT)  
Dr<sup>a</sup> Marta Corvo (UNL-FCT)  
Professora Maria Manuel Marques (UNL-FCT)

MONTE DE CAPARICA, July 2011

# **“Development of cyclodextrin-hydrogel polymeric systems in scCO<sub>2</sub> for drug delivery”**

Joana Isabel Sobral Romão, *Copyright*

“A Faculdade de Ciências e Tecnologia e a Universidade Nova de Lisboa têm o direito perpétuo e sem limites geográficos, de arquivar e publicar esta dissertação através de exemplares impressos reproduzidos em papel ou de forma digital, ou por qualquer outro meio conhecido ou que venha a ser inventado, e de a divulgar através de repositórios científicos e de admitir a sua cópia e distribuição com objectivos educacionais ou de investigação, não comerciais, desde que seja dado crédito ao autor e editor.”



# Acknowledgements

In the first place I would like to thank Dr<sup>a</sup>.Teresa Casimiro and Dr<sup>a</sup>. Maria Manuel Marques for the opportunity they gave me, allowing me to understand what I truly like to achieve in my future career. This change proves that sometimes life, or destiny, decides what the best for us.

To Dr<sup>a</sup> Maria Manuel Marques for the opportunity of constant learning, for all the scientific conversation at 8:00 am, for all the support and continuous motivation during the realization of this work.

To Dr<sup>a</sup> Teresa Casimiro, I thank for the knowledge transfer and for the ongoing availability.

To Mara Silva, I thank for the collaboration, the availability, help and support.

In the same way, I thank all my work colleagues of laboratory 202 for sharing the good and bad times of science.

I would also like to thank all my friends, especially those who accompanied me in my academic path: Ana Neto, Ana Fernandes, Daniel Silva, Marta Silva, João Domingos, Keno, Bruno for all the support, to Silvia for always being present and a big thanks to Alex for all the unconditional help and friendship, particularly this last year.

My parents and my sister, I thank for doing everything in their power for me and for always staying by my side.

Last but not least, I thank David Barata for all the support in my best and worst days, for always reminding me how lucky I truly am, for the smiles and good moments, for all the constructive discussions and opinions, for always pushing me one step ahead. I hope that life continue to smile at us.

Thanks to FCT/MCTES project PTDC/ QUI/ 66086/2006 for the financial support.



# Abstract

This work describes the studies on the development of new cyclodextrin-hydrogel systems in supercritical carbon dioxide (scCO<sub>2</sub>) with potential application in drug delivery. Three β-cyclodextrin (CDs) derivatives were synthesized: 6-monoacryloyl-β-CD, 2-monoacryloyl-β-CD and 6-monoacryloyl-heptakis-(2,3-di-*O*-benzyl)-β-CD. Their structures were assigned by nuclear magnetic resonance (NMR), infrared (IR) and mass spectrometry (MS) using the technique of matrix-assisted laser desorption/ionisation-time-of-flight (MALDI-TOF). These functionalized β-CDs were co-polymerized in scCO<sub>2</sub> and the resulting co-polymers were characterized by high resolution magnetic angle spinning (HR-MAS) NMR. Swelling tests were performed showing that the presence of CD decreases the swelling capacity of the corresponding co-polymers. The β-CD co-polymers were impregnated with a model drug, metronidazole, using a batch supercritical fluid impregnation process. Experiments *in vitro* were realized in order to evaluate the performance of the cyclodextrin-hydrogel system as drug release device at different pHs, 2.2 and 7.4. The co-polymer with 2.5 % of 2-monoacryloyl-β-CD was the one that impregnated more drug and showed more interesting results, since at pH 2.2 the release is more controlled. The effect of the percentage of β-CD in the co-polymers performance was also investigated. The co-polymer with more percentage of 2-monoacryloyl-β-CD (8.8%) showed a more controlled drug release at pH 7.4. The results with 2.5 % of β-CD indicate that the co-polymer would be more suitable for oral administration, whereas with 8.8 % would be suitable for parenteral administration.





# Resumo

Este trabalho descreve os estudos realizados no desenvolvimento de sistemas de ciclodextrinas (CDs)-hidrogel, em dióxido de carbono supercrítico com potencial aplicação para a liberação controlada de fármacos. Três derivados de  $\beta$ -CDs foram sintetizados: 6-monoacrilada- $\beta$ -CD, 2-monoacrilada- $\beta$ -CD e a 6-monoacrilada-hepta-(2,3-di-*O*-benzilo)- $\beta$ -CD. As suas estruturas foram determinadas por ressonância magnética nuclear, infravermelho e espectrometria de massa através da técnica de MALDI-TOF. As  $\beta$ -CDs funcionalizadas foram co-polimerizadas em dióxido de carbono supercrítico e os resultantes co-polímeros foram caracterizados por ressonância magnética nuclear usando a técnica de HR-MAS. Foram realizados testes de *swelling* que demonstraram que a presença da  $\beta$ -CD nos co-polímeros diminui o *swelling*. Os co-polímeros da  $\beta$ -CD foram impregnados com um fármaco, o metronidazol, usando um processo de impregnação em dióxido de carbono supercrítico. Realizaram-se estudos *in vitro* com o intuito de avaliar a performance do sistema CDs-hidrogel para a liberação controlada do metronidazole a pH 2.2 e a pH 7.4. O co-polímero com 2.5 % de 2-monoacrilada- $\beta$ -CD foi o que conseguiu impregnar mais metronidazol e também aquele que demonstrou um resultado mais interessante, uma vez que a pH 2.2 teve uma liberação mais controlada do fármaco. A percentagem de  $\beta$ -CD nos co-polímeros também foi um factor estudado. O co-polímero com mais percentagem de 2-monoacrilada- $\beta$ -CD (8.8 %) apresentou uma liberação do fármaco mais controlada a pH 7.4. Os resultados indicam que o co-polímero com 2.5 % de 2-monoacrilada- $\beta$ -CD será mais adequado para uma aplicação futura por administração oral e o co-polímero com 8.8 % de 2-monoacrilada- $\beta$ -CD será mais adequado para administração parenteral.



# Index

Acknowledgements.....	v
Abstract.....	vii
Resumo .....	ix
Index .....	xi
List of Figures.....	xv
List of Tables .....	xix
Keywords.....	xxi
List of Abbreviations .....	xxiii
1. Introduction .....	1
1.1 Cyclodextrins.....	2
1.1.1 Fundamentals of CD chemistry .....	3
1.1.2 Chemical Modification of CDs .....	5
1.1.3 NMR Studies .....	10
1.1.4 CD inclusion complexes in aqueous solution.....	12
1.1.5 CD inclusion complexes in scCO <sub>2</sub> .....	13
1.2 Polymers.....	15
1.2.1 scCO <sub>2</sub> in polymer and impregnation process .....	15
1.2.2 Polymers in drug delivery .....	16
1.3 CD complexes and pharmaceutical applications .....	20
1.3.1 Complexation and mechanism of drug release from CD complexes .....	20
1.3.2 Pharmaceutical applications of drug-CD complexes.....	23
2. Results Discussion.....	25
2.1 Objective .....	26
2.2 Synthesis of functionalized CDs .....	27
2.3 Exploration of novel approach towards the functionalization of β-CD.....	41

2.4	Polymerization.....	46
2.4.1	Synthesis of CD-MAA-PNIPAAm co-polymer in scCO <sub>2</sub> .....	46
2.4.2	Characterization of polymers .....	47
2.5	Final Conclusions .....	60
3.	Experimental Part.....	63
3.1	Preamble.....	64
3.2	Synthesis.....	66
3.2.1	Synthesis of compound 10 (6-monoacryloyl-β-CD) .....	66
3.2.2	Synthesis of compound 11 (2-monoacryloyl-β-CD) .....	68
3.2.3	Synthesis of 12 (6-monoacryloyl-heptakis-(2,3-di- <i>O</i> -benzyl)-β-CD).....	69
3.2.4	Synthesis of acetylation β-CD.....	72
3.3	Studies in scCO <sub>2</sub> .....	74
3.3.1	General methods for co-polymer synthesis in scCO <sub>2</sub> .....	74
3.3.2	General methods for scCO <sub>2</sub> -assisted impregnation .....	75
3.3.3	General methods for <i>in vitro</i> drug release experiments.....	75
4.	References .....	79
	Appendix 1.....	87
	Appendix 2.....	97
	Appendix 3.....	107
	Appendix 4.....	111
	Appendix 5.....	127
	Appendix 6.....	131
	Appendix 7.....	137
	Appendix 8.....	141
	Appendix 9.....	155
	Appendix 10.....	165
	Appendix 11.....	169

Appendix 12.....	177
Appendix 13.....	183
Appendix 14.....	187
Appendix 15.....	191



# List of Figures

Figure 1.1: Generic representation of the structure of the different types of CD.....	2
Figure 1.2: CDs history, by József Szejtli.....	3
Figure 1.3: Structure of $\alpha$ (1)-, $\beta$ (2)- and $\gamma$ -CD (3). .....	3
Figure 1.4: Schematic 3D representation of CD . .....	4
Figure 1.5: Conversion of a 6-substituted CD to a 3,6-anhydro CD. X is a good leaving group.....	6
Figure 1.6: Strategies for pertosylation (I-IV) and peralkylation (I-VI). R <sub>1</sub> : TBDMS, R <sub>2</sub> : methyl or acetyl group, R <sub>3</sub> : alkyl group. ....	6
Figure 1.7: Strategy for synthesis of per-6-substituted CD <i>via</i> halogenated CD. X: Halogen atoms. R: Alkoxy, alkylamino, thio.....	7
Figure 1.8: Summary of several pathways for the monosubstitution at 6-position of CDs. R <sub>1</sub> = I, N <sub>3</sub> <sup>-</sup> , alkyl. ....	8
Figure 1.9: Strategies for modifications at the 2-positions of CDs. R: Sulfonyl group, R: R <sub>1</sub> :TBDMS.....	9
Figure 1.10: Representation of <sup>1</sup> H-NMR spectra of $\beta$ -CD: A- in D <sub>2</sub> O and B- in DMSO. C- Structure of the $\beta$ -CD numbered. ....	11
Figure 1.11: Schematic representation of CD inclusion complex formation. The guest molecule is <i>p</i> -Xylene and small circles represent the water molecules. ....	12
Figure 1.12: Schematic illustration of the association of free CD and drug to form drug-CD complexes. ....	12
Figure 1.13: Representation of the equilibrium constant of inclusion complexes. ....	13
Figure 1.14: Schematic phase diagram for pure CO <sub>2</sub> . A- The critical point at the critical temperature and the pressure marks the end of the vapor-liquid equilibrium line and the beginning of the supercritical fluid region. B - Density of CO <sub>2</sub> as a function of pressure at different temperatures (solid lines) and at the vapor-liquid equilibrium line (dashed line). ....	16
Figure 1.15: Graphical representations of A and B-type phase-solubility profiles. ....	21
Figure 1.16: Classes of CDs-containing polymers. ....	22
Figure 2.1: Functionalized $\beta$ -CDs ( <b>10</b> , <b>11</b> and <b>12</b> ) which were synthesized for application on polymerization reaction, to study the formation of inclusion complexes with drugs.....	27
Figure 2.2: Mechanisms of mono-tosylation reaction with different reagents to obtain <b>5</b> .....	28
Figure 2.3: Structure of <b>5</b> and a representation of the corresponding <sup>1</sup> H-NMR spectrum obtained. ....	29
Figure 2.4: Mechanism of reaction to obtain <b>10</b> and <b>13</b> .....	30
Figure 2.5: Structure of compounds <b>10</b> and <b>13</b> and a representation of the corresponding <sup>1</sup> H-NMR spectrum obtained. ....	30

Figure 2.6: NOESY HR-MAS NMR spectrum and correlations between the protons of $\beta$ -CD and acryloyl group of <b>10</b> . .....	31
Figure 2.7: Mechanism of preparation of acryloyl- $\beta$ -CD.....	32
Figure 2.8: Structure of <b>11</b> and a representation of the corresponding $^1\text{H-NMR}$ spectrum obtained. ....	32
Figure 2.9: Plausible mechanism proposed to the formation of <b>11</b> . a) Reaction of pyridine with acryloyl chloride. b) Mechanism of reaction forming an inclusion complex with pyridine salt.....	33
Figure 2.10: Synthetic plan to obtain <b>12</b> . .....	34
Figure 2.11: Mechanism of reaction with TBDMSCl to afford <b>4</b> . .....	34
Figure 2.12: Structure of <b>4</b> and the corresponding $^1\text{H-NMR}$ spectrum obtained. ....	35
Figure 2.13: Mechanism of reaction with benzyl bromide to fill the cavity of $\beta$ -CD and obtain <b>14</b> . ....	35
Figure 2.14: Structure of <b>14</b> and a representation of the corresponding $^1\text{H-NMR}$ spectrum obtained. ....	36
Figure 2.15: Mechanism of deprotection of primary hydroxyl group to obtain <b>15</b> .....	36
Figure 2.16: Structure of compound <b>15</b> and $^1\text{H-NMR}$ spectrum characterization. ....	37
Figure 2.17: Mechanism of reaction to obtain the final product ( <b>12</b> ) with acryloyl chloride. ....	37
Figure 2.18: Structure of compound <b>12</b> and $^1\text{H-NMR}$ spectrum characterization. ....	38
Figure 2.19: Mechanism of the acetylation reaction. ....	41
Figure 2.20: Examples of application of <i>N</i> -acylbenzotriazole (Bt: benzotriazole) .....	42
Figure 2.21: a) Synthesis of <i>N</i> -acetylbenzotriazole ( <b>17</b> ), b) Mechanism of acetylation reaction with benzotriazole as transfer agent of the acetyl group. ....	43
Figure 2.22: Structure of compound <b>19</b> and $^1\text{H-NMR}$ spectrum characterization. ....	44
Figure 2.23: a) Scheme of membrane for UF. 1-Ultrafiltrate, 2-UF equipment, 3-Pressure supply. b) UF equipment. ....	45
Figure 2.24: Synthesized $\beta$ -CDs that were co-polymerized in $\text{scCO}_2$ .....	46
Figure 2.25: Scheme of the co-polymerization reaction.....	46
Figure 2.26: Schematic representation of equipment used in polymerization reaction and impregnation. 1- Nitrogen cylinder; 2-Gas regulator; 3-Rupture disc; 4- High-pressure manometer; 5- Check-valve; 6- Line filter; 7-Water bath; 8-Immersible stirrer; 9-High pressure cell; 10- Platinum resistance RTD probe; 11- Temperature controller; 12-Vent; 13- Pneumatic $\text{CO}_2$ compressor; 14- $\text{CO}_2$ cylinder; M1,M2- bourbon manometers; wp-water recirculation pump; V1 to V7- HIP valves. ....	47
Figure 2.27: Appearance of the co-polymer obtained. ....	47
Figure 2.28: SEM images of: A - compound <b>10</b> ; B - NIPAAm-MAA-EGDMA co-polymer <b>10</b> ; C- NIPAAm-MAA-EGDMA co-polymer <b>11</b> ; D - NIPAAm-MAA-EGDMA co-polymer <b>12</b> . ....	48
Figure 2.29: NOESY HR-MAS NMR spectrum and representation of co-polymer of compound <b>10</b> .....	49
Figure 2.30: Types of $\beta$ -CD polymer: A-catenanes, B-rotaxanes and C-pseudorotaxanes.....	50



Figure 2.31: XRD of P(NIPPAm-MAA) (blue), P(NIPAAm-MAA- <b>10</b> ) co-polymer (orange) and compound <b>10</b> (gray).	51
Figure 2.32: XRD of P(NIPPAm-MAA) (blue), P(NIPAAm-MAA- <b>11</b> ) co-polymer (green) and compound <b>11</b> (gray).	51
Figure 2.33: Swelling of co-polymers at two different pHs 2.2 and 7.4. P(NIPAAm-MAA) (blue), P(NIPAAm-MAA- <b>10</b> ) co-polymer (orange), P(NIPAAm-MAA- <b>11</b> ) co-polymer (green) and (NIPAAm-MAA- <b>12</b> ) (purple).	52
Figure 2.34: Test of swelling. A-(pH2.2); B-(pH7.4).	52
Figure 2.35: Structure of metronidazole.	53
Figure 2.36: High-pressure cell used for impregnation.	53
Figure 2.37: Drug release from the synthesized P(NIPAAm-MAA) (blue), P(NIPAAm-MAA-10) co-polymer (orange), P(NIPAAm-MAA-11) co-polymer (green) and (NIPAAm-MAA-12) (purple) at pH 2.2 (A) and pH 7.4 (B).	56
Figure 2.38: Drug release from the synthesized P(NIPPAm-MAA) (blue), P(NIPAAm-MAA-11) co-polymer with 2.5% (green) and P(NIPAAm-MAA-11) co-polymer with 8.8% (gray) at pH 2.2 (A) and pH 7.4 (B).	58
Figure 2.39: Drug release from the synthesized P(NIPAAm-MAA-11) co-polymer with 8.8% at pH 2.2 (blue) and P(NIPAAm-MAA-11) co-polymer with 8.8% at pH 7.4 (gray).	58
Figure 2.40: Temperature test of co-polymers A- 23°C, B- 45°C.	59
Figure 3.1: Synthetic scheme to obtain products <b>10</b> and <b>13</b> .	66
Figure 3.2: Structure of product <b>11</b> .	68
Figure 3.3: Synthetic scheme to obtain compound <b>12</b> .	69
Figure 3.4: Structure of product <b>4</b> .	70
Figure 3.5: Structure of product <b>14</b> .	70
Figure 3.6: Structure of product <b>15</b> .	71
Figure 3.7: Structure of product <b>12</b> .	71
Figure 3.8: Structure of product <b>16</b> .	72
Figure 3.9: Reaction between the acid anhydride and benzotriazole to obtain product <b>17</b> .	72
Figure 3.10: Structure of product <b>18</b> .	73
Figure 3.11: Structure of product <b>19</b> .	74



# List of Tables

Table 1.1: Properties of $\alpha$ -, $\beta$ - and $\gamma$ -CD. ....	4
Table 1.2: Examples of CDs pendent polymers. ....	22
Table 1.3: Approved and marketed drug-CD complexes. ....	23
Table 2.1: Yields of mono-tosylation reactions with different reagents. ....	28
Table 2. 2: Summary of structural characterization and yields of all compounds involved in synthesis of <b>10</b> , <b>11</b> and <b>12</b> . ....	40
Table 2.3: Number of equivalents of reagent used in the reactions of peracetylation and the products obtained. ....	42
Table 2.4: Conditions of the reactions with <i>N</i> -acylbenztriazole and products obtained ....	44
Table 2.5: Polymer loading during scCO <sub>2</sub> -assisted impregnation with Metronidazole. ....	54
Table 3.1: Results of metronidazole release of each co-polymer at pH 2.2. ....	76
Table 3.2: Results of metronidazole release of each co-polymer at pH 7.4. ....	77



# Keywords

$\beta$ -Cyclodextrin

Functionalization of  $\beta$ -Cyclodextrin

Supercritical carbon dioxide

Polymerization

Controlled drug Delivery



# List of Abbreviations

$^{13}\text{C}$ -NMR	Carbon Nuclear Magnetic Resonance Spectroscopy
$^1\text{H}$ -NMR	Proton Nuclear Magnetic Resonance Spectroscopy
AIBN	Azobisisobutyronitrile
Bt	Benzotriazole
CD	Cyclodextrin
DCC	Carbodiimide
DMF	<i>N,N'</i> -Dimethylformamide
DMP	Dess-Martin periodinane
DMSO	Dimethyl sulfoxide
DMSO- $d_6$	Deuterated Dimethyl sulfoxide
EGDMA	Ethylene glycol dimethylacrylate
h	Hours
HR-MAS	High Resolution Magnetic Angle Spinning
IR	Infrared Spectroscopy
$K_c$	Stability Constant
MAA	Methacrylic acid
MALDI-TOF	Matrix-assisted laser desorption/ionisation-time-of-flight mass spectrometer
min	Minutes
MS	Mass Spectrometry
NIPAAm	<i>N</i> -isopropylacrylamide
NMR	Nuclear Magnetic Resonance Spectroscopy
NOESY	Nuclear Overhauser effect spectroscopy
PGE	Prostaglandins
RP	Reverse Phase
RTD	Resistance Temperature Detector
scCO $_2$	Supercritical carbon dioxide
SEM	Scanning Electron Microscope
TBAF	Tetra- <i>n</i> -butylammonium fluoride
TBDMS	<i>Tert</i> -Butyldimethylsilyl
THF	Tetrahydrofuran
TLC	Thin layer chromatography
TMS	Trimethylsilyl

Ts	<i>p</i> -Toluenesulfonyl
UF	Ultrafiltration
UV	Ultraviolet
XRD	X-Ray Diffraction



# **1. Introduction**

## 1.1 Cyclodextrins

In 1981, A. Villiers, a French scientist, reported the formation of a crystalline substance by fermentation of starch and determined its composition as  $(C_6H_{10}O_5)_2 \cdot 3H_2O$  naming it as “cellulosine”.<sup>[1-3]</sup>

In 1903, an Austrian microbiologist, Franz Schardinger, isolated from the microorganism *Bacillus macerans*, two distinct crystalline substances and identified them as a cyclic structure of glucose oligomers, called  $\alpha$ -cyclodextrin (CD) and  $\beta$ -CD. In 1935,  $\gamma$ -CD was discovered by Freudenberg and Jacobi.<sup>[1, 2, 4]</sup>

The corrected chemical structure of  $\alpha$ -,  $\beta$ -,  $\gamma$ -CD was elucidated by Freudenberg and co-workers in 1938, featuring them as cyclic structures composed of  $\alpha$ -1,4-linked glucose units (Figure 1.1). In the following years their molecular weight was determined.<sup>[1, 5, 6]</sup>

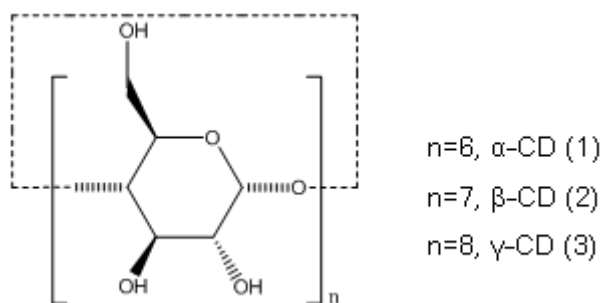


Figure 1.1: Generic representation of the structure of the different types of CD.

In 1953 the first patent on CD and their inclusion complex ability was registered by Freudenberg, Cramer and Plieninger, who recognize the potential of these compounds to form complexes. Later, in the 70s, only a small amount of CD could be produced with a high production cost. However, advances in the biotechnology field allowed the improvement of CDs production in terms of costs and purity.<sup>[2]</sup>

Using genetic engineering techniques, highly active and specific enzymes, cyclodextrin glucosyltransferases (GCTases) were isolated, which can selectively produce CD subtypes. Nowadays, the use of these enzymes as well as the progress in purification processes, has been leading to production of high yields of pure CD subtypes on large scale.<sup>[2, 7-9]</sup>

Figure 1.2 summarizes the main CDs development phases: the discovery period, the exploratory period, and the utilization period. [2, 7-9]

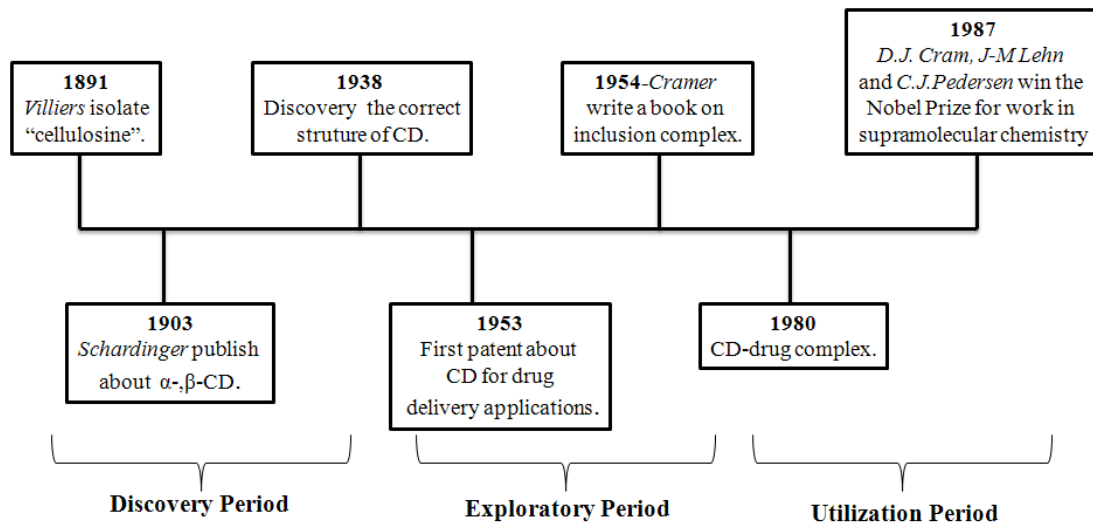


Figure 1.2: CDs history, by József Szejtli.<sup>[9]</sup>

### 1.1.1 Fundamentals of CD chemistry

CDs also known as cycloamyloses, cyclomaltooses or Schardinger dextrans, are macrocyclic oligosaccharides, most commonly composed by 6, 7 or 8 D-glucose units, known as  $\alpha$ -,  $\beta$ - and  $\gamma$ -CD, respectively (Figure 1.3).<sup>[8, 9]</sup> These CDs are crystalline and homogeneous substances, built up from glucopyranose units.<sup>[8, 9]</sup>

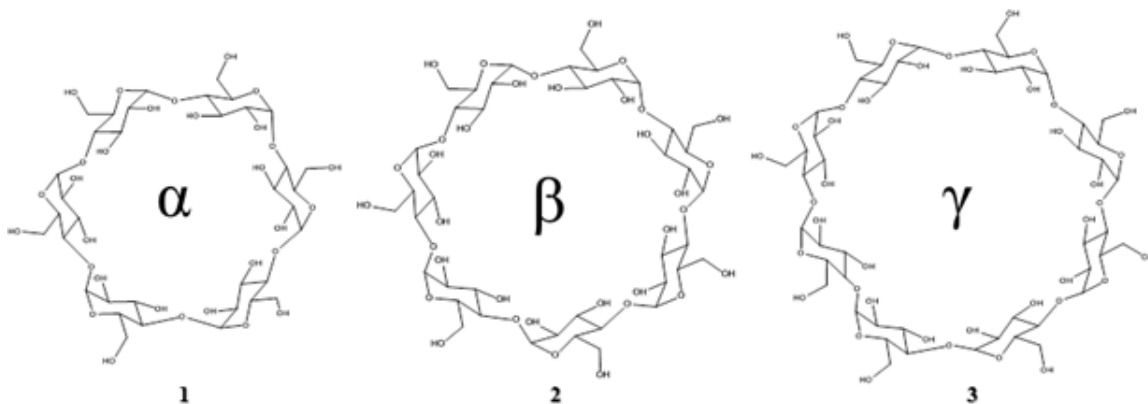


Figure 1.3: Structure of  $\alpha$  (1)-,  $\beta$  (2)- and  $\gamma$ -CD (3).<sup>[8]</sup>

The most important properties of CDs are summarized in Table 1.1.<sup>[1, 5, 8-10]</sup>

Table 1.1: Properties of  $\alpha$ -,  $\beta$ - and  $\gamma$ -CD.<sup>[5]</sup>

	$\alpha$ -CD	$\beta$ -CD	$\gamma$ -CD
Number of glucose units	6	7	8
Molecular weight	972	1134	1296
Approximate inner cavity diameter (pm)	50	620	800
Approximate outer diameter (pm)	1460	1540	1750
Approximate volume of cavity ( $10^6 \text{ pm}^3$ )	174	262	427
$[\alpha]_D$ at 25°C	$150.0 \pm 0.5$	$162.5 \pm 0.5$	$177.4 \pm 0.5$
Solubility in water (room temperature, g/100 ml)	14.5	1.85	23.2
Melting temperature range (°C)	255-260	255-265	240-245
Water molecules in cavity	6	11	17

The units of D-glucose are attached by  $\alpha$ -1,4-linkages, and the rigid  ${}^4\text{C}_1$ -chair conformation gives to the macrocycle structure the shape of a hollow truncated cone.<sup>[5]</sup> The hydroxyl groups located at the outer surface of the CD molecule are the primary hydroxyl groups that are located at the narrow face of the cone, while the secondary hydroxyls are located at the wide face, Figure 1.4. The cone is formed by the carbon skeletons of the glucose units and the glycosidic oxygen atoms in between.<sup>[1, 6, 8]</sup>

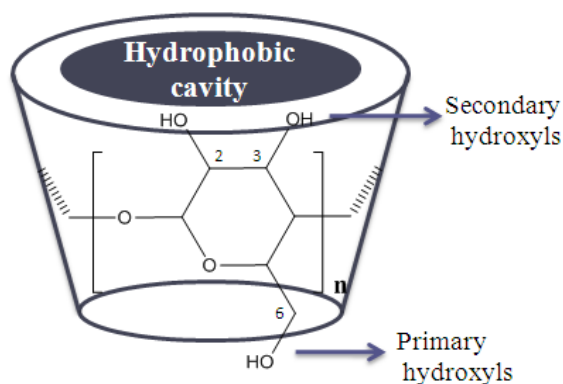


Figure 1.4: Schematic 3D representation of CD.<sup>[8]</sup>

The C<sub>2</sub>-OH group of glucopyranoside unit can form a hydrogen bond with the C<sub>3</sub>-OH group of the adjacent glucopyranose unit, forming a complete secondary belt, which may explain the rigid structure of β-CD and the lower water solubility comparing with the other CDs (Table 1.1).<sup>[5, 9, 11]</sup> In Table 1.1, it is possible to observe the different size and diameter of the cavities from the different CDs.<sup>[5, 8, 9]</sup>

The primary hydroxyl groups on the outside of the CDs cavity make them soluble in water, but simultaneously the secondary hydroxyl groups generate a cavity that is relatively hydrophobic<sup>[8, 9]</sup> or lipophilic<sup>[12, 13]</sup> (Figure 1.4).

## 1.1.2 Chemical Modification of CDs

The strategies for selective modification of CDs explored to date involve the exploration of the different reactivity of hydroxyl groups in CDs, and the selective modification is often adverted by regioselective protection and deprotection sequential steps.<sup>[6, 11, 14]</sup>

All modifications of CDs take place at the hydroxyl groups (C<sub>2</sub>-OH, C<sub>3</sub>-OH and C<sub>6</sub>-OH), which nucleophilic nature directs the regioselectivity and extension of modifications on all subsequent reactions.<sup>[14, 15]</sup>

The glucose units of CDs contain three different types of hydroxyl groups: primary hydroxyl groups at position C<sub>6</sub>, and secondary hydroxyl groups at C<sub>2</sub> and C<sub>3</sub>. The primary side C<sub>6</sub>-OH groups are the most basic and the most nucleophilic, the C<sub>2</sub>-OH groups are the most acidic and the C<sub>3</sub>-OH groups are the most inaccessible.<sup>[5, 14-16]</sup> The different reactivity between both secondary hydroxyl groups is due to the fact that C<sub>2</sub>-OH is closer to the hemi-acetal than the C<sub>3</sub>-OH.<sup>[5, 14]</sup>

Some of the reported methods to functionalize CDs will be described next.

### 1.1.2.1 Modification at the primary face

The primary hydroxyl groups are the easiest to modify due to their high nucleophilicity and accessibility. Selective permodification of all the primary hydroxyl groups is relatively easier than mono- or disubstitution, because persubstitution is achieved when the reaction is allowed to run for a longer time with appropriate amounts of reagents. Normally, these products require chromatographic purification.<sup>[5, 11, 14]</sup>

### Permodification at the C6-Position

Opposite to the mono-substitution of CDs, the persubstitution at C<sub>6</sub> such as the persulfonates derivatives are normally prepared directly from CDs by treatment with a large amount of sulfonyl chloride in pyridine. The 6-position tends to change to the 3,6-anhydro form, even in the absence of a base at room temperature (Figure 1.5).<sup>[14]</sup> This represents a limitation to this method, and in order to get reproducible results, the use of freshly prepared persulfonates is required.<sup>[14]</sup>



Figure 1.5: Conversion of a 6-substituted CD to a 3,6-anhydro CD. X is a good leaving group.<sup>[14]</sup>

Another approach reports for pertosylation or –mesylation involves silylation at the primary side of CDs with the TBDMS group (Figure 1.6, **4**) as the first step, followed by esterification of the secondary side, subsequent desilylation and finally tosylation at the primary side (Figure 1.6, **I-IV**).<sup>[14, 17]</sup>

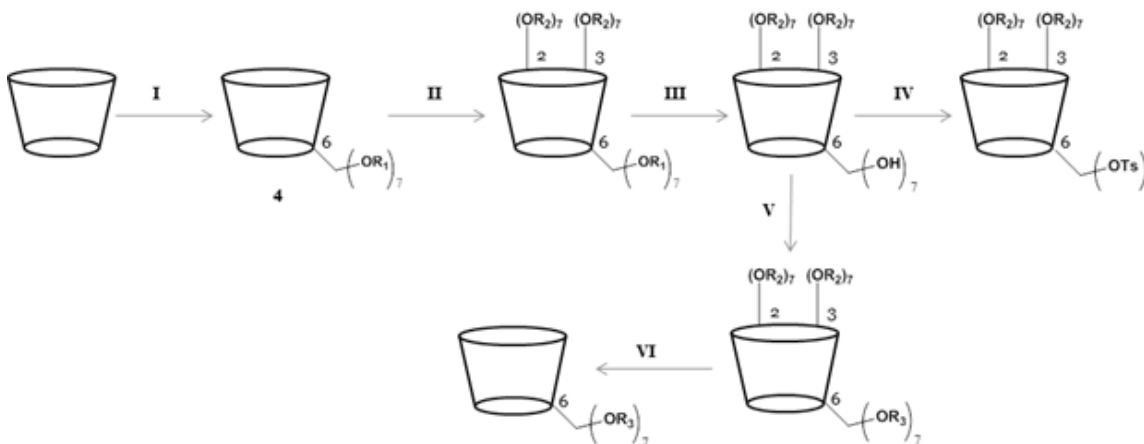


Figure 1.6: Strategies for pertosylation (I-IV) and peralkylation (I-VI). R<sub>1</sub>: TBDMS, R<sub>2</sub>: methyl or acetyl group, R<sub>3</sub>: alkyl group.<sup>[14]</sup>

Peralkylation of the primary hydroxyl groups is not direct and requires many synthetic steps. The strategy consists on the protection of the primary face with silyl groups as the first step, followed by esterification of the secondary face, subsequent desilylation, and finally reaction with an alkyl halide, under strongly basic conditions to produce the alkyl ether (Figure 1.6, **I-VI**).<sup>[14]</sup> Indeed, the per-*O*-6-silylated (Figure 1.6, **4**) CDs are extremely useful and are widely used in

multi-step sequences, due to the good stability and easy removal of the silyl protecting groups.<sup>[14, 18]</sup>

Per-6-halogenocyclodextrins are important classes of compounds that, due to their greater stability compared to per-6-sulfonates, can be used for the selective functionalization of the primary face. However, these compounds are only soluble in polar solvents such as pyridine, *N,N'*-dimethylformamide (DMF), dimethyl sulfoxide (DMSO), among others.<sup>[14]</sup> The secondary side of halogenated CDs can be acetylated in order to increase the solubility or allow a more selective functionalization (Figure 1.7).<sup>[14]</sup>

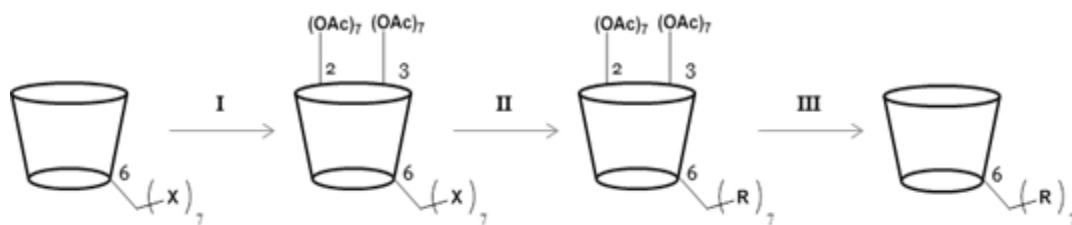


Figure 1.7: Strategy for synthesis of per-6-substituted CD *via* halogenated CD. X: Halogen atoms. R: Alkoxy, alkylamino, thio.<sup>[14]</sup>

### Monosubstitution at C-6-position

The most popular method for monomodifications at the 6-position of CDs is by nucleophilic attack to a properly functionalized CD, for example containing a good leaving group such as the tosyl group.<sup>[14, 16]</sup> The three main functional groups used for a variety of modification in CDs are the 6-tosyl (**5**), the 6-azide (**6**) and the 6-aldehydic (**7**)  $\beta$ -CDs (Figure 1.8).<sup>[5, 14]</sup> One of the most commonly used methods to perform mono-functionalizations at C<sub>6</sub>-OH is *via* the monotosyl CD (Figure 1.8, **I**), which formation involves treatment of CD with tosyl chloride in pyridine or DMF.<sup>[14, 16, 19-21]</sup> However, this reaction produces a mixture of mono, di and tri-tosylated CDs. In order to obtain the desired product an extensive purification is required leading to low product yields. This compound is an important intermediate to achieve other desired modified products (Figure 1.8, **II**).<sup>[14, 16]</sup>

Many derivatives can be obtained from 6-monotosyl CD (**5**) by nucleophilic displacement of the tosyl group by a suitable nucleophile such as iodide, azide, thioacetate, hydroxylamine, alkyl, among others. This reaction allows the selective introduction of new functionalities at this position (Figure 1.8, **II**).<sup>[14, 15]</sup>

The 6-monoazide CD (**6**) can be obtained by two different methods: *via* the 6-monotosyl CD (**5**) under heating with sodium or lithium azide salt in DMF (Figure 1.8, **V**); or *via* the Vilsmeier-Haack type reactions in which the CDs are heated with sodium azide containing

triphenylphosphine in DMF (Figure 1.8, **III**). The 6-monoazide CD (**6**) derivative is often used to obtain the 6-monoamine (**8**).<sup>[5, 14]</sup>

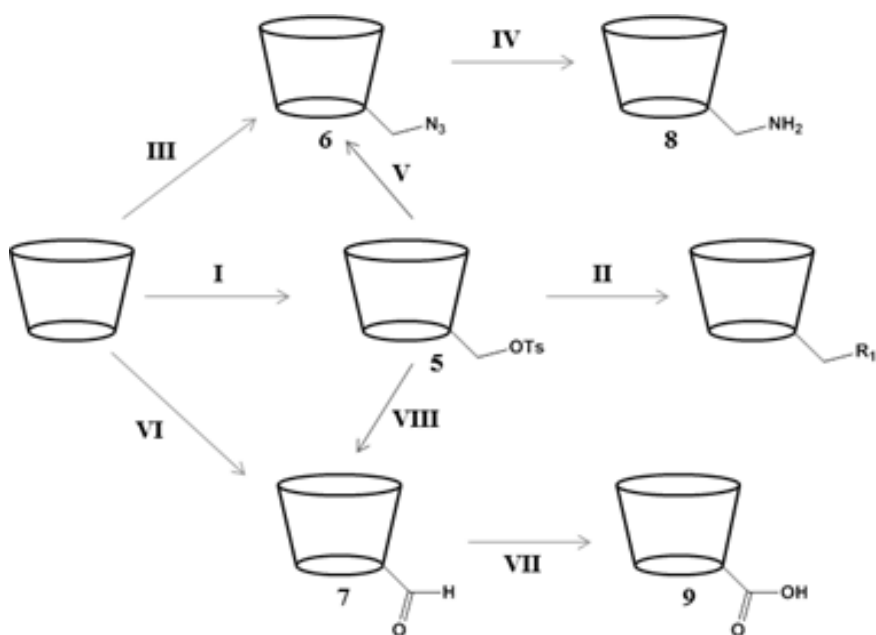


Figure 1.8: Summary of several pathways for the monosubstitution at 6-position of CDs. R<sub>1</sub>= I, N<sub>3</sub><sup>-</sup>, alkyl.<sup>[14]</sup>

6-Monoaldehydic CDs (**7**) provide another route for further modifications (Figure 8, **VI**). The 6-monoaldehyde (**7**) has been synthesized by oxidizing 6-monosyl-β-CD (**5**) using DMSO (Figure 1.8, **VIII**) or directly synthesized by reacting CDs with Dess-Martin periodinane (DMP), with a high yield (Figure 1.8, **VI**). Oxidation of 6-monoaldehyde (**7**) leads to the corresponding carboxylic acid (**9**) (Figure 1.8, **VII**).<sup>[5, 14]</sup>

### 1.1.2.2 Modification reaction at the secondary face

The secondary side is very important, especially to allow studies about the influence and role of the CD cavity. At the secondary side, the hydrogen bonding between hydroxyl groups at C<sub>2</sub>-OH and C<sub>3</sub>-OH positions makes them rigid and less flexible when compared with the primary C<sub>6</sub>-OH hydroxyl groups.<sup>[11]</sup> All these factors make the secondary side less reactive and harder to selectively functionalize, comparing to the primary face.<sup>[11]</sup> During the course of a reaction, as the degree of substitution increases, the secondary side becomes more crowded. This results in steric hindrance for the incoming nucleophile, which forces the attacking group toward the other



position, decreasing the selectivity. Positional isomerism in the secondary side, contributes to an increase in complexity.<sup>[5, 14]</sup>

### Permodification at the C2-Position

Selective perfunctionalization of the secondary side is a difficult process due to the higher reactivity of the primary hydroxyl groups. A strong base selectively produces a 2-alcooxide ion which reacts with alkyl or sulfonyl chloride (Figure 1.8, **I**). This discriminatory behavior becomes less significant with increasing degree of substitution due to the steric crowding, where, as the reaction proceeds, the incoming electrophile finds the attack at the available primary hydroxyl groups more attractive. This problem can be overcome by protecting the primary face of CDs with suitable group such as TBDMS (Figure 1.9, **II**).<sup>[5, 14]</sup>

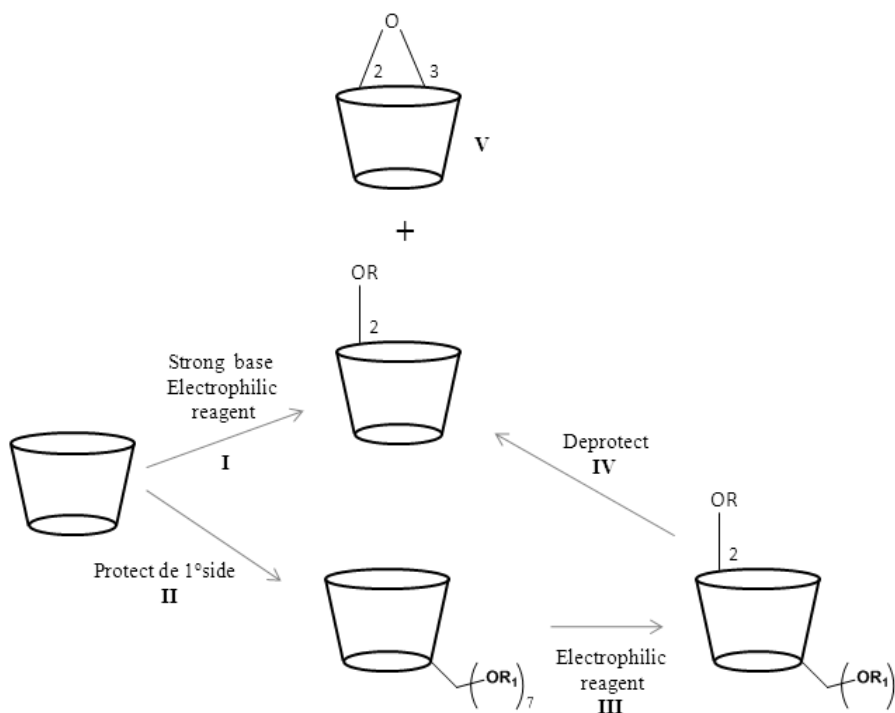


Figure 1.9: Strategies for modifications at the 2-positions of CDs. R: Sulfonyl group, R<sub>1</sub>: TBDMS.<sup>[14]</sup>

In order to prepare per-2-sulfonylation of CDs it is necessary to protect the primary hydroxyl groups due to their higher reactivity. The silyl group is usually selected as protecting group due to its easy removal with tetra-*n*-butylammonium fluoride (TBAF) (Figure 1.9, **IV**). After protection of the primary side, the product of per-2-tosylation is prepared by using tosyl chloride as reagent and pyridine as solvent. Subsequent desilylation affords the desired compound (Figure 1.9, **III-IV**).

Due to the tendency to form 2,3-epoxy (Figure 1.9, **V**) derivatives in the basic medium, the yield of tosylation reaction is low.<sup>[14]</sup>

The direct alkylation of CDs at C<sub>2</sub>-OH is scarcely reported in literature, but an interesting approach has been described for the synthesis of per-2-alkylated CDs. This strategy involved the alkylation of per-2,6-di-*O*-TBDMS CD, due to the migratory property of the silyl group (from *O*-2 to *O*-3). The per-2-alkylated compound was obtained after removal of the silyl groups from positions *O*-3 and *O*-6.<sup>[14]</sup>

### **Per-modification at the C3-Position**

The hydroxyl groups at the C<sub>3</sub> are the least reactive groups, probably because of the hydrogen bonding with C<sub>2</sub> hydroxyl groups. This position is hardly accessed and less reactive; consequently the modification in this position is not easy.<sup>[5, 14]</sup>

Selective per-3-sulfonation has not yet been reported, since sulfonyl chlorides fail to react with C<sub>3</sub>-OH hydroxyl groups. Indeed, strategies that involve protection of *O*-2- and *O*-6 positions with TBDMS, lead to a high steric hindrance due to the bulky silyl functionality.<sup>[17]</sup> Moreover, the TBDMS groups have a tendency to migrate from the *O*-2 to *O*-3-hydroxyl groups under strongly basic conditions, which also limits the attack of *O*-3-hydroxyl groups to the sulfonyl reagent.<sup>[17]</sup> The use of TMS group for protection at the *O*-2- and *O*-6 positions does not constitute a better choice, since these groups are easily hydrolyzed under neutral or acidic conditions.<sup>[14]</sup> Per-2-sulfonated CDs, when under basic condition, lead to per-2,3-epoxy-CDs (Figure 1.9, **V**).<sup>[14]</sup>

### **1.1.3 NMR Studies**

To perform an analysis and structural assignment of each monomer and polymer of CD, it is important to be familiar with NMR of non-functionalized β-CD.

The NMR spectroscopy has become the most important tool for structural elucidation of organic compounds. This technique allows structural assignment of compounds obtained by synthetic modifications in the different units of glucose of CD, by different 2D NMR experiments.<sup>[11, 22]</sup>

In the <sup>1</sup>H-NMR spectra it is possible to identify most of the CD protons, facilitated by the high symmetry of these macrocycles (Figure 1.10).<sup>[11, 22]</sup> The solvents have an influence in the <sup>1</sup>H-NMR spectra, due to fast exchange of OH protons, in the case of D<sub>2</sub>O and DMSO-d<sub>6</sub> as a

solvent. These different solvents allow a detailed insight into the intramolecular CDs hydrogen-bond network.<sup>[22]</sup>

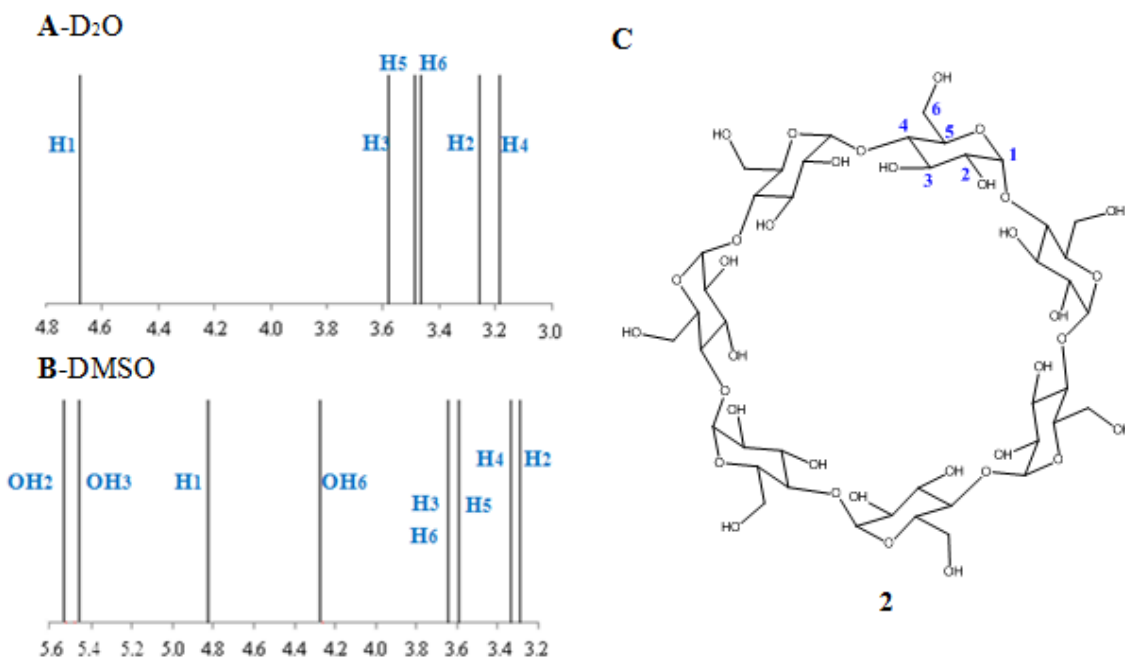
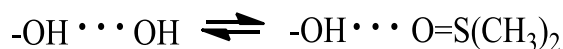


Figure 1.10: Representation of chemical shift spectra of β-CD: A- in D<sub>2</sub>O and B- in DMSO-d<sub>6</sub>. C- Structure of the β-CD numbered.<sup>[22]</sup>

In protic solvents such as D<sub>2</sub>O, intermolecular exchange between solute and solvent is too fast on the NMR time scale for the observation of separate OH signals. The intramolecular hydrogen bond is visible by hydrogen-deuterium exchange rate constants in D<sub>2</sub>O for the equilibrium:<sup>[22]</sup>



In a solvent such as DMSO-d<sub>6</sub> it is possible to observe separate signals for the OH groups and analyze the coupling of the vicinal C-H protons. The resonances of C<sub>3</sub>-OH and C<sub>2</sub>-OH were found to appear in DMSO-d<sub>6</sub> between 5.4 and 5.6 ppm, clearly separated from the signals of the free, more shielded OH-6 group at 4.3 ppm (Figure 1.10, b). In DMSO-d<sub>6</sub> as hydrogen bonding acceptor, the following hydrogen-bonding equilibrium is present:<sup>[22]</sup>



The left side stands for intramolecular hydrogen bonds in the CD, while the right side for the solvent-solute association.<sup>[22]</sup>

### 1.1.4 CD inclusion complexes in aqueous solution

Each CD has its own characteristics to form inclusion complexes with specific molecules, which is determined by the characteristics of the guest molecules, such as polarity, size and geometry that should be appropriate to the hydrophobicity and cavity size of a particular CD.<sup>[23]</sup>

In an aqueous solution, the slightly apolar CD cavity is occupied by water molecules which are energetically unfavored (polar-apolar interaction) and can be readily substituted by an appropriate guest molecule less polar than water (Figure 1.11).<sup>[7, 9, 10, 15]</sup> The dissolved CD is the “host” molecule and the driving force for complex formation is the substitution of the high-enthalpy water molecules by an appropriate guest molecule (Figure 1.11).<sup>[7, 10, 24]</sup>

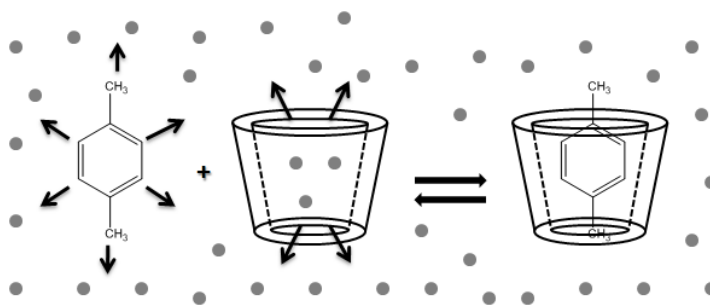


Figure 1.11: Schematic representation of CD inclusion complex formation. The guest molecule is *p*-Xylene and small circles represent the water molecules.<sup>[7]</sup>

Frequently, the host:guest ratio is 1:1, however, 1:2, 2:1, 2:2 or other association can occur, sometimes simultaneously (Figure 1.12).<sup>[9, 24]</sup>

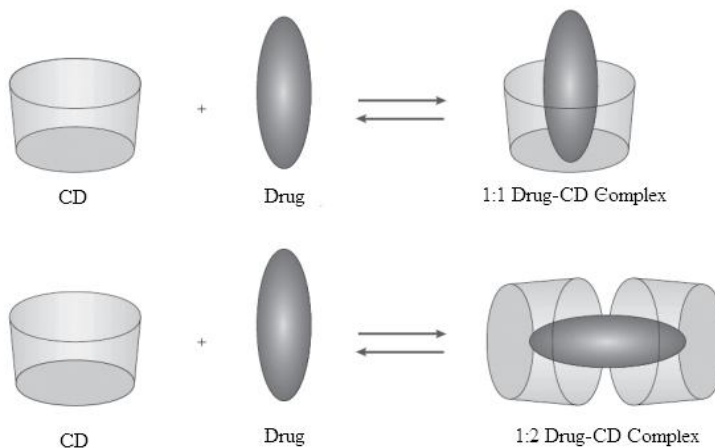
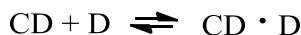


Figure 1.12: Schematic illustration of the association of free CD and drug to form drug-CD complexes.<sup>[23]</sup>

The cavity size of  $\alpha$ -CD allows the formation of complexes with aliphatic chains and small molecules, whereas  $\beta$ -CD is appropriate for aromatic ring and  $\gamma$ -CD has a larger cavity so can form complexes with larger molecules, as steroids.<sup>[23, 25]</sup>

Upon dissolving these complexes, an equilibrium is established between dissociated and associated species, and this is expressed by the complex stability constant  $K_c$ . The association of the CD and guest (D) molecules, and the dissociation of the formed CD/guest complex is governed by the thermodynamic equilibrium (Figure 1.13).<sup>[9, 15]</sup>



$$K_{1:1} = \frac{[\text{CD} \cdot \text{D}]}{[\text{CD}][\text{D}]}$$

Figure 1.13: Representation of the equilibrium constant of inclusion complexes.<sup>[15]</sup>

This association and dissociation reactions of guest molecules from the CDs are dynamic processes that occur quite fast (in few milliseconds), even for complexes with high stability constants.<sup>[23]</sup> According to this properties, the kinetics of drug release from CDs will not be a limiting factor in absorption, other mechanisms may also be responsible for the release of the drug inclusion complex, as the effect of pH on CDs or ionizable drugs.<sup>[23]</sup> The change of pH can change the state of ionization of the drug or the CD and lead the dissociation of the complex by decreasing its  $K_c$ . The way all these factors mentioned will influence the dissociation of the complex depends on the route of administration, the volume of distribution of the drug, the  $K_c$  and the complex concentrations of the drug, the CD and other competitive entities.<sup>[23]</sup>

### 1.1.5 CD inclusion complexes in scCO<sub>2</sub>

Nowadays, the combinatorial chemistry and high throughput screening, allow the discovery of new drugs with good pharmacological activities, but many of them have low solubility.<sup>[26]</sup> The drug-CD complexes can bring substantial advantages like improvement of solubility, stability and bioavailability of drugs. The two main techniques to form complexes between CD and drugs in scCO<sub>2</sub> are impregnation of CD matrixes with guest compounds and co-precipitation of CDs and guest molecules.<sup>[27]</sup>

The impregnation of CD in scCO<sub>2</sub> has been applied to generate inclusion compounds between CDs and therapeutic drugs. However, the formation of inclusion complexes depends on time and experiment conditions. The first step in the formation of the guest/host complex is the

solubilization of the drug in CO<sub>2</sub> and the complexation of the solubilized drug with CD that would shift the equilibrium toward the dissolution of extra drug. A driving mechanism for the formation of CD inclusion complexes is the substitution of water of crystallization molecules in the CD cavity with hydrophobic guest. Since the removal of water of crystallization makes the hydrophobic cavity of the CD free to include other guest molecules, the extraction of the included water molecules in CO<sub>2</sub> would favor the formation of the inclusion complex between the CD and the drug. The efficacy of CO<sub>2</sub> in extracting water from the CD depends on the water solubility.<sup>[27]</sup>

The co-precipitation of CDs and guest compounds is another method that allows formation of complexes in CO<sub>2</sub>. The CD and the guest molecule are separately dissolved in different fluids and the two solutions were concomitantly contacted with the CO<sub>2</sub> that expanded the two solvents, lowering their solvent power and causing the solutes precipitation. The solvents were removed from the systems by the CO<sub>2</sub> and the product was collected in the form of dry powder.<sup>[27]</sup>

This is a technique to be explored since the CO<sub>2</sub> constitute an environmentally sustainable technology and can be applied in several areas like biomedical and green chemistry.<sup>[27]</sup>

## 1.2 Polymers

### 1.2.1 scCO<sub>2</sub> in polymer and impregnation process

In this work, scCO<sub>2</sub> was used as an alternative green media of polymerization, once it offers numerous advantages compared with other traditional methods that use solvents.<sup>[28, 29]</sup> Conventional production routes involve an excessive use of organic solvents, either as a reaction medium in the polymerization step or as a processing medium for shaping, extraction, impregnation, and viscosity reduction. In each of these steps, most of the effort of the process is put into solvent recovery.<sup>[30]</sup> Therefore, it is highly desirable from environmental, safety and economical point of view, to develop alternative routes to reduce the use of solvents in polymerization processes.<sup>[28, 29, 31]</sup>

The scCO<sub>2</sub> allows the preparations of hydrogels completely dry and free-flowing powders, with no solvent residues and with no need for intensive drying steps before processing.<sup>[32]</sup> Additionally, more attractive features are available: an easily accessible critical point (31.1 °C and 73.8 bar), abundance, non-flammable, non-toxic and relatively inexpensive.<sup>[29, 31, 33]</sup> Due to the favorable practical physical and chemical properties of CO<sub>2</sub>, it is a solvent for monomers and a non-solvent for polymers, which facilitates the separation.<sup>[30]</sup>

A supercritical fluid is defined as a substance for which the temperature and pressure are above their critical values and which has a density close to or higher than its critical density.<sup>[29, 30]</sup> Above the critical temperature, the vapor-liquid coexistence line no longer exists. The supercritical fluids are versatile because their properties can be tuned from liquid to gas without crossing a phase boundary by simply changing the pressure or the temperature.<sup>[30]</sup>

In Figure 1.14, two projections of the phase behavior of carbon dioxide are shown. In the Figure 1.14, **A**, the pressure-temperature phase diagram, the boiling line, is observed, which separates the vapor and liquid regions and ends in the critical point.<sup>[29, 30, 34]</sup> At the critical point, the densities of the equilibrium liquid phase and the saturated vapor phases become equal, resulting in the formation of a single supercritical phase, which can be observed in the density-pressure phase diagram (Figure 1.14, **B**).<sup>[30]</sup> The density of scCO<sub>2</sub> at its critical point is 450 kg/m<sup>3</sup>, however the transport properties of a supercritical fluid depend strongly of density, which in turn is sensitive to the pressure and temperature (Figure 1.14, **B**).<sup>[34]</sup>

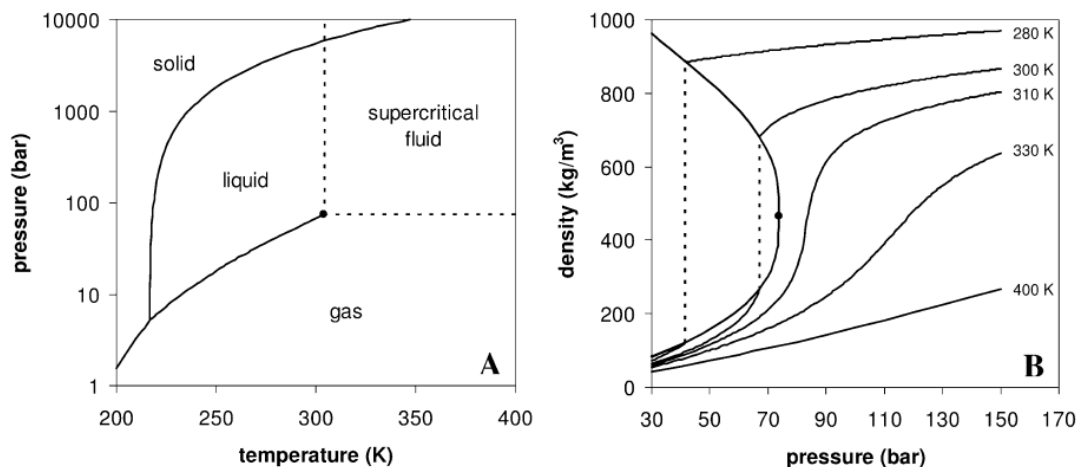


Figure 1.14: Schematic phase diagram for pure CO<sub>2</sub>. A- The critical point at the critical temperature and the pressure marks the end of the vapor-liquid equilibrium line and the beginning of the supercritical fluid region. B - Density of CO<sub>2</sub> as a function of pressure at different temperatures (solid lines) and at the vapor-liquid equilibrium line (dashed line).<sup>[30]</sup>

Supercritical carbon dioxide is a non-toxic and non-flammable solvent with a low viscosity and high diffusion rate and no surface tension.<sup>[28, 29]</sup> The disadvantage of CO<sub>2</sub> is that only volatile or relatively non-polar compounds are soluble,<sup>[28, 29]</sup> however, the polarity can be turned by adding some amount of co-solvents and also several polymerizations approaches can be followed depending on the initial reaction phase behavior.<sup>[29, 33]</sup>

## 1.2.2 Polymers in drug delivery

*Controlled drug delivery* has emerged as a truly interdisciplinary science that aims to improve human health. The basic goal of controlled drug delivery systems is to deliver biologically active molecules at a desired rate and for a desired period, maintaining the drug levels in the body within the therapeutic window.<sup>[35]</sup>

Most of the initially developed drug delivery systems were based on nondegradable polymers. However, the advent of synthetic biodegradable polymers coupled with the fact that macromolecules can be effectively delivered from these matrices, gave a new impetus to this branch of science.<sup>[35]</sup>

Based on the nature of the carrier, controlled drug delivery systems can be broadly classified into liposomal, electromechanical and polymeric delivery systems. Liposomes belong to a family of vesicular structures based on lipid bilayers surrounding aqueous compartments. In the majority of cases, lipid complexes and liposomal pharmaceuticals provide less toxicity and better efficacy



than the active ingredient.<sup>[36]</sup> Micro- and nano-electromechanical have many potentialities in drug release, like control the time and the doses administered. Micro-electromechanical has been used to construct microreservoirs, micropumps, nanoporous membranes, nanoparticles, valves, sensors, and other structures using biocompatible materials appropriate for drug administration. The focus of this section is polymeric drug delivery systems.<sup>[35]</sup>

In polymeric drug delivery systems, the drugs are incorporated in a polymer matrix. The rate of release of drugs from such a system depends on a multitude of parameters such as nature of the polymer matrix, matrix geometry, properties of the drug, initial drug loading, and drug-matrix interaction.<sup>[35]</sup> Therefore, controlled drug delivery can be used to achieve:<sup>[37]</sup>

- Sustained constant concentration of therapeutically active compounds in the blood with minimum fluctuations;
- Predictable and reproducible release rates over a long period time;
- Protection of bioactive compounds having a very short half-life;
- Elimination of side-effects waste of drug and frequent dosing;
- Optimized therapy and better patient compliance
- Solution to drug stability problems.

Furthermore, the mechanisms for drug delivery systems can be classified into diffusion controlled systems, chemically controlled systems, and solvent-activated systems.<sup>[38]</sup>

In diffusion systems, drugs diffuse through polymer: the polymer may undergo in subsequent biodegradation on exhaustion of the drug. Two types of diffusion-controlled devices have been used in drug delivery, these are reservoir devices and matrix devices.<sup>[38]</sup> The reservoir systems are hollow devices in which an inner core of dissolved, suspended or neat drug is surrounded by a polymer membrane. In this device, the drug core is encapsulated in a polymeric membrane. Drug diffusion through the membrane is rate limiting and controls the overall drug release rate, and a saturated concentration of reservoir of the drug inside the reservoir is essential to maintain a constant concentration gradient across the membrane. The drug transport mechanism through the membrane is usually a solution-diffusion mechanism, and it occurs first by dissolution of the drug in the membrane in the one side, being followed by diffusion through the membrane and desorption in the other side.<sup>[37, 38]</sup> In matrix systems, the drug is uniformly dissolved or dispersed. An inherent drawback of the matrix systems is their first-order release behavior with continuous decrease of release rate, which is due to the increasing diffusion path length and the decreasing area at the penetrating diffusion front (as the matrix release proceeds). The matrix device is easy

to formulate and gives higher initial release rate than a reservoir device and can be made to release at a nearly constant rate.<sup>[37]</sup>

In chemically controlled drug delivery systems, the release of a pharmacologically active agent usually takes place in the aqueous environment by one or more of the following mechanism:<sup>[37]</sup>

- Gradual biodegradation of a drug containing polymer system;
- Biodegradation of unstable bonds by which the drug is coupled to the polymer system;
- Diffusion of a drug from injectable and biodegradable microbeads.

In biodegradable systems, the main advantages are elimination of the need for surgical removal, their small size and potential low cost. On the other hand, all biodegradable products as well as their metabolites must be non-toxic and non-carcinogenic, these requirements are not easily met and must be subject to careful scrutiny.<sup>[37]</sup>

In pendent chain systems, the drug molecule is chemically bonded to a polymer backbone and the drug is released by hydrolytic or enzyme cleavage. The rate of drug release is controlled by the rate of hydrolysis. This approach provides an opportunity to target the drug to a particular cell type or tissue.<sup>[37]</sup>

### **1.2.2.1 Aspects to approve a new drug**

A number of factors that create hurdles for ultimate approval of the drug-loaded system in polymer medicine must be considered. Some of this factors are biocompatibility of the device, cytotoxicity, efficiency, inconvenience caused to patients, cost effectiveness, etc.<sup>[37]</sup>

For the design of drug delivery systems with optimum performance in specific circumstances, the drug delivery systems has to confront the following challenges:<sup>[37]</sup>

1. Improved efficacy;
2. Targeted delivery and reduced side effects;
3. Optimum performance;
4. Interfacing and pacing with modern methodologies;
5. Guarantees of safe environment;
6. Ease of fabrication and application in reality.

The polymer hydrogels of different chemical architecture with novel physic-chemical properties have shown potential to find applications as promising drug carrying vehicles in several drug delivery platforms. Although their synthesis and *in vivo* study seems to be simple, from the point of view *in vivo* applications the polymers systems need to be judged with extreme care before they can be accepted ultimately for commercial applications.<sup>[37]</sup>

## 1.3 CD complexes and pharmaceutical applications.

The potential uses of CDs in pharmaceutical industry have been increasing in the last few decades and may explain their main application in drug delivery field. The CDs have the ability to form inclusion complexes with some drugs and improve some of their features like solubility, stability, safety and bioavailability.<sup>[12, 39]</sup> However the most desirable attribute for a drug carrier is the ability to deliver a drug to targeted site.<sup>[40]</sup>

CDs with hydrophobic liner cavities and hydrophilic outer surfaces are capable of interacting with a large variety of guest molecule to form noncovalent inclusion complexes. The cavity size of  $\alpha$ -CD is insufficient for many drugs and  $\gamma$ -CD is expensive.  $\beta$ -CD has been widely used in the early stages of pharmaceutical studies because of its availability and cavity size, which gives a character suitable to interact with the widest range of drugs.<sup>[12]</sup>

The effect of CDs on chemical stability of drugs is a useful property and has been extensively studied.<sup>[41]</sup> CDs can be used to reduce or prevent gastrointestinal and ocular irritations, reduce/eliminate unpleasant smell or taste, prevent drug-drug or drug-additive interactions, or even to convert oils and liquid drugs into microcrystalline or amorphous powder.<sup>[13, 39]</sup> Besides this the CDs can improve the stability of several labile drugs against dehydration, hydrolysis, oxidation and photodecomposition and thus increase the shelf life of drugs.<sup>[12]</sup>

### 1.3.1 Complexation and mechanism of drug release from CD complexes

#### 1.3.1.1 Aqueous Solution

In aqueous solutions, CDs are able to form inclusion complexes with many drugs by taking up the drug molecule or some hydrophobic moiety of the molecule into the central cavity. No covalent bonds are formed or broken during the complex formation and the drug molecules in complex find rapid equilibrium (with free molecules in the solution).<sup>[3, 39, 42]</sup>

Phase-solubility analysis about the effect of complexing agents on the compound being solubilized is a traditional approach to determine not only the value of the stability constant but also to give insight into the stoichiometry of the equilibrium.<sup>[3]</sup> The phase-solubility profiles as shown in Figure 1.15. In **A** systems, the apparent solubility of substrate increases as a function of CD concentration. Three subtypes have been defined: **A<sub>L</sub>**, when the complex is first order with respect to ligand and first or higher order with respect to substrate (drug); **A<sub>P</sub>**, systems indicate an isotherm wherein the curve deviates in a positive direction from linearity, i.e. the complex is first

order with respect to the substrate, but second or higher order with respect to the ligand and  $A_N$  relationships indicate a negative deviation from linearity, i.e the CD proportionally less effective at higher concentrations. The A-type phase-solubility profiles indicate that water-soluble complexes are being formed with solubility higher than that of uncomplexed substrate.<sup>[3, 39, 42]</sup> Type **B** phase-solubility profiles indicate formation of complexes with a limited solubility in the aqueous complexation medium.  $B_S$ -type isotherms indicate that the CD concentration increases, a soluble complex forms which increase the total solubility of the substrate. The  $B_I$  systems are similar in form to the  $B_S$  profiles except that the complexes being formed are so insoluble that they do not give rise to the initial ascending component of the isotherm.<sup>[3, 39, 42]</sup>

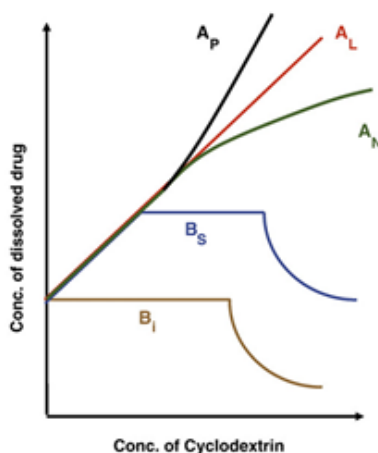


Figure 1.15: Graphical representations of A and B-type phase-solubility profiles.

When the complexation of CD/drug is in aqueous solution two parameters are important, dilution and competitive displacement, because the complexation constant (K) and the lifetime of the complex are very important for the drug release mechanism.<sup>[13]</sup>

### 1.3.1.2 Polymerization

There are different classes of CD containing polymers. One of the types of polymers are those possessing a crosslinked structure (Figure 1.16, **a**), one of the first agents used for crosslink in CDs was epichlorohydrin (1-chloro-2,3-epoxypropane).<sup>[11, 25]</sup> These were the initial CD-containing polymers investigated for drug delivery applications. Other agents used for crosslinking are the diepoxides and diisocyanates. Another class of polymers are those containing CDs as pendent moieties in the polymers backbone (Figure 1.16, **b**), however this type of

polymers are prepared by functionalized CDs. In Table 1.2, some examples of pendent polymers are referred.<sup>[15, 25]</sup>

Table 1.2: Examples of CDs pendent polymers.

Types of polymer	CDs	Preparation method
<b>Polyacrylic esters</b>	$\alpha$ and $\beta$	Polymerization of vinyl CD derivatives
<b>Poly(allylamine)s</b>	$\beta$ and $\gamma$	Grafting of CD to preformed polymer
<b>Polymethacrylates</b>	$\alpha$ , $\beta$ and $\gamma$	Polymerization of CD methacrylate monomers
<b>Polyester</b>	$\beta$	Gratting of CD to preformed polymer

A different type of CDs polymerized possesses a tubular structure, these polymers are then formed from the tubular configuration by crosslink between the CDs (Figure 1.16, c). The last class of polymers studied has a linear structure and contains CD as part of the backbone, as it can be seen in Figure 1.16, d.<sup>[15, 25]</sup>

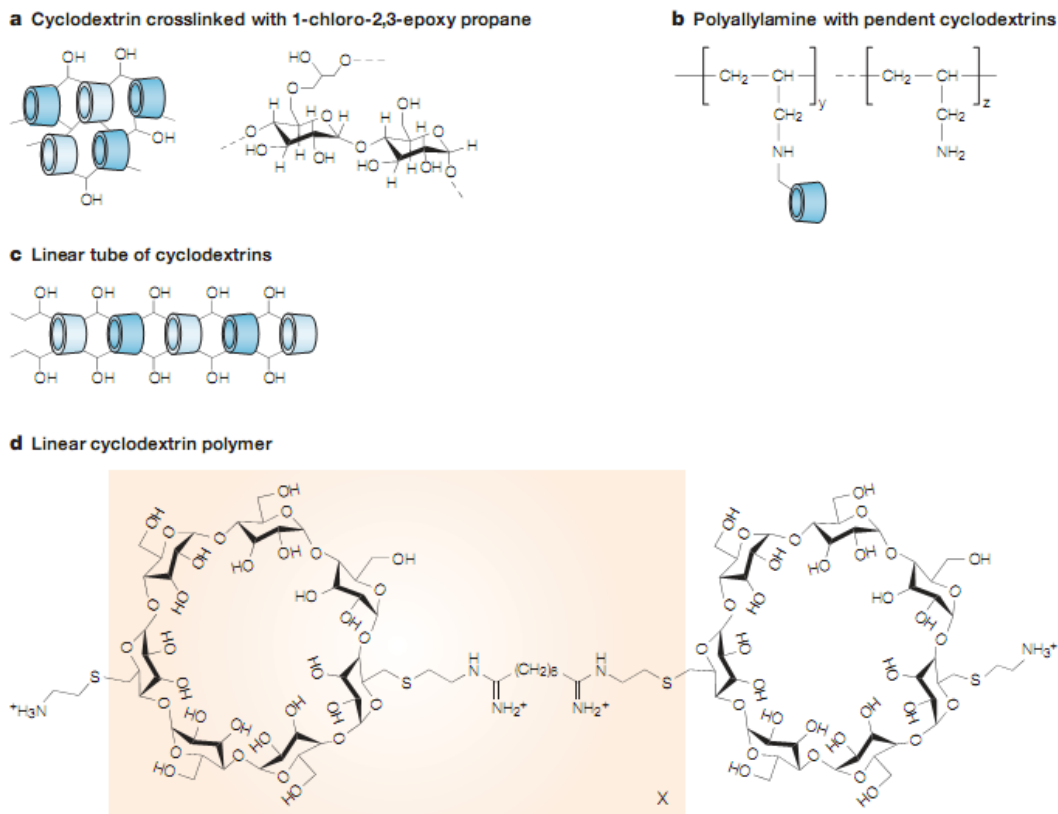


Figure 1.16: Classes of CDs-containing polymers.<sup>[25]</sup>

### 1.3.2 Pharmaceutical applications of drug-CD complexes

Nowadays many drugs with CDs are available in the market with application in several areas of medicine, as shown in Table 1.3.<sup>[1, 25, 43]</sup>

Table 1.3: Approved and marketed drug-CD complexes.<sup>[1, 25, 43]</sup>

Drug	Administration route	Treatment	Trade name	Market
<b><math>\alpha</math>-CD</b>				
<b>Alprostadil (PGE<sub>1</sub>)</b>	Intravenous	Vasodilation	Prostavastin, Edex	Europe, Japan, USA
<b>Cefotiam Hexetil HCl</b>	Oral	Antibiotic	Pansporin T	Japan
<b><math>\beta</math>-CD</b>				
<b>Dinoprostone (PGE<sub>2</sub>)</b>	Sublingual	Labor induction	Prostarmon E	Japan
<b>Benexate</b>	Oral	Antiulcer	Ulgut, Lonmiel	Japan
<b>Dexamethasone</b>	Dermal	Analgesic	Glymesason	Japan
<b>Nicotine</b>	Sublingual	Reducing the symptoms of absence	Nicorette	Europe
<b>Omeprazol</b>	Oral	Antiulcer	Omebeta	Europe
<b><i>2-Hydroxypropyl-<math>\beta</math>-CD</i></b>				
<b>Hydrocortisone</b>	Buccal	Anti-inflammatory	Dexocort	Europe
<b>Indomethacin</b>	Eye drops	Anti-inflammatory	Indocid	Europe
<b><i>Random methylated <math>\beta</math>-CD</i></b>				
<b>17<math>\beta</math>-Oestradiol</b>	Nasal spray	Hormone therapy	Aerodiol	Europe
<b>Chloramphenicol</b>	Eye drops	Antibiotic	Clorocil	Europe
<b><i>Sulphobutylether <math>\beta</math>-CD</i></b>				
<b>Voriconazole</b>	Intravenous	Antimycotic	Vfend	Europe, USA
<b><i>2-Hydroxypropyl <math>\gamma</math>-CD</i></b>				
<b>Diclofenac sodium</b>	Eye drops	Anti-inflammatory and analgesic	Voltaren	Europe

The first studies about the application of CDs in drug delivery experiments were with the prostaglandins (PGE). CDs complexes of PGE<sub>1</sub> and PGE<sub>2</sub> resulted in a significant increase in their solid-state stability, and a product designed along these lines was approved for the first time in Japanese market in 1976. Prostaglandins are used to relax smooth muscles and increase blood flow, and were initially developed in the therapeutic of peripheral circulatory disorders. Just after, in 1979, alprostadil alphasex (Prostavasin) was approved for the treatment of peripheral vascular complications and showed activity against chronic arterial occlusions and arteriosclerosis. CDs were applied to this compound in an effort to improve several properties, including safety and drug dissolution rate. These improved characteristics reduced gastrointestinal irritation, and allowed faster drug absorption and faster onset of analgesic effect.<sup>[25]</sup>

The implementation of structural changes in the CD allowed different pharmaceutical applications. For instance, the randomly methylated  $\beta$ -CD avoids a number of issues related to oral or transdermal administration and allows administration strategies like eye drop and nasal. The hydroxypropylated  $\beta$ -CD is available in registered oral, intravenous, buccal, rectal and ophthalmic products. The sulphobutyl ether  $\beta$ -CD has products like intravenous formulation of the antifungal agent voriconazole and an intramuscular dosage form for the antipsychotic agent ziprasidone.<sup>[25]</sup>

These are only some examples about the available commercial applications of the CDs in pharmaceutical industry. There are many exciting possibilities for the future applications of CDs including new uses for existing derivatives, as well as the development of new derivatives.



## **2. Results Discussion**

## 2.1 Objective

From the point of view of pharmacotherapy optimization, drug release should be controlled in accordance to the therapeutic purpose and the pharmacological properties of active substances. There has been a growing interest in the development of a delivery system with rate- or time-controlled oral administration, because appropriate drug release from dosage forms have critical importance for efficient therapeutics.<sup>[44]</sup>

Cyclodextrins (CDs) are potential candidates for controlled drug delivery, once their cavities provide microenvironments where molecules can enter and form inclusion complexes. Supercritical CO<sub>2</sub> (scCO<sub>2</sub>) is a sustainable alternative comparing to processes with organic solvents, and a very attractive medium for the preparation of these inclusion complexes.<sup>[45]</sup>

This work aims to develop a new pH responsive CDs-hydrogel system in scCO<sub>2</sub> with potential application on controlled drug delivery. The first part of this study consists on functionalization of  $\beta$ -CD with a group, such as activated double bonds that allow polymerization in scCO<sub>2</sub>. In order to prepare the desired  $\beta$ -CDs, two different approaches were used: regioselective functionalization in the most reactive hydroxyls groups (C<sub>6</sub>-OH) and functionalization of a complete set of hydroxyls groups.<sup>[3]</sup> The second part of this work envisages the polymerization of the functionalized  $\beta$ -CD in scCO<sub>2</sub> and the investigation of the potential ability of polymer-CD to form inclusion complexes with the drug. *In vitro* experiments will be performed in order to evaluate the performance of the CDs-hydrogel system as drug release device at different pHs, 2.2 and 7.4, which simulate the gastric and colon experiments. The intent is to study the most appropriate application of these complexes.<sup>1</sup>

In order to investigate the importance and role of CD cavity, three different  $\beta$ -CD derivates need to be prepared: the first involves the synthesis the of a monoacrylate- $\beta$ -CD *via* the 6-monotosyl- $\beta$ -CD approach (Figure 2.1,1); the second consists of acrylation by a direct method (Figure 2.1, 2); and the third involves the exploration of a filled CD cavity to study its role in the polymerization and interaction with the drug (Figure 2.1,3).

---

<sup>1</sup> The co-polymerization in scCO<sub>2</sub> and the *in vitro* drug release experiments were performed with the collaboration of a PhD student (Mara Soares da Silva) from the group of Polymer Synthesis and Processing using Supercritical Carbon Dioxide (REQUIMTE).

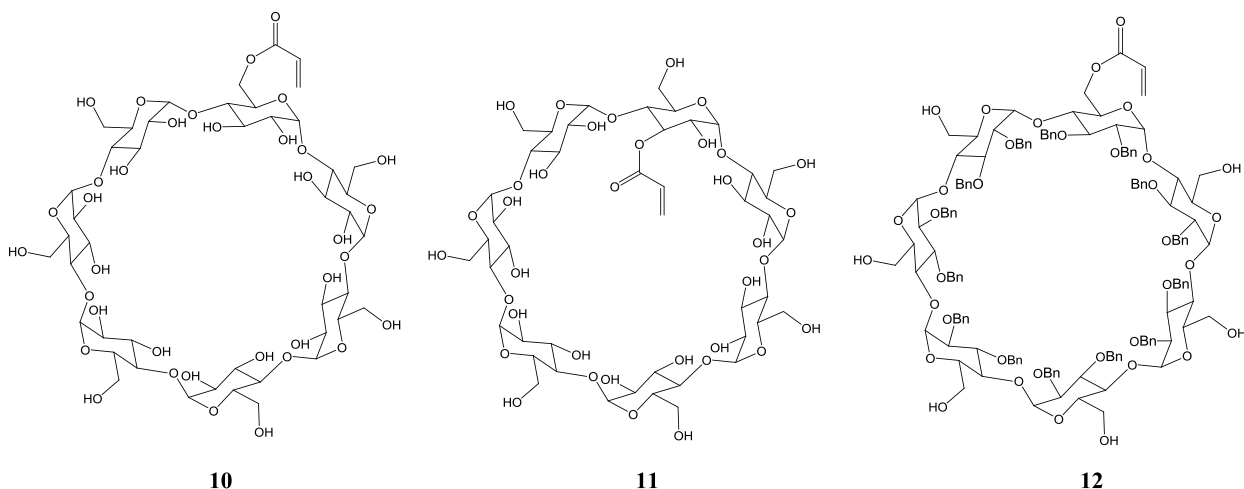


Figure 2.1: Functionalized  $\beta$ -CDs (**10**, **11** and **12**) which were synthesized for application on polymerization reaction, to study the formation of inclusion complexes with drugs.

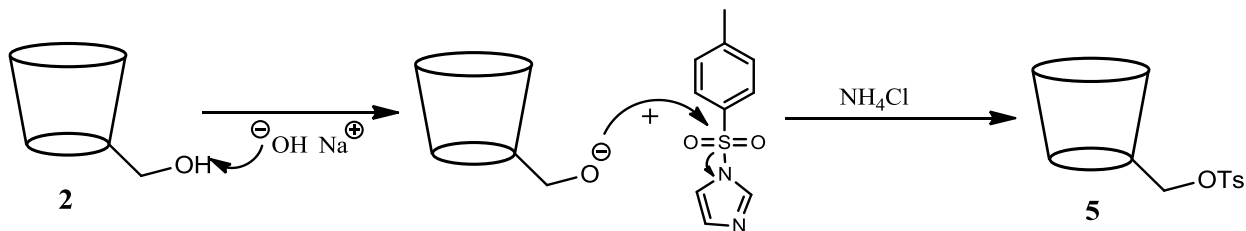
## 2.2 Synthesis of functionalized CDs

The objective of synthesizing the compound **10** was to introduce a crosslink, a group with a double bond possessing an electron withdrawing group that allows subsequent polymerization in  $s\text{CCO}_2$ .

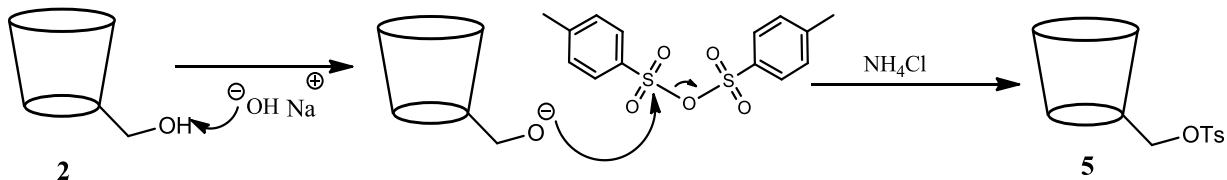
In the first chapter, the main approaches described in literature (Chapter 1.1.3.1) to selectively functionalize CDs were presented. From the reported approaches, a route for a selective modification at C<sub>6</sub>-OH consists on to the introduction of the tosyl group, a good leaving group and then substitution by the desired functional group, by tosyl group displacement (Figure 1.18).<sup>[14]</sup>

To synthesize the 6-monotosyl- $\beta$ -CD (**5**) three procedures were tested in order to achieve high yields of conversion. The first attempts of mono-tosylation were performed by treatment with *p*-toluenesulfonyl imidazole,<sup>[21]</sup> *p*-toluenesulfonic anhydride<sup>[20]</sup> and *p*-toluenesulfonyl chloride<sup>[19]</sup>. The mechanisms of these reactions are very similar as noted in the Figure 2.2 and consist in a S<sub>N</sub>2 mechanism. In the first step, the base sodium hydroxide will remove the proton of the hydroxyl group forming an anion that will act as a nucleophile and attack the sulfur atom of the tosylation reagent, releasing: imidazole ion (**a**), tosyl ion (**b**) and chloride ion (**c**).<sup>[19-21]</sup> The reactions a) and b) were quenched with ammonium chloride. The precipitate was a white powder that was filtered and washed with water.<sup>[19-21]</sup>

a) Reaction of tosylation with toluenesulfonyl imidazole.



b) Reaction of tosylation with *p*-toluenesulfonic anhydride.



c) Reaction of tosylation with *p*-toluenesulfonyl chloride.

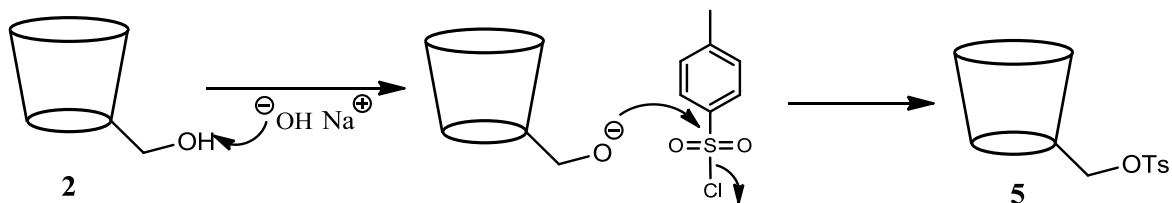


Figure 2.2: Mechanisms of mono-tosylation reaction with different reagents to obtain **5**.

The yield of isolated and purified **5** varies depending on the tosylation reaction conditions (Table 2.1). Thus, a higher yield of **5** was obtained when *p*-TsCl was used as tosylation agent.

Table 2.1: Yields of mono-tosylation reactions with different reagents.

Reagents	Yields
<i>p</i> -Toluenesulfonyl Imidazole	19%
Toluenosulfonic Anhydride	10%
<i>p</i> -Toluenesulfonyl Chloride	21%

The NMR spectra of the 6-monotosyl- $\beta$ -CD (**5**) were performed in DMSO- $d_6$ . In the  $^1\text{H-NMR}$  spectrum was possible to observe two types of resonance signals that indicated the presence of

this compound: the aromatic protons (7.4-7.7 ppm) and the methylic protons (2.5 ppm) of tosyl group (Figure 2.3).<sup>[19-21]</sup> The NMR spectrum was in accordance with literature.<sup>[19-21, 46]</sup>

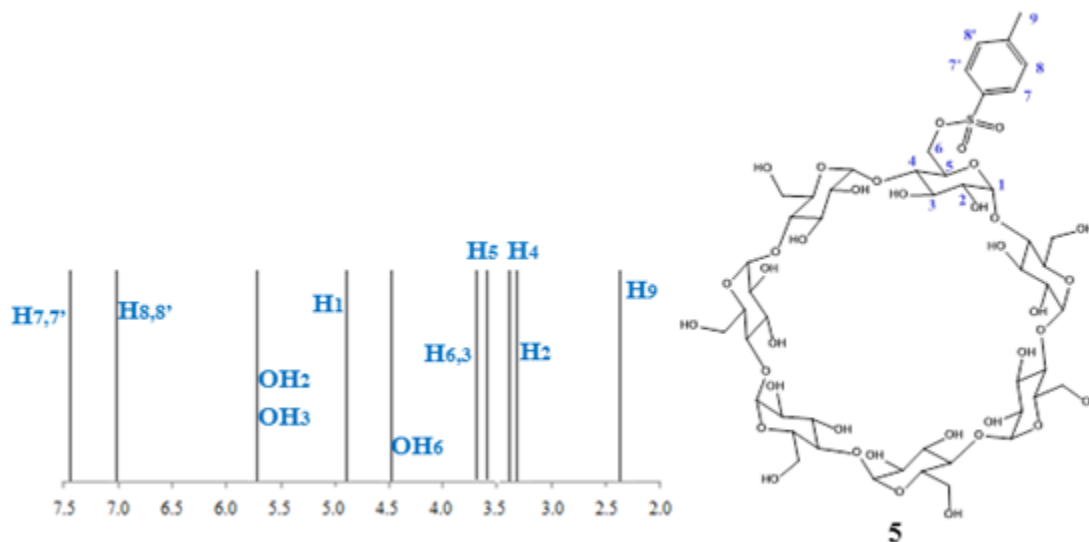


Figure 2.3: Structure of **5** and a representation of the chemical shift.

The next step to obtain the desired products 6-mono-acryloyl/methacryloyl/- $\beta$ -CD (**10/13**), consisted on the displacement of tosyl group by a proper nucleophile.<sup>[47]</sup> The salt of methacrylic acid or acrylic acid was previously prepared by treatment with cesium hydroxide (Figure 2.4, 1<sup>st</sup> step). The salt formed was then added to a solution of **5**, reacting as nucleophile and attacking the secondary carbon atom of 6-monotosyl- $\beta$ -CD (**5**), releasing the tosyl group (Figure 2.4, 2<sup>nd</sup> step).<sup>[48]</sup> The final product was obtained as a white solid, after several washing with ethyl ether and ethanol. The 6-mono-acryloyl- $\beta$ -CD (**10**) was isolated with 79% yield and 6-mono-methacryloyl- $\beta$ -CD (**13**) was not possible to obtain completely pure. The overall yield to achieve compound **10** through compound **5** was 17%. This was the compound used for the studies of polymerization and interaction with a drug.

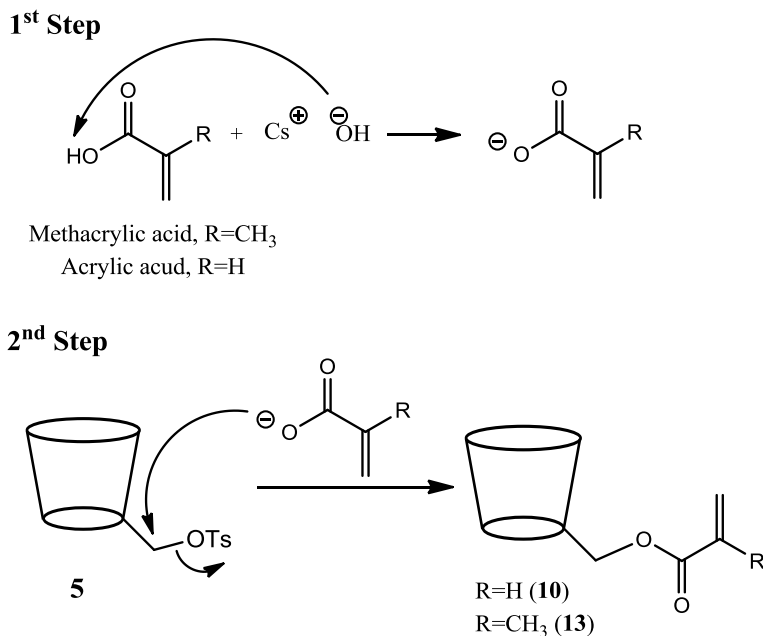


Figure 2.4: Mechanism of reaction to obtain **10** and **13**.

The NMR spectra of **10** and **13** were performed in D<sub>2</sub>O. In the case of 6-mono-methacryloyl- $\beta$ -CD (**13**) two signals were expected in the <sup>1</sup>H-NMR around 5.6-6.3 ppm, due to the presence of the double bond and 2 ppm due to the methyl group (Figure 2.5).<sup>[46, 48]</sup>

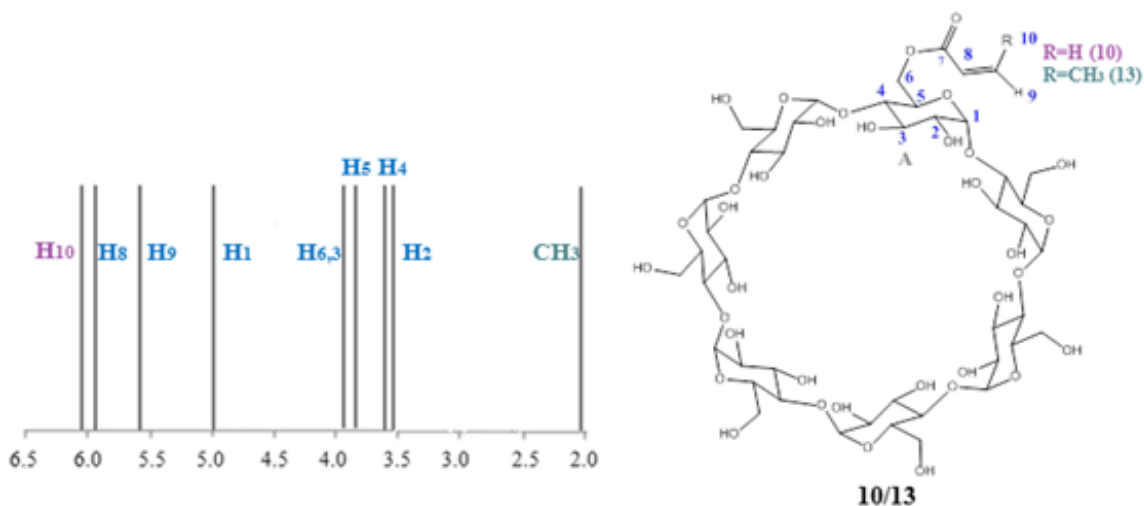


Figure 2.5: Structure of compounds **10** and **13** and a representation of the corresponding chemical shift.

In spite of all efforts to remove the unreacted 6-monotosyl- $\beta$ -CD (**5**), through washing and recrystallization, it was not possible to remove it completely. From the <sup>1</sup>H-NMR spectrum of 6-mono-acryloyl- $\beta$ -CD (**10**) it was possible to observe three signals corresponding to resonances of the double bond protons between 5.5-6.4 ppm (Figure 2.5).<sup>[19-21]</sup> In the <sup>13</sup>C-NMR spectrum the

resonance signal correspondent to the carbon of carbonile carbon at 175.6 ppm and the signals of two carbons of the double bonds at 133.9 and 126.5 ppm were observed.<sup>[46]</sup> From all 2D spectra only in the NOESY experience was possible to see a correlation between the anomeric ( $H_1$ ) protons and the double bond protons ( $H_{9,10}$ ) (Figure 2.6).

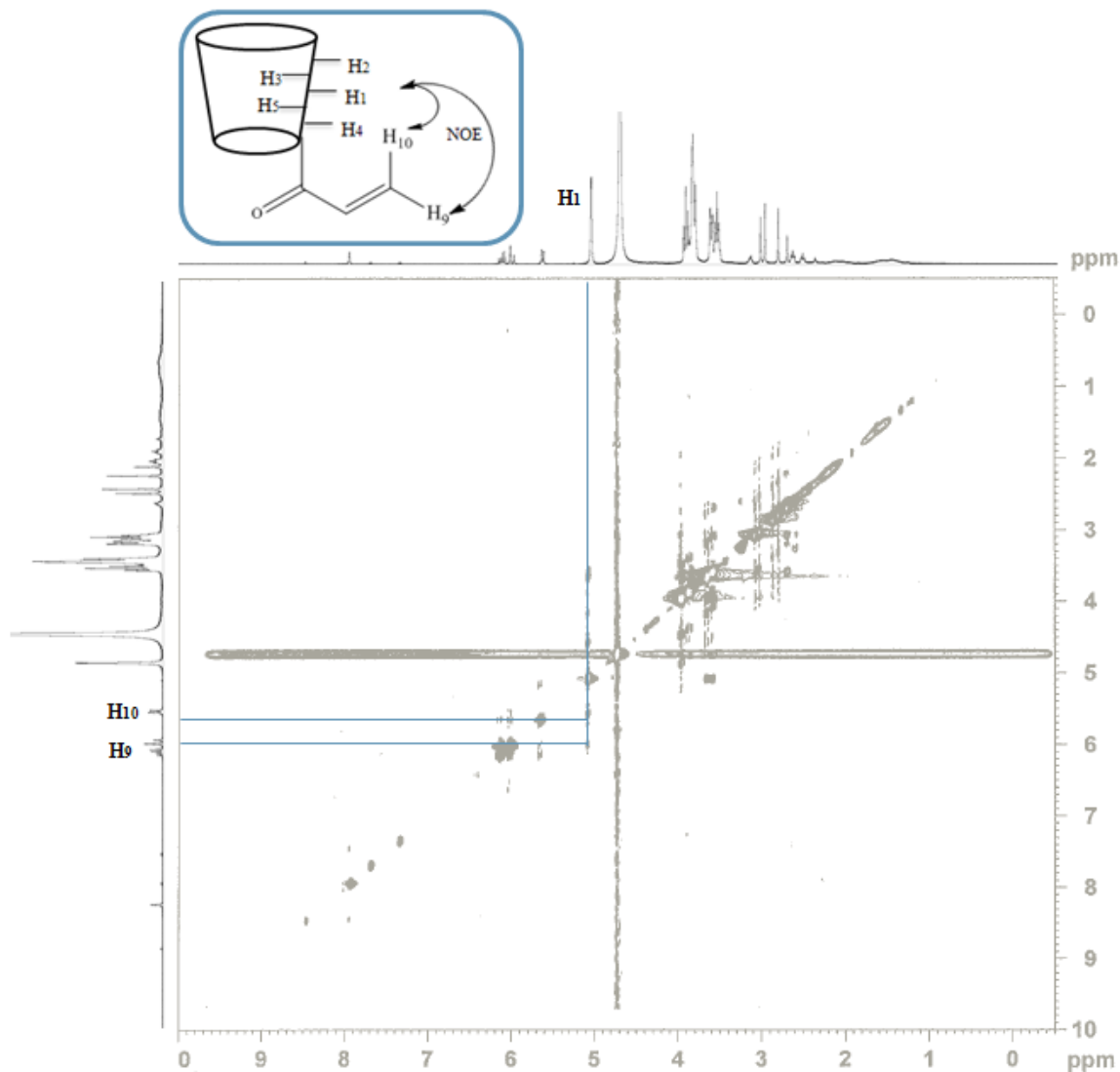


Figure 2.6: NOESY HR-MAS NMR spectrum and correlations between the protons of  $\beta$ -CD and acryloyl group of **10**.

Due to the difficulty in preparing the 6-mono-acryloyl/methacryloyl- $\beta$ -CD (**10/13**) completely pure, and in large amount needed for the  $scCO_2$  study, a less selective method was used to overcome this problem and have enough product to start the polymerization and drug delivery studies.<sup>[49]</sup>

In this second approach the  $\beta$ -CD (**2**) was slowly dissolved in pyridine to prevent the formation of a gel and subsequently the acryloyl chloride in THF was added dropwise.<sup>[50]</sup> The mechanism of this reaction is basically the attack of the oxygen atom to the carbonyl group with the release of chloride ion, which is a good leaving group. In Figure 2.7, is represented a mechanism for the acrylation of  $\beta$ -CD (**11**).

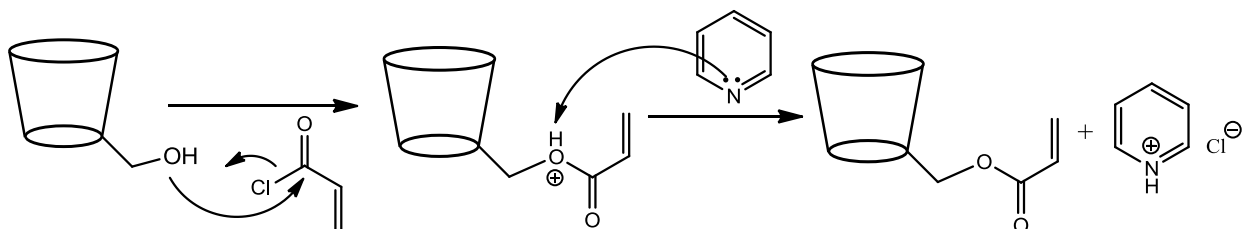


Figure 2.7: Mechanism of preparation of acryloyl- $\beta$ -CD.

The product **11** was obtained with 94 % yield and presented a yellow/brown color. To characterize **11** by NMR DMSO- $d_6$  and  $D_2O$  were used as solvents. In the  $^1H$ -NMR spectra performed in  $D_2O$  it was possible to observe a signal correspondent to the resonance of double bound protons between 5.9- 6.4 ppm (Figure 2.8).<sup>[50]</sup>

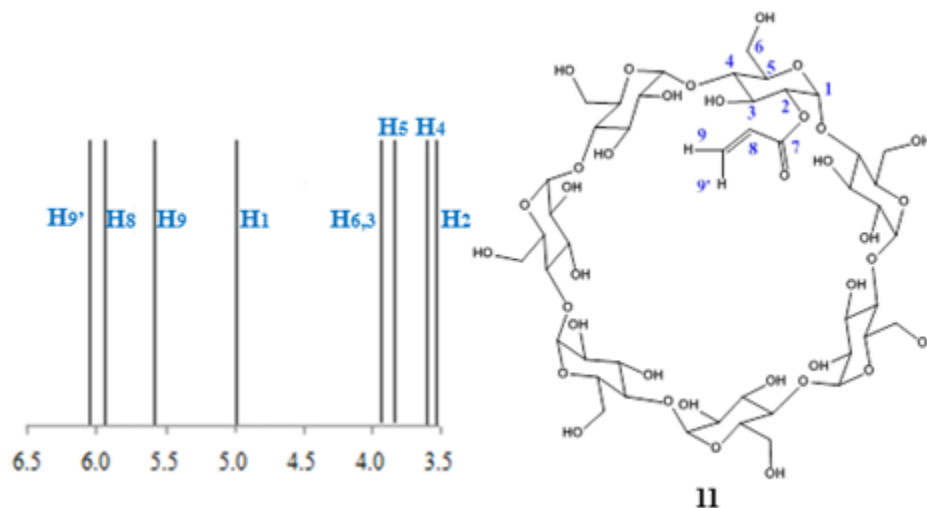


Figure 2.8: Structure of **11** and a representation of the corresponding chemical shift.

In the  $^{13}C$ -NMR spectrum it was possible to observe the resonance signal of the carbon of the carbonile group at 165.9 ppm and the carbons of the double bond between 132.0 and 128.0 ppm.<sup>[47, 50]</sup> However, in the 2D spectrum it was not possible to observe any correlation between the protons of the acryloyl group and protons of the  $\beta$ -CD. Moreover, the NMR study was realized in DMSO- $d_6$  to analyze the signals of hydroxyls groups. Despite the fact of the 2D



experiments did not show evidence of an acryloyl group covalently bonded to CD, in the  $^1\text{H-NMR}$  spectrum the integration of the number of protons for the hydroxyl groups ( $\text{C}_2\text{-OH}$ ,  $\text{C}_3\text{-OH}$ ,  $\text{C}_6\text{-OH}$ ) suggests that the acryloyl group is bonded to the  $\text{C}_2\text{-OH}$ . The resonance signals of  $\text{C}_2\text{-OH}$  and  $\text{C}_3\text{-OH}$  appear in the same chemical shift while  $\text{C}_6\text{-OH}$  appears at a higher field, thus integration suggests that the reaction occurred at  $\text{C}_2\text{-OH}$  or  $\text{C}_3\text{-OH}$  instead of the most reactive hydroxyl group,  $\text{C}_6\text{-OH}$ . However, due to the known higher reactivity of  $\text{C}_2\text{-OH}$  it is proposed that the reaction occurred at this position.<sup>[5]</sup> Figure 2.9, shows a proposed mechanism to explain the fact that acrylation reaction occurred inside the cavity of the  $\beta\text{-CD}$ . In MALDI-TOF spectrum, the peak observed at  $1268.6\text{ m/z}$  corresponds to monoacrylate- $\beta\text{-CD}$  and in the IR spectrum a band at  $1735\text{ cm}^{-1}$  confirms the presence of an ester group.<sup>[47]</sup>

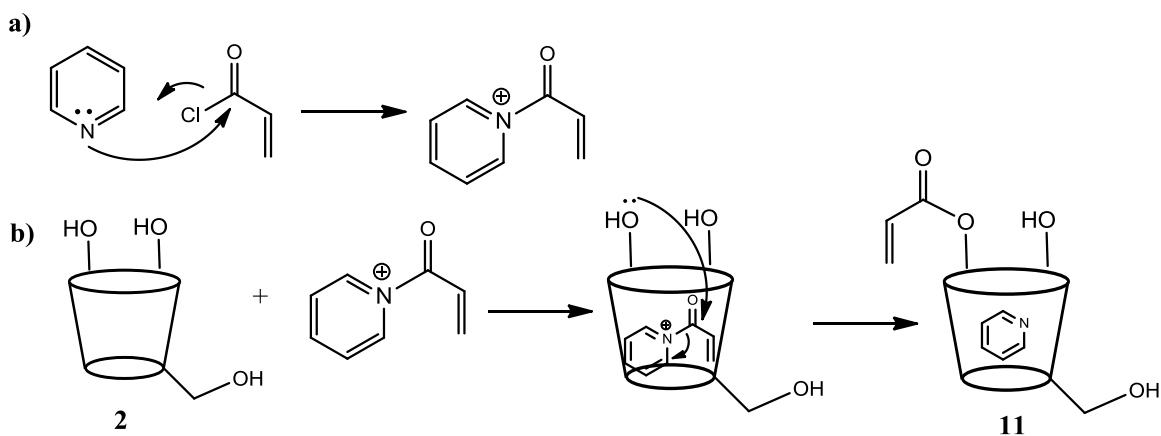


Figure 2.9: Plausible mechanism proposed to the formation of **11**. a) Reaction of pyridine with acryloyl chloride. b) Mechanism of reaction forming an inclusion complex with pyridine salt.

The next synthesis envisaged the investigation of the importance of the free cavity of  $\beta\text{-CD}$ , in the process of polymerization and impregnation with a drug.

To plan a modification in secondary hydroxyl group was necessary first to protect the primary hydroxyl groups, since these are the most reactive.<sup>[14]</sup> Figure 2.10, shows the synthetic plan to obtain the desired product.<sup>[18, 49-51]</sup>

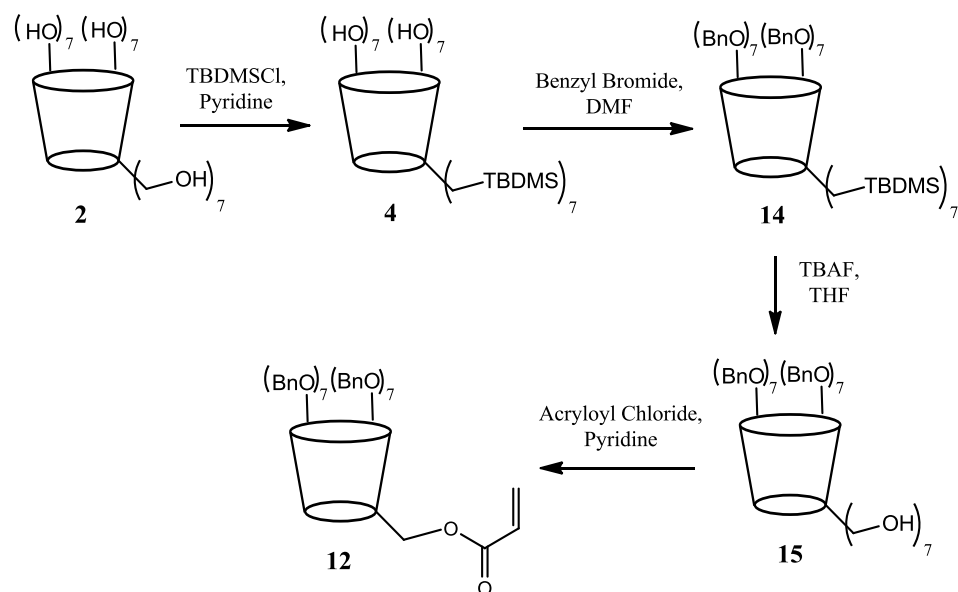


Figure 2.10: Synthetic plan to obtain **12**.

The requirements for the choice of the protecting group are their stability in the following reaction steps and the conditions to remove them. The deprotection conditions should not affect the groups introduced in the secondary hydroxyl groups. From all the protective groups and procedures described in literature, the TBDMS was the group of choice due to its easy removal by treatment with TBAF and also due to its stability under the proposed synthetic sequence.<sup>[18]</sup> The synthesis of persilylated CD consisted on the use of TBDMSCl, that due to its bulkiness prevents the silylation at secondary hydroxyl groups.<sup>[50]</sup> However, it was necessary to purify the resulting crude in a chromatography column with a gradient of solvents (MeOH:CH<sub>2</sub>Cl<sub>2</sub>). The persilylate- $\beta$ -CD (**4**) was collected as a white solid and a yield of 81% was obtained.

The mechanism of this reaction is depicted in Figure 2.11.

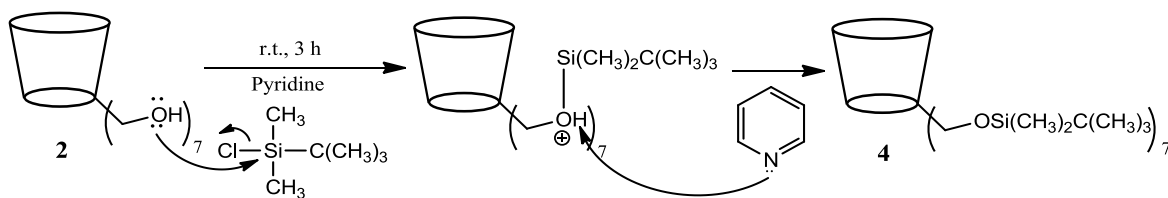


Figure 2.11: Mechanism of reaction with TBDMSCl to afford **4**.

The NMR spectra were performed in CDCl<sub>3</sub>. The <sup>1</sup>H-NMR spectrum showed two signals that indicate the presence of TBDMS group, the resonance signal at 0.04 ppm of the methyl groups and at 0.87 ppm correspondent to the protons of the *tert*-butyl groups (Figure 2.12). The MALDI-

TOF spectrum confirmed that the silylation occurred at all C<sub>6</sub>-OH positions by the presence of the peak at 1956.0 m/z.<sup>[50]</sup>

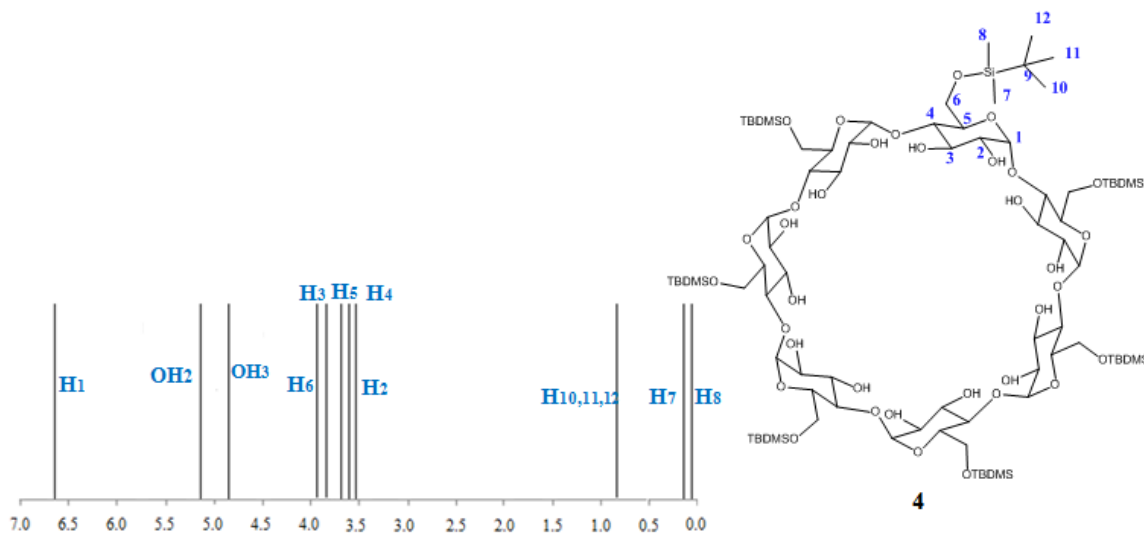


Figure 2.12: Structure of **4** and the corresponding chemical shift.

The next step aimed to occupy the cavity of  $\beta$ -CD with benzyl groups, a large group that would fill the cavity and allow achievement of this study.<sup>[51]</sup>

One of the procedures reported, involved the use of benzyl bromide.  $\beta$ -CD was dissolved in DMF and sodium hydride was added, a base to remove protons from the secondary hydroxyl group forming the corresponding anion. This anion will act as nucleophile and when benzyl bromide is added, the attack to the carbon atom that is bound to bromine occurs since bromine is a good leaving group (Figure 2.13).<sup>[51]</sup> The product was collect as a white solid in 43% yield.

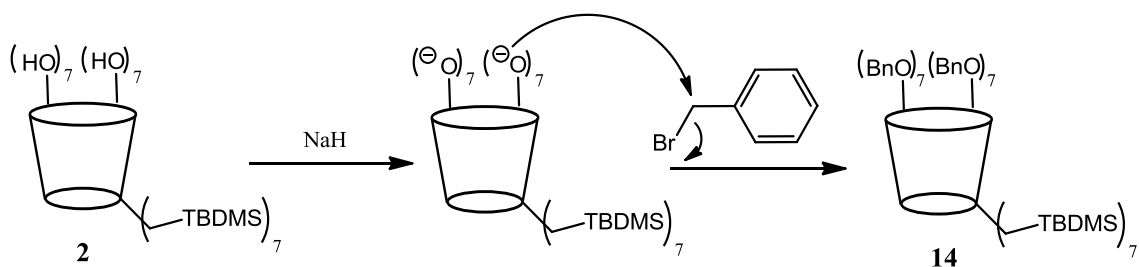


Figure 2.13: Mechanism of reaction with benzyl bromide to fill the cavity of  $\beta$ -CD and obtain **14**.

The NMR spectra were performed in  $\text{CDCl}_3$ . The  $^1\text{H}$ -NMR spectrum shows the signal of correspondent to the resonance of the protons of TBDMS group which proves that this compound is stable under these reaction conditions. The  $^1\text{H}$ -NMR signals around the 7.0-7.3 ppm show that the benzyl groups are present in the cavity of  $\beta$ -CD (Figure 2.14).<sup>[51]</sup> The MALDI-TOF proves

that all the positions of secondary hydroxyl group are substituted by the presence of peak at 3217.8 m/z.<sup>[51]</sup>

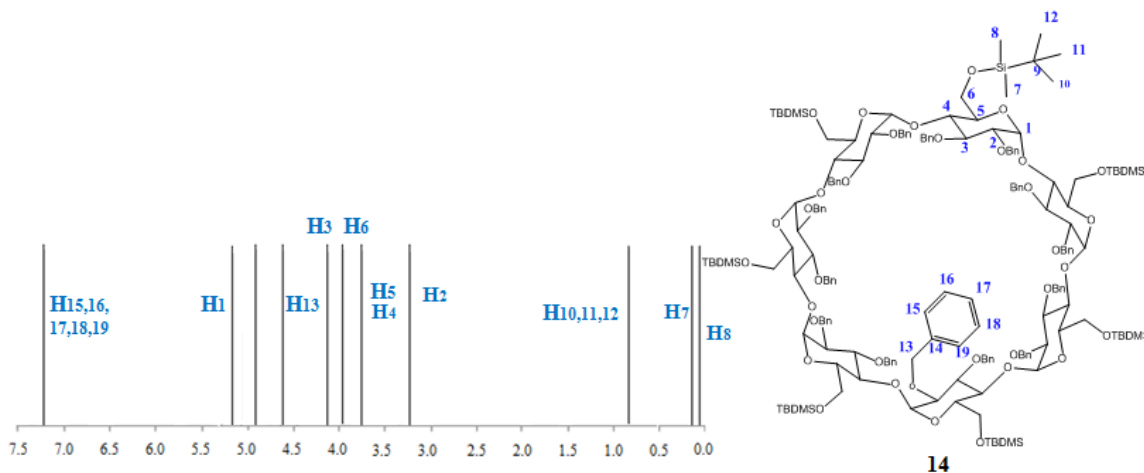


Figure 2.14: Structure of **14** and a representation of the corresponding chemical shift.

The third step of this synthetic route consisted on the deprotection of primary hydroxyl group, removing the TBDMS group. This reaction was performed in tetrahydrofuran (THF) with the TBAF reagent, a quaternary ammonium salt (Figure 2.15).<sup>[18]</sup>

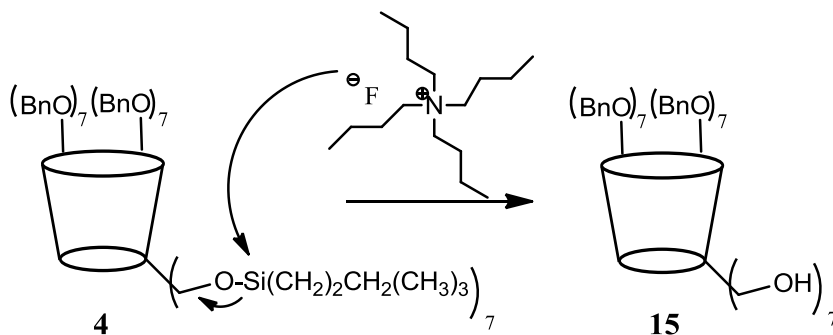


Figure 2.15: Mechanism of deprotection of primary hydroxyl group to obtain **15**.

The product **15** was obtained with a 94% yield and presented a yellow/brown color. The NMR spectra were performed in CDCl<sub>3</sub>, and in the <sup>1</sup>H-NMR spectrum the absence of the signals correspondent to the resonance of methylic protons from the TBDMS groups indicated that the deprotection was successful (Figure 2.16).<sup>[18, 46]</sup>

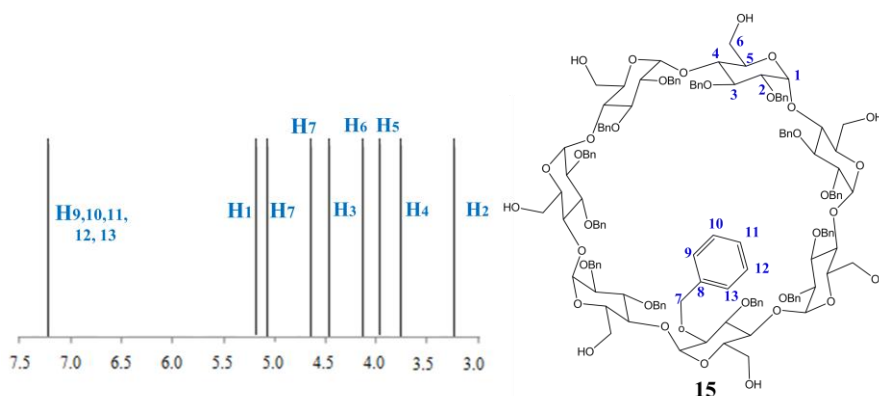


Figure 2.16: Structure of compound **15** and representation of chemical shift.

The last step consisted on the introduction of the cross-linking to polymerize the  $\beta$ -CD with filled cavity. The procedure for this step was the same used before for the product **11**, by reaction with the acryloyl chloride (Figure 2.17).<sup>[49]</sup>

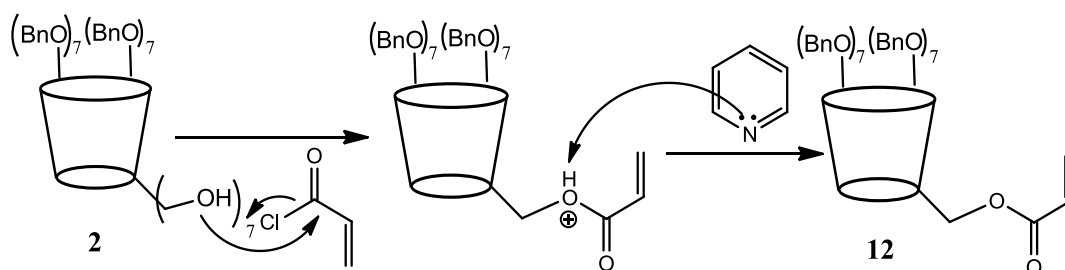


Figure 2.17: Mechanism of reaction to obtain the final product (**12**) with acryloyl chloride.

The product was obtained with 65% yield. The  $^1\text{H-NMR}$  spectrum of compound **12** reveals the resonance signals of aromatic ring around 7.2-7.4 ppm (Figure 2.18). It was not possible to observe the resonance signals of the double bond protons due to the “ring –current effect”. This is an example of diamagnetic anisotropy that causes the large deshielding of benzene ring protons as well as protons near the aromatic ring.<sup>[46]</sup> Due to the effect described, above the protons of double bond are deshielded, and their resonance signals are shifted to lower field appearing in the same field as the aromatic protons.<sup>[46]</sup> Moreover, it was observed that the resonances of CD ring were also affected by the presence of the aromatic rings. This observation was already described in the literature.<sup>[51]</sup> In MALDI-TOF the fragment at 2529.1 m/z corresponds to  $\beta$ -CD benzylated and acrylate in one position. Furthermore the IR spectrum showed the band at  $1731\text{ cm}^{-1}$  correspondent to the carbonyl of an ester group.<sup>[46, 51]</sup>

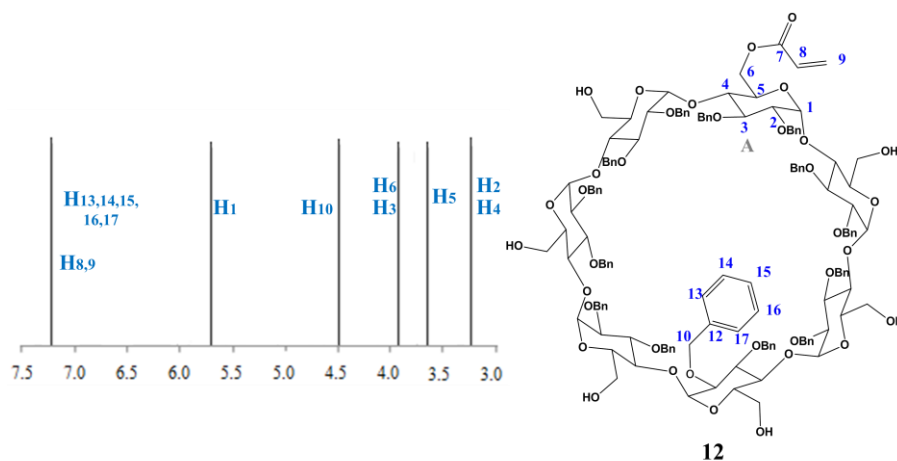


Figure 2.18: Structure of compound **12** and representation of chemical shift.

In order to co-polymerize the compound **12** with functional monomers and study the interaction of the resulting polymer with a drug, a large amount was needed. With an overall yield of 21% it was necessary to reproduce the synthetic scheme many times to obtain the amount of product needed.

Table 2.2 presents the summary of the structural characterization (NMR, IR and ME) and yields of all compounds involved in synthesis of **10**, **11** and **12**.

Table 2. 2: Summary of structural characterization and yields of all compounds involved in synthesis of **10**, **11** and **12**.



## 2.3 Exploration of novel approach towards the functionalization of $\beta$ -CD

The selective modifications of CDs are a challenge, due the hydrophobic cavity and the large number of hydroxyl groups. Due to the hydrophobic cavity there is a tendency to form inclusion complexes with reagents of the synthetic scheme.<sup>[14, 24]</sup> The hydroxyl groups C<sub>2</sub>-OH, C<sub>3</sub>-OH and C<sub>6</sub>-OH compete for the reagent and make the selective modification extremely difficult.<sup>[14, 24]</sup> In literature, the main methods to selectively functionalize the CDs at C<sub>6</sub>-OH are *via* the use of 6-monotosly- $\beta$ -CD (**5**), but the synthesis of this compound has a very low yield.<sup>[5, 14]</sup> Due to the importance of developing new methods that allow the regioselective functionalization of  $\beta$ -CD (**2**) with a good yield, synthetic studies were performed using the acetyl group as an alternative to protect the primary hydroxyl groups (C<sub>6</sub>-OH).

The first attempt consisted in the reproduction of a literature procedure using the acetyl chloride as acetylating agent (Figure 2.19).<sup>[52]</sup> Two assays were performed, one with seven equivalents of base and reagent and other with ten equivalents.

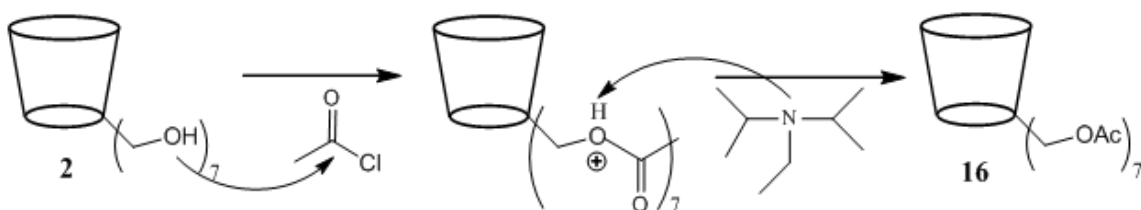


Figure 2.19: Mechanism of the acetylation reaction.

In both experiments performed, two different reaction mixtures were obtained and analyzed by NMR. The NMR experiments of product obtained in the reaction with seven equivalents were performed in DMSO-d<sub>6</sub>. In the <sup>1</sup>H-NMR spectrum it was possible to observe the resonance signal of methylic protons from the acetyl group at 2.16 ppm.<sup>[46, 52]</sup> The MALDI-TOF spectrum revealed that the product obtained was a mixture of acetylated  $\beta$ -CD in one, two, three, four and five positions. However, the diacetylate  $\beta$ -CD was the major product (Table 2.3). The product obtained in the second reaction with ten equivalents, presented a <sup>1</sup>H-NMR with the characteristic resonance signal at 2.16 ppm of the methylic protons, but the MALDI-TOF spectrum revealed that the product was acetylated mainly in three and four positions. Moreover, it was possible to observe a mixture of  $\beta$ -CDs acetylated until seven positions (Table 2.3).

Table 2.3: Number of equivalents of reagent used in the reactions of peracetylation and the products obtained.

N° equivalents of Acetyl Chloride	Mass Spectrum (m/z)
7	1241.7 (2 acetyl groups)
10	1283.7 (3 acetyl groups) and 1325.7 (4 acetyl groups)

As the previous procedure did not result in the expected product and revealed to be a non-selective approach, another approach was explored – use of benzotriazole as acetyl group transfer agent.<sup>[53]</sup> The most used acylating agents are acetic anhydride, acetyl chloride, between others, which are small compounds, can easily access the CD cavity and thus the regioselective functionalization of the  $\beta$ -CD is difficult.<sup>[16]</sup> The *N*-acylbenzotriazole reagent is reported in the literature as a general reagent for *N*-acylation of amines and amides, the *O*-acylation of aldehydes, and the *C*-acylation of ketones and heteroaromatics, alksulfones, alkylcyanides and alkylazines (Figure 2.20).<sup>[54-56]</sup> Acylation with the stable and crystalline *N*-acetylbenzotriazole (**17**)<sup>[56]</sup> has a great potential to selectively functionalize the  $\beta$ -CD, due to the size of the benzotriazole unit, the access to the cavity hydroxyls group C<sub>2</sub>-OH and C<sub>3</sub>-OH, will be more difficult.

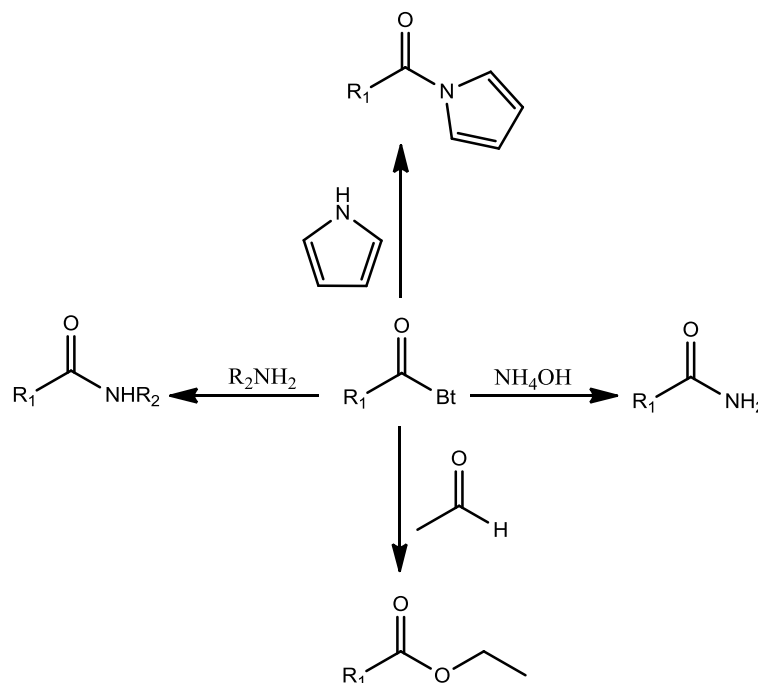


Figure 2.20: Examples of application of *N*-acylbenzotriazole (Bt: benzotriazole)

The first step consisted on the synthesis of the *N*-acetylbenzotriazole (**17**). The reaction was run in DMF and diisopropylethylamine was added as base, subsequently the acetic anhydride was added and the desired product was obtained (Figure 2.21, a).<sup>[53]</sup> The second step consisted on the reaction of the  $\beta$ -CD with **17** and the desired product **18** was obtained (Figure 2.21, b).<sup>[53]</sup>

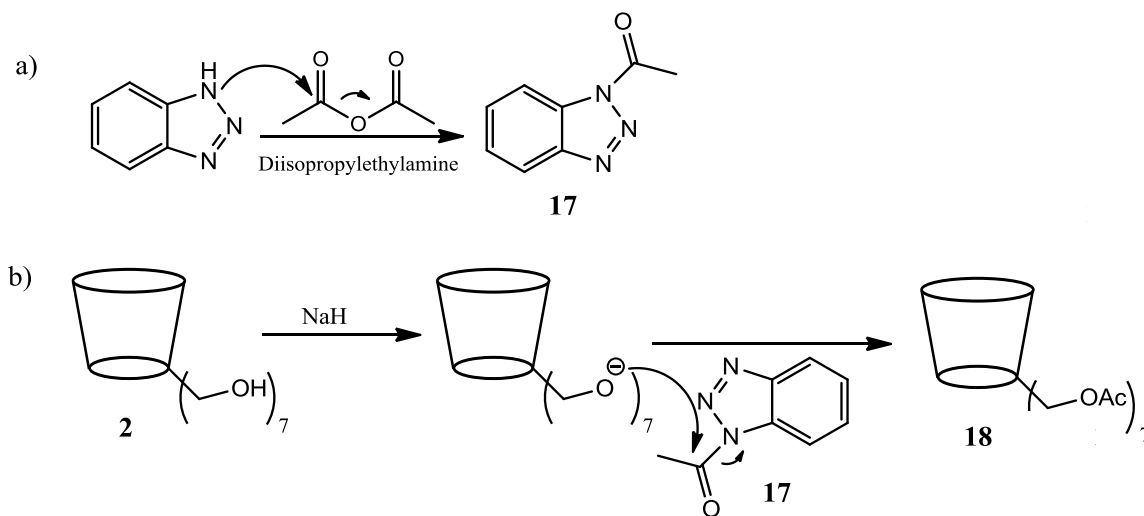


Figure 2.21: a) Synthesis of *N*-acetylbenzotriazole (**17**), b) Mechanism of acetylation reaction with benzotriazole as transfer agent of the acetyl group.

The first attempt to the peracetylation at C<sub>6</sub>-OH was performed with 14 equivalents of **17** and the reaction run during 24 h (**18**). In the <sup>1</sup>H-NMR spectrum, in D<sub>2</sub>O, it was observed the signal correspondent to the resonance of methylic protons at 2.0 ppm.<sup>[46, 53]</sup> The mass spectrum (MALDI-TOF) showed that the product is acetylated at eleven positions, but the major product has seven and eight acetyl groups. Another entry was performed with 2 equivalents of **17** with time reaction of 2 h in order to achieve mono-substitution at C<sub>6</sub> and obtain the 6-monoacety- $\beta$ -CD (**19**). Figure 2.22 is <sup>1</sup>H-NMR spectrum of the compound obtained (**19**) and in the MALDI-TOF spectrum it was possible to observe that the product is acetylated mostly in one and two positions. The yields were not calculated because the significant quantity of benzotriazole present in the final product.

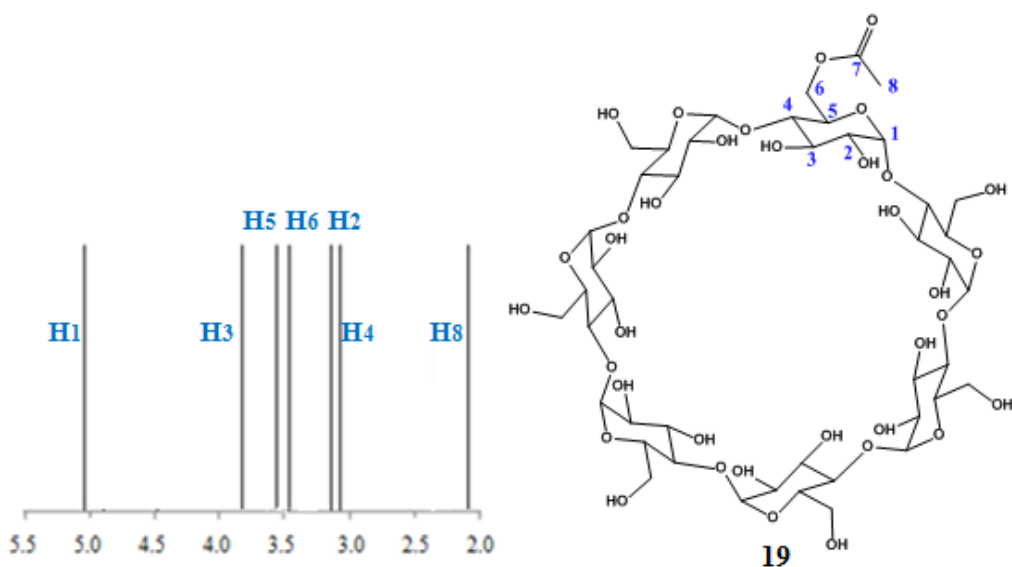


Figure 2.22: Structure of compound **19** and representation of chemical shift..

Table 2.4 summarizes the conditions and the products obtained by this method.

Table 2.4: Conditions of the reactions with *N*-acylbenzotriazole and products obtained

Compounds	N <sup>o</sup> equivalents of 17	Time of reaction (h)	Mass Spectrum (m/z)
<b>18</b>	14	24 h	1451.5 (9 acetyl groups), 1535.5 (8 acetyl groups).
<b>19</b>	2	2 h	1199.2 (1 acetyl group), 1241.2 (2 acetyl groups).

This method needs to be optimized in two aspects: first, to improve reaction time and the number of equivalent of reagent; and second, improve the product isolation and separation from the benzotriazole ring. At the end of reaction the benzotriazole is released but difficult to isolate from the product due to similar solubility. One purification method tested was through a reverse phase column chromatography RP-18 with eluent H<sub>2</sub>O: MeOH (10:1), but the separation was not efficient, since the retention time of the compound and the benzotriazole in RP-18 is very similar. Another technique used was the process of ultrafiltration (UF). The UF is characterized by a membrane pore size between 2 nm and 0.05 μm and operating pressures between 1 and 10 bar.<sup>[57, 58]</sup> UF can be used to separate macromolecules (β-CD) from small molecules (benzotriazole), hence it is a method with potential to isolated the peracetylated-β-CD (**18**). Figure 2.23 shows a

scheme of UF and the cell used in the process.<sup>[59]</sup> The membrane used had a pore size of 1000 atomic mass units (daltons). By performing successive washes with H<sub>2</sub>O, compound **18** was retained in the membrane since it has a molecular weight of 1428.44 g/mol, while the benzotriazole crosses the membrane (119.12 g/mol). The number of washing operations was controlled by TLC, observing the presence of benzotriazole in UV lamp. However, the yield of this purification was low. In the future, in order to optimize the purification method, a membrane with a pore size of less than 1000 Da will be used to ensure that the peracetyl- $\beta$ -CD does not cross the membrane and no losses will be observed.

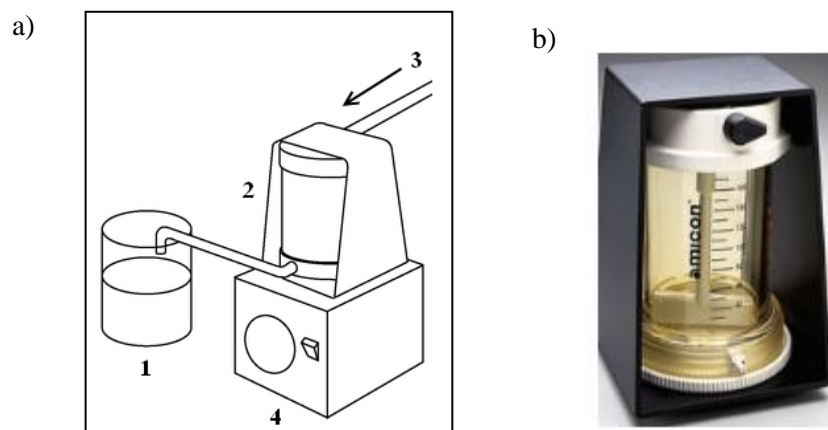


Figure 2.23: a) Scheme of membrane for UF. 1-Ultrafiltrate, 2-UF equipment, 3-Pressure supply. b) UF equipment.<sup>[59]</sup>

## 2.4 Polymerization

### 2.4.1 Synthesis of CD-MAA-PNIPAAm co-polymer in scCO<sub>2</sub>

The previously synthesized compounds **10**, **11** and **12**, shown in Figure 2.24, were co-polymerized in scCO<sub>2</sub> with the functional monomers methacrylic acid (MAA), a pH sensitive monomer and *N*-isopropylacrylamide (NIPAAm), a temperature sensitive monomer.<sup>[60]</sup> Ethyleneglycol dimethacrylate (EGDMA) was used as crosslinker and azobisisobutyronitrile (AIBN), as the radical initiator.<sup>[61]</sup> In a typical polymerization 3.81 mmoles of a mixture of functional monomers the MAA and NIPAAm are in the proportion of 1:3,<sup>[62]</sup> the compounds **10**, **11** and **12** are in 2.5% molar and the EGMA is in 1% molar, with respect to the total molar amount of functional monomers and crosslink (Figure 2.25). A co-polymer with 8.8 % molar of compound **11** was also prepared in order to study the effect of the CD content in the co-polymer. The AIBN is in 1 wt%, with respect to the total mass of MAA, NIPAAm and EGDMA.

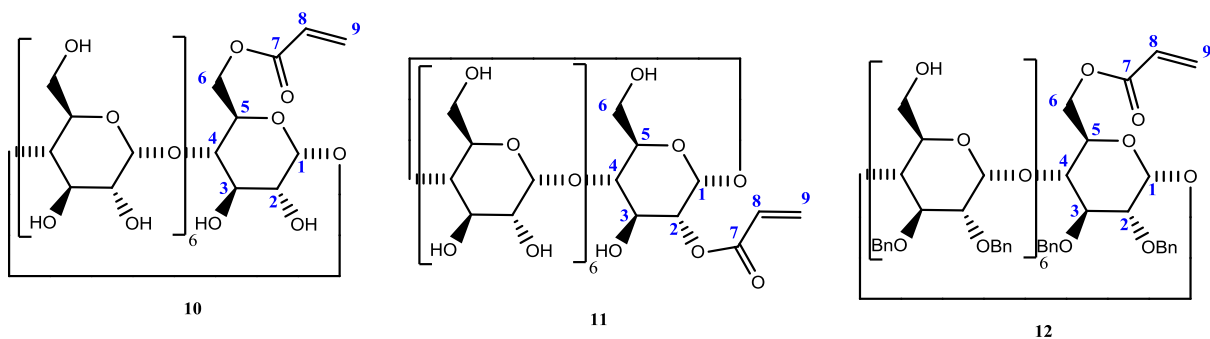


Figure 2.24: Synthesized  $\beta$ -CDs that were co-polymerized in scCO<sub>2</sub>.

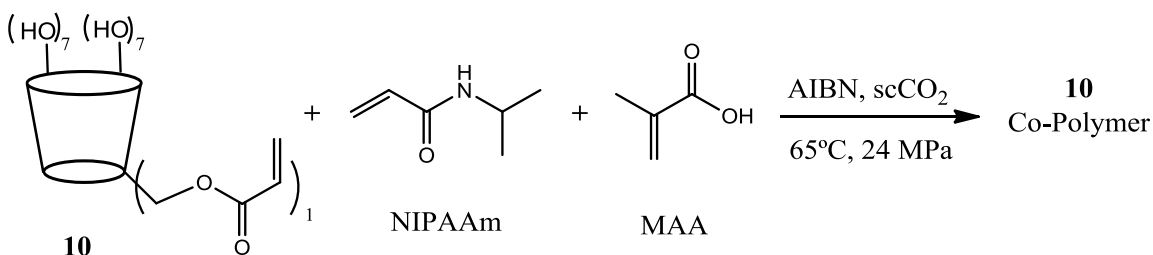


Figure 2.25: Scheme of the co-polymerization reaction.

The co-polymerization reactions were performed in a high pressure apparatus already existing in the host laboratory as described elsewhere<sup>[28]</sup> and schematically presented in Figure 2.26.

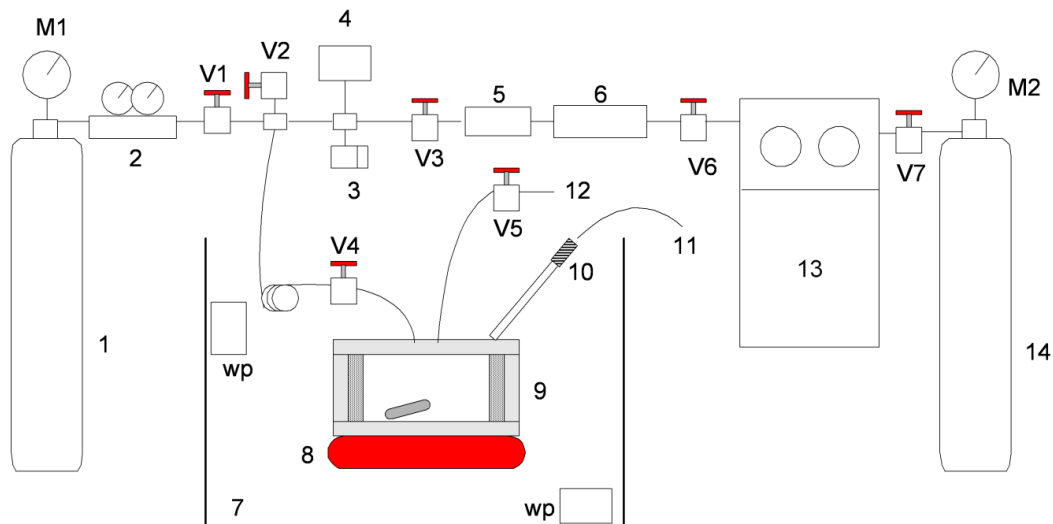


Figure 2.26: Schematic representation of equipment used in polymerization reaction and impregnation. 1- Nitrogen cylinder; 2-Gas regulator; 3-Rupture disc; 4- High-pressure manometer; 5- Check-valve; 6- Line filter; 7-Water bath; 8-Immersible stirrer; 9-High pressure cell; 10- Platinum resistance RTD probe; 11- Temperature controller; 12-Vent; 13- Pneumatic CO<sub>2</sub> compressor; 14- CO<sub>2</sub> cylinder; M1,M2- bourbon manometers; wp-water recirculation pump; V1 to V7- HIP valves.

The polymerization reaction was performed in scCO<sub>2</sub> in a stainless steel high-pressure cell at 65 °C and 24 MPa, for 24 h.<sup>[61]</sup> The cell is equipped with two aligned sapphire windows, which allow full observation of the reaction mixture during the polymerization and assure that a homogeneous phase is attained at the beginning of the reaction. At the end of the reaction the system is quickly depressurized, and the polymer is collected inside the cell.

## 2.4.2 Characterization of polymers

The synthesized polymers were obtained as white, dry, free flowing powders at the end of the reaction as it can be seen in Figure 2.27.



Figure 2.27: Appearance of the co-polymer obtained.

Figure 2.28 shows scanning electron microscope (SEM) images of compound **10** (A) and of the synthesized co-polymers (B, C, and D). As it can be seen in Figure 2.28A the compound **10** appears as irregularly shaped crystals. The co-polymers of respective compounds **10** (B), **11** (C) and **12** (D) are very homogeneous in terms of particle size, with slightly agglomerated discrete particles sizing less than 1  $\mu\text{m}$ . It seems that the nature of the CD in the co-polymer does not interfere much in the morphology of the co-polymers. Another type of structural characterization that could have been made was the measurement of porosity of the co-polymers, since the molecular-sized pores have a great influence in the capacity of absorption and liberation of a drug. However, this was not possible in this thesis due to the little amount of polymer samples available.

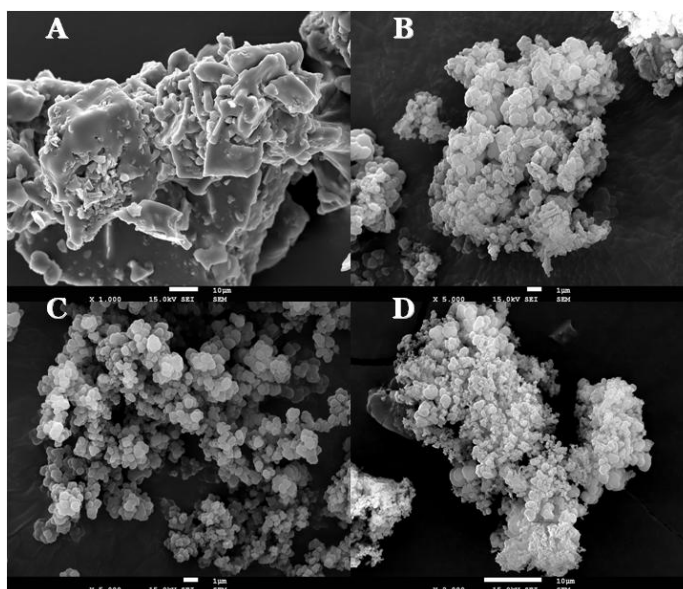


Figure 2.28: SEM images of: A - compound 10; B - NIPAAm-MAA-EGDMA co-polymer 10; C- NIPAAm-MAA-EGDMA co-polymer 11; D - NIPAAm-MAA-EGDMA co-polymer 12.

The major problem faced in the structural characterization of the synthesized co-polymers by NMR was their low solubility in organic solvents and water, as expected due to crosslinking. Several studies of solubility in mixed solvents were realized and only a small amount was dissolved being in the limits of detection of NMR in solution. An alternative was to characterize the polymers by High Resolution Magnetic Angle Spinning (HR-MAS), a well developed NMR technique that offers many possibilities to further investigate samples between the liquid and the solid state.<sup>[63]</sup> The structural framework required an intensive study of the appropriate parameters (pulse sequence, spectral window, acquisition time, mixing time) to allow structural assignment of the  $\beta$ -CD co-polymers.



In the  $^1\text{H}$  HR-MAS NMR of co-polymer of compound **10** was not possible to observe the resonance signals of double bond protons between 5.5-6.4 ppm, which means that the polymerization was initiated there and all the double bond reacted. In 2D spectra only the NOESY spectrum gives relevant information, since it is possible to observe interaction between the protons of polymer and the protons  $\text{H}_5$  and  $\text{H}_3$  of the cavity of  $\beta$ -CD (Figure 2.29). The polymer in NOESY spectrum does not show correlations with the protons outside the cavity of  $\beta$ -CD, probably due to distances higher than 6 Å, which is the limit of detection of interaction in NOESY experiment.

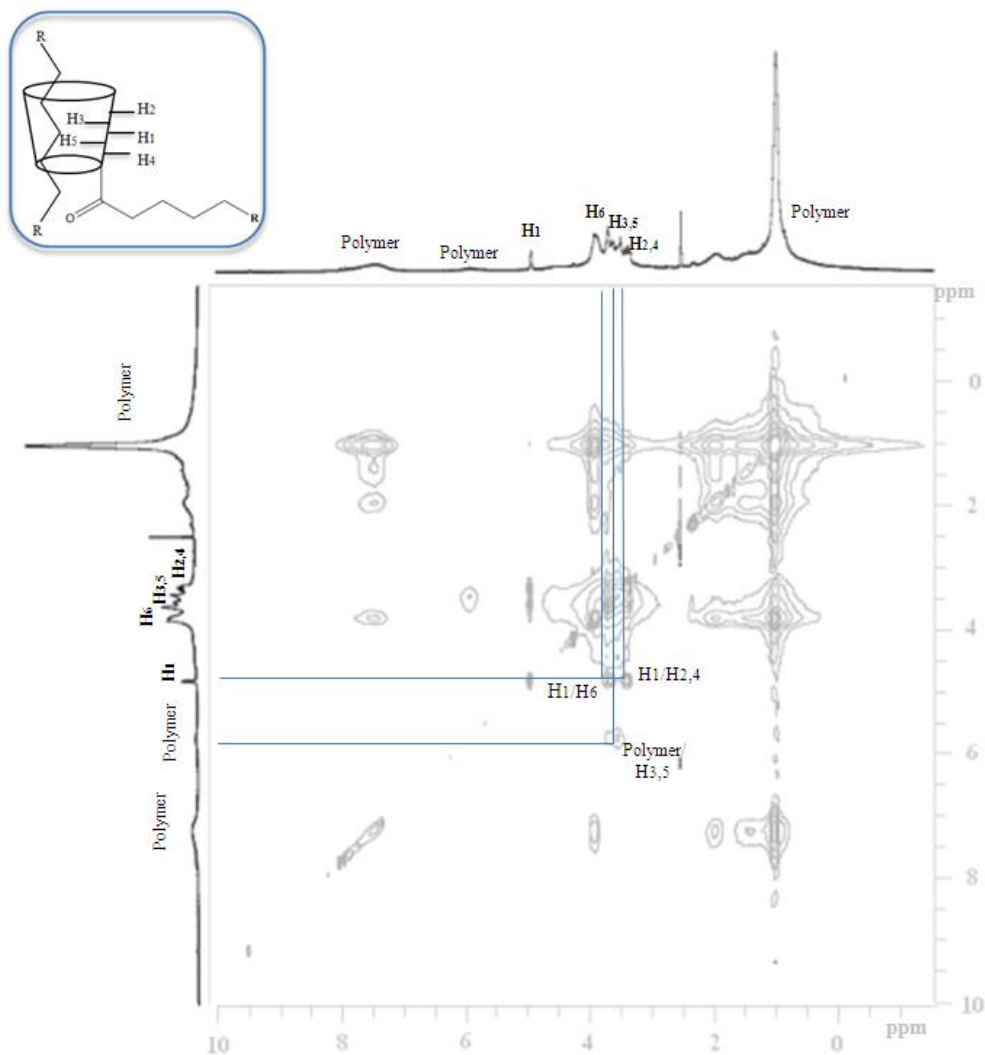


Figure 2.29: NOESY HR-MAS NMR spectrum and representation of co-polymer of compound **10**.

The co-polymer of compound **11** presents a  $^1\text{H}$  HR-MAS NMR where signals of double bond protons are observed, meaning that not all the acryloyl group led to a starting point for co-

polymerization. In the NOESY HR-MAS NMR spectrum interaction between the polymer chain and the proton H<sub>3</sub> or H<sub>5</sub> of the β-CD cavity can be observed.

In <sup>1</sup>H HR-MAS NMR spectrum of the polymer of compound **12**, the due to the presence of multiple aromatic rings, the signals of aromatic protons do not allow the observation the signals of double bound protons. The interaction between the protons of polymer and the CH<sub>2</sub> of benzyl group, in the NOESY HR-MAS NMR spectrum confirms that the polymer crosses the β-CD cavity.

In literature three types of β-CD polymers are described: catenanes - molecules that contain two or more interlocked ring (Figure 2.30, **A**); rotaxanes which are macrocycles trapped on the ends with compounds larger than the internal diameter of the ring, to prevent the disassociation of the components (Figure 2.30, **B**); and the pseudorotaxanes that are similar to the rotaxanes but with or without groups at the end (Figure 2.30, **C**).<sup>[15, 64, 65]</sup> In the characterization of co-polymers by HR-MAS NMR it was observed the interaction between the polymer and the protons of the cavity of β-CD, which means that our co-polymers can be characterized as pseudo-polyrotaxanes.

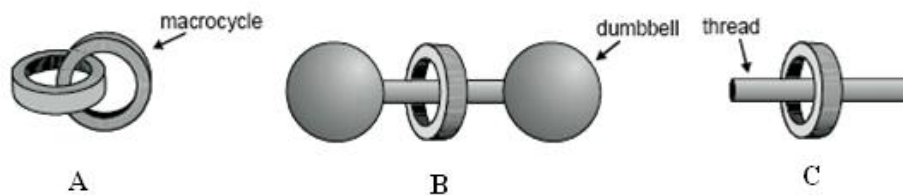


Figure 2.30: Types of β-CD polymer: A-catenanes, B-rotaxanes and C-pseudorotaxanes.<sup>[64]</sup>

Another technique of structural characterization used was the X-Ray Diffraction (XRD). Figure 2.31 shows XRD of the synthesized co-polymer with and without the derivate of β-CD and the compound **10**. As it can be seen and as expected in a polymerization in scCO<sub>2</sub>, the polymer is completely amorphous. The compound **10** shows a quite crystalline pattern. This compound was dissolved in scCO<sub>2</sub> and precipitated in order to be compared with the polymers processed in scCO<sub>2</sub>. The pattern suggests that compound **10** maintained a crystalline structure even after being processed in scCO<sub>2</sub>. The co-polymer from compound **10** shows a quite amorphous structure. However, it presents two sharp peaks at two predominant diffraction peaks located at 22° and 31° of 2θ. This suggests that some polymer parts are crystalline, probably due to the presence of derivate **10**, since these peaks are also in the compound **10** pattern. Nevertheless, these peaks show a slight shift which suggest that a new entity was formed (in this case the co-polymer) and it is not a physical mixture.

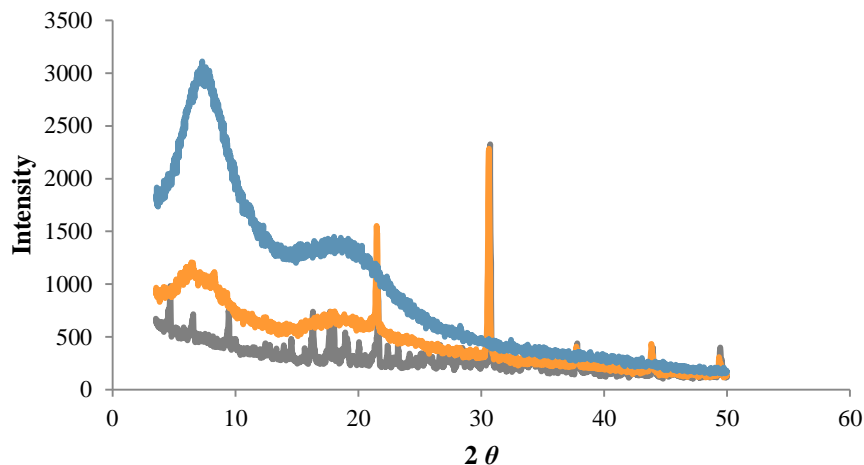


Figure 2.31: XRD of P(NIPPAAm-MAA) (blue), P(NIPAAm-MAA-**10**) co-polymer (orange) and compound **10** (gray).

Figure 2.32 shows the XRD of the synthesized polymer with and without the derivate of  $\beta$ -CD and the compound **11**. As it can be seen this polymer is also completely amorphous. The pattern of the **11** is typical of a crystalline structure. The resultant co-polymer also shows an amorphous structure. The pattern shows some low intensity peaks which are in accordance with the existence of crystalline parts of the co-polymer. The pattern of the polymer does not correspond to the sum of the patterns of the **11** and the polymer without  $\beta$ -CD, meaning that the co-polymer **11** it is a new entity.

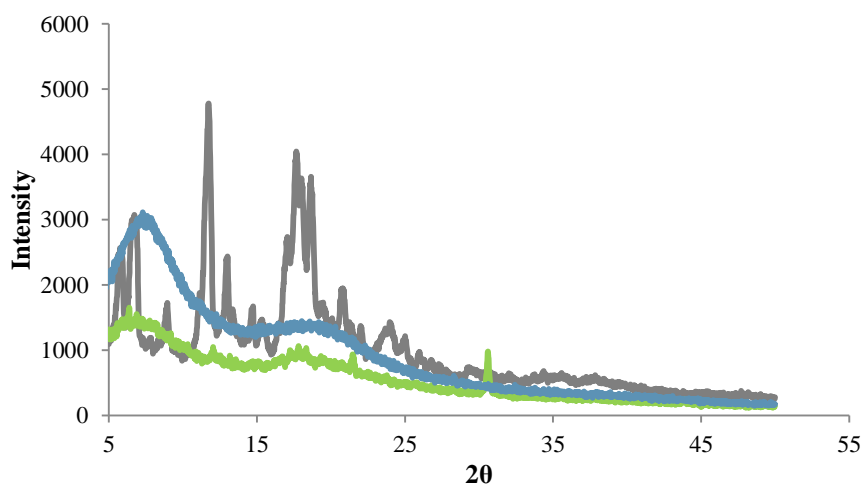


Figure 2.32: XRD of P(NIPPAAm-MAA) (blue), P(NIPAAm-MAA-**11**) co-polymer (green) and compound **11** (gray).

Swelling tests were performed to the synthesized co-polymers at different pHs (Figure 2.33). The polymer showing higher swelling is the one without  $\beta$ -CD. These results suggest that the introduction of the CDs in the co-polymer can decrease the flexibility of the polymeric chains in solution. A possible explanation is an increase of the crosslink degree or the interference of the  $\beta$ -CD in the interchain interactions of the pH responsive backbones of the polymer. From the polymers containing  $\beta$ -CD the co-polymer prepared using the  $\beta$ -CD with the acrylated functionalization inside the cavity, compound **11**, shows a slightly higher swelling.

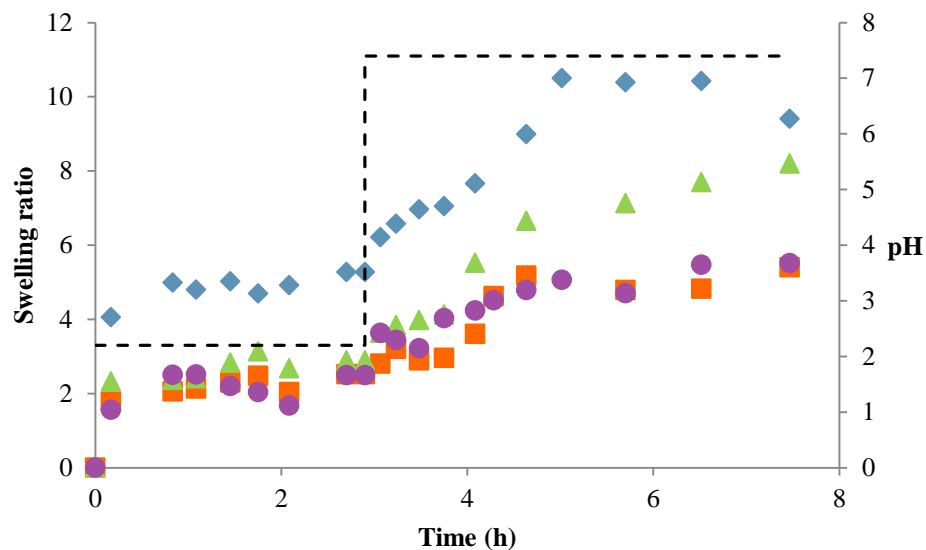


Figure 2.33: Swelling of co-polymers at two different pHs 2.2 and 7.4. P(NIPAAm-MAA) (blue), P(NIPAAm-MAA-**10**) co-polymer (orange), P(NIPAAm-MAA-**11**) co-polymer (green) and (NIPAAm-MAA-**12**) (purple).

The pH responsive character of the polymers can be easily seen in Figure 2.34, where the water uptake and swelling is quite visible.

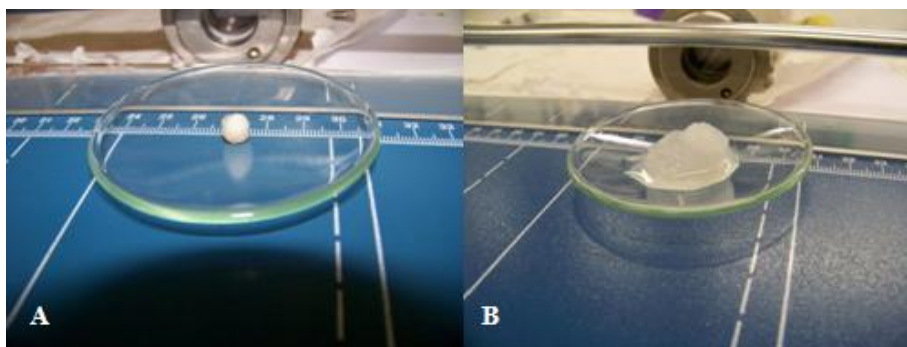


Figure 2.34: Test of swelling. A-(pH2.2); B-(pH7.4).

After co-polymerization of the derivatives of  $\beta$ -CD (**10**, **11** and **12**) and in order to test the polymeric materials as drug delivery devices, the co-polymers were impregnated with a drug using a  $scCO_2$ -assisted method. Metronidazole (Figure 2.35) is an antibacterial drug and it is used in combination with other antibiotics.<sup>[66]</sup> It was chosen drug because its solubility in solution is independent on pH.<sup>[67]</sup> This is important because the release profiles obtained will be only dependent on the co-polymer itself and not on the drug solubility at the different studied pHs. Additionally this drug is soluble in  $scCO_2$ .<sup>[68]</sup>

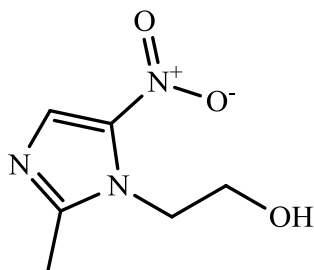


Figure 2.35: Structure of metronidazole.

The impregnation of metronidazole was undertaken in a cell similar to the one used in the polymerization, with an inner porous support which divides the cell in two compartments, as it can be seen through the sapphire window of the cell shown in Figure 2.36. This prevents physical contact between the drug and the co-polymers that could interfere in the impregnation process.

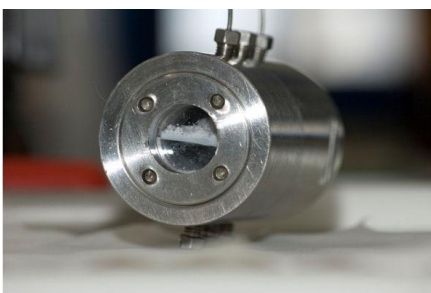


Figure 2.36: High-pressure cell used for impregnation.

The drug was placed in the downer compartment, under the porous support with a magnetic stirring bar, and in quantity enough to obtain a saturated solution at 65°C and 24 MPa. The co-polymers were loaded into cellulose membranes which were placed in the upper compartment of the cell. After 24 h, the system was quickly depressurized.

After impregnation with metronidazole, *in vitro* drug release experiments were performed, in order to evaluate the performance of the cyclodextrin-hydrogel system as drug release device at

pH 2.2, to simulate the gastric conditions and at pH 7.4 to reproduce the colon environment. The co-polymers were transferred to porous membranes and added to a buffer solution (pH 2.2 and 7.4) at controlled temperature 37°C. Aliquots were withdrawn at time intervals and the same volume of fresh medium was added to the solution. Quantification was performed by making a calibration curve in a spectrophotometer (Perkin Elmer, Lambda 25) at 265 nm (pH 2.2) and 318 nm (pH 7.4) and the total mass released was determined considering the aliquots and the dilution produced by addition of fresh buffer solution.

Table 2.5 summarizes the impregnation loading obtained for each polymer using the supercritical assisted method.

Table 2.5: Polymer loading during scCO<sub>2</sub>-assisted impregnation with Metronidazole.

Entries	Compounds	Metronidazole loaded (mg/g)*
1	Poly	7.85
2	Co-polymer 10 (2.5%)	6.69
3	Co-polymer 11 (2.5%)	11.30
4	Co-polymer 12 (2.5%)	3.54
5	Co-polymer 11 (8.8%)	21.04

\* wt Metronidazole (mg) with respect to the co-polymer sample (g).

The impregnation in scCO<sub>2</sub> depends mainly in the high scCO<sub>2</sub> diffusivity within the polymer structure, swelling and drug solubility, and has two contributions: the impregnation within the polymeric chains and into the β-CDs cavities.<sup>[69]</sup> As it can be seen by comparing entries 3 and 5 of Table 2.5 corresponding to the same co-polymer but with different percentages of β-CD. The increase of the β-CD content leads to a very significant increase of the loaded drug. This could be explained by the accessibility of part of the β-CD cavities since probably not all cavities have polymeric chains passing through. Also the polymer that has the wider opening of the β-CD obstructed by voluminous groups (co-polymer **12**) presents the lowest metronidazole loading, even less than the polymer without CDs. This fact could be explained by the inaccessibility of the cavities as well as to different intermolecular interaction within the polymer due to the lack of hydroxyl groups available at the CD to establish hydrogen bonding. This can lead to different polymer conformations and also to different porosities that influence the impregnation.

These differences are difficult to explain since one may expect that similar drug loads would be obtained due to the high diffusivity of CO<sub>2</sub> within similar polymeric matrixes. However as it was already discussed above, these polymers can have different porosities, which can greatly interfere with the accessibility of the drug into the copolymer. Additionally the different swellings of the matrixes in scCO<sub>2</sub> have to be taken into account, which study was not in the scope of this thesis but is known to greatly influence the impregnation in scCO<sub>2</sub>.

After the impregnation the pressure is rapidly decreased leading to a sudden change in the medium density and in all the properties density-dependent as solubility, thus the drug stays entrapped in the polymeric net whereas the CO<sub>2</sub> is released as a gas.

Figure 2.37 presents the *in vitro* drug release of metronidazole from the different synthesized co-polymers for a period of 5 h at pH 2.2 (A) and pH 7.4 (B). Figure 2.37A shows the percentage of drug released at pH 2.2 where it is possible to see that polymers of **10** and **12** have similar behavior to the polymer without β-CD, releasing almost all the drug in the first hour. Polymer **11** shows a more controlled release, since at the end of the first hour only 60% of the metronidazole was released and after 3 h the maximum was achieved, although not reaching a complete release. Figure 2.37B represents the behavior of the co-polymers at pH 7.4 where it is possible to observe that polymer of **11** was the one that released the drug more quickly, 80% after 30 min and 100% after 1 h. Polymers **10** and **12** released the maximum metronidazole in approximately 2 h, while polymer **10** releases the drug in a slightly more controlled way: after 1 h only 70% of the metronidazole was release, and after 5 h 85-90% of the drug was liberated.

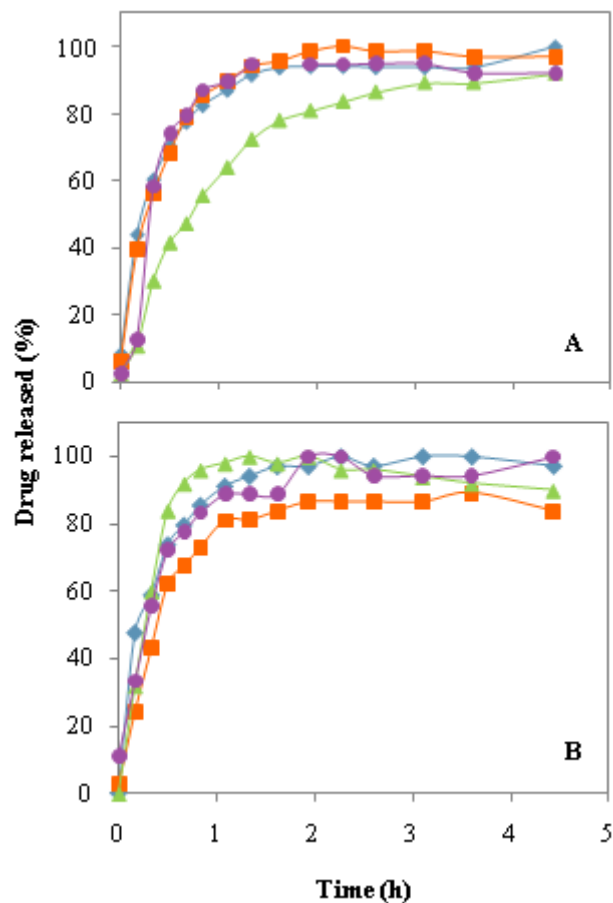


Figure 2.37: Drug release from the synthesized P(NIPAAm-MAA) (blue), P(NIPAAm-MAA-10) co-polymer (orange), P(NIPAAm-MAA-11) co-polymer (green) and (NIPAAm-MAA-12) (purple) at pH 2.2 (A) and pH 7.4 (B).

From these results it is possible to conclude that the polymer synthesized with compound **11**, is the only one that shows some of the expected pH responsiveness trend. At pH 2.2 the release is slower and at pH 7.4 presents the highest release of all the polymers. This behavior suggests that probably the polymeric MAA backbone (pH sensitive) of the polymer is available to interact with the medium, inducing changes in the polymer conformation. The co-polymer **11** showed a higher swelling than the other polymers at pH 7.4 meaning that at this pH condition the polymeric matrix is more hydrated, thus the drug diffusion from the matrix is likely to be slightly more rapid.

In the swelling test it was possible to observe that the presence of  $\beta$ -CD decreases the swelling of the co-polymer and that different swellings are obtained at the different pHs, thus being sensitive to the pH.



Since the co-polymer of compound **11** shows the better swelling, was the co-polymer that impregnated more drug and have a significant response at different pHs, this was the co-polymer chosen to repeat the polymerization reaction with a higher percentage of compound **11**, 8.8 % (molar). Figure 2.38 compares the release of metronidazole from the polymers with 2.5% and 8.8% of compound **11**. At pH 2.2 the polymers with 2.5% and 8.8% of **11** have a similar drug release profiles (Figure 2.38, A) not achieving 100% of metronidazole release. At pH 7.4 the polymer with 2.5% of **11**, released 75% of the drug after one hour achieving its maximum in 4 h while polymer with 8.8% of **11** presented a very different behavior (Figure 2.38, B). The polymer with 8.8% of **11** has a significant controlled drug release, only 30% of the metronidazole was released after one hour, 60% were released after three hours and the maximum release is achieved only in nine hours. According to the observed result with 2.5%  $\beta$ -CD, this result was unexpected. This strongly suggests that when the percentage of  $\beta$ -CD is increased more  $\beta$ -CDs are available, free cavities and external hydroxyl groups, within the polymer.

Moreover, as it can be seen in Figure 2.39 the drug release is more sustained at the highest pH, achieving the maximum release in 8 h while at pH 2.2 this maximum is achieved around 3 h. This behavior can also be explained by the pKa value of the  $\beta$ -CD (12.2)<sup>[15]</sup> and of metronidazole (16.0)<sup>[70, 71]</sup>. At pH 2.2 both the CD and the drug are totally protonated. At pH 7.4 both the CD and the drug are neutral thus are available to establish hydrogen bonding interactions between them. Therefore the polymer has the capacity to establish hydrogen bonding with the drug at the highest pH, and thus leads to a more sustained release of the drug. This controlled release at pH 7.4 suggests a new application for this material as parenteral rectal delivery device.

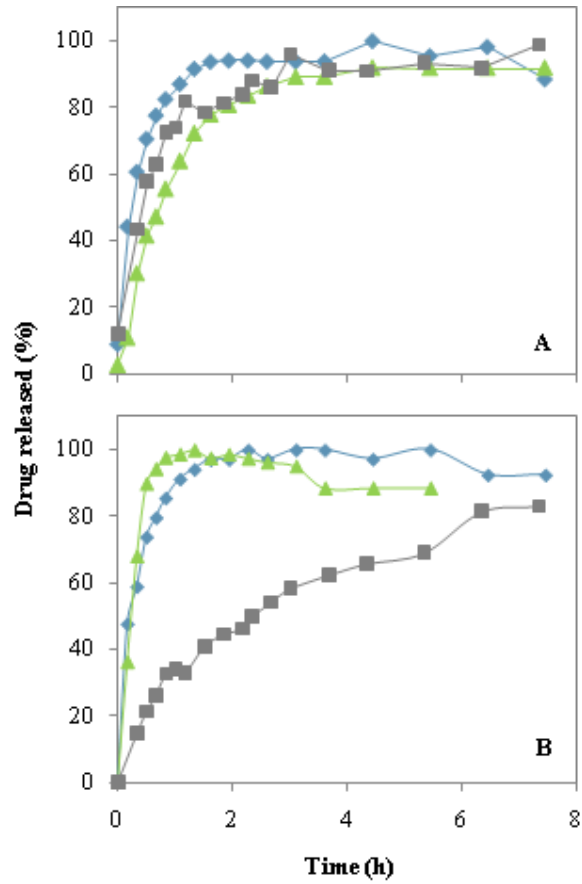


Figure 2.38: Drug release from the synthesized P(NIPAAm-MAA) (blue), P(NIPAAm-MAA-11) co-polymer with 2.5% (green) and P(NIPAAm-MAA-11) co-polymer with 8.8% (gray) at pH 2.2 (A) and pH 7.4 (B).

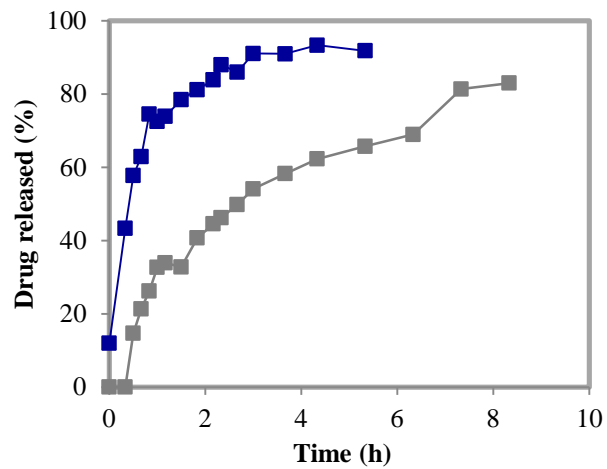


Figure 2.39: Drug release from the synthesized P(NIPAAm-MAA-11) co-polymer with 8.8% at pH 2.2 (blue) and P(NIPAAm-MAA-11) co-polymer with 8.8% at pH 7.4 (gray).

Figure 2.40 shows one of the co-polymers in water. As it can be seen, the polymer shows a significant temperature responsive behavior, although it would be expected that the co-polymer with the ratio 25:75 (MAA:NIPPAm) would exhibit a strong pH responsiveness but would not be temperature dependent.<sup>[62]</sup> Nevertheless, the polymers reported in literature were synthesized by conventional methods. In this case different interactions are established during polymerization and consequently different polymer conformations can be obtained which obviously can lead to different polymer-solvent interactions during the drug release experiments. From Figure 2.40 it is obvious that the co-polymers show a LCST (lower critical solution temperature), which was not determined in this work. It is clear that at room temperature the polymeric chains are completely free to establish hydrogen bonding with water, although it does not dissolve due to crosslinking. At higher temperature (Fig 2.40, B at 45°C) the co-polymer chains are collapsed due to the disruption of these bonds, so the polymer shrinks.

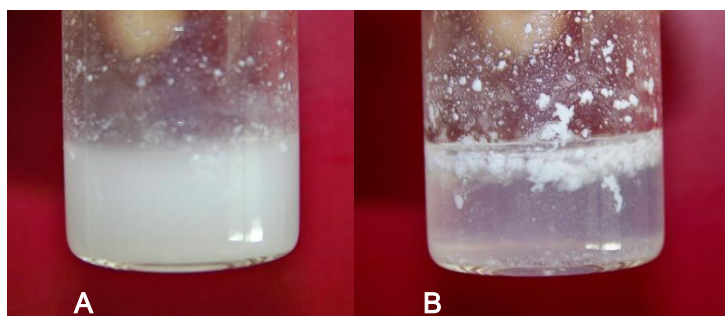


Figure 2.40: Temperature test of co-polymers A- 23°C, B- 45°C.

In the swelling test it was observed that the presence of  $\beta$ -CD units decreases the swelling of the co-polymer and that this is sensitive to the pH. The metronidazole was impregnated in the co-polymers and the one that had more capacity to permeate the drug was the co-polymer of **11** (2-monoacryloyl- $\beta$ -CD, 2.5%). This result is in accordance with the fact that this polymer presented a better swelling.

## 2.5 Final Conclusions

The purpose of this study was to synthesize polymerizable CDs in order to develop new CD-hydrogel systems in scCO<sub>2</sub> for pH-responsive drug delivery.

The first part of this thesis consisted on the synthesis of polymerizable  $\beta$ -CD, by functionalization of  $\beta$ -CD with a group that allows the polymerization (activated double bonds). This was the first challenge of this work, since the reactions performed had low yield, and were difficult to reproduce in a large scale. Moreover, for the co-polymerization reactions using supercritical fluid technology, high amounts of these compounds were needed. Thus, three functionalized  $\beta$ -CDs were prepared by different synthetic sequences: 6-monoacryloyl- $\beta$ -CD (**10**), 2-monoacryloyl- $\beta$ -CD (**11**) and 6-monoacryloyl-heptakis-(2,3-di-*O*-benzyl)- $\beta$ -CD (**12**). The 6-monoacryloyl- $\beta$ -CD (**10**) was obtained *via* 6-monotosyl- $\beta$ -CD, while the 2-monoacryloyl- $\beta$ -CD (**11**) was prepared by direct acrylation using acryloyl chloride. For the 6-monoacryloyl-heptakis-(2,3-di-*O*-benzyl)- $\beta$ -CD, a longer synthetic sequence was needed, the primary hydroxyl groups was first protected by silylation and the secondary hydroxyl groups was then benzylated. Removal of the silyl groups and subsequent direct acrylation afforded the final functionalized  $\beta$ -CD. The 6-monoacryloyl- $\beta$ -CD (**10**) was obtained with a yield of 17 %, while the 2-monoacryloyl- $\beta$ -CD (**11**) with 94 % and the 6-monoacryloyl-heptakis-(2,3-di-*O*-benzyl)- $\beta$ -CD (**12**) with 21 %. Compounds structures were confirmed by NMR, IR and MS by MALDI-TOF technique.

The second part of this work consisted in the synthesized CD-co-polymers for a pharmaceutical targeted application. The polymerizable  $\beta$ -CD derivatives previously prepared were co-polymerized with functional monomers using a clean technology, supercritical fluid technology. The characterization of these materials were difficult, mainly due to the co-polymers have low solubility as a consequence of crosslinking. Through HR-MAS NMR, structural information about the co-polymers, were obtained being observed that polymeric chains interact with the  $\beta$ -CD cavity, what strongly suggest the formation of supramolecular structures: pseudo-polyrotaxanes.

Moreover, supercritical fluid technology was found to be a suitable “green” process to impregnate polymeric materials with a drug. The impregnation degree was affected by the percentage of  $\beta$ -CD units present in the polymer and by the different positions of the  $\beta$ -CD where polymerization occurred (related to the position in which acrylation took place in the CD).

From the studied co-polymers with  $\beta$ -CD derivates, co-polymer **11** demonstrated a higher capacity to impregnate the drug. The results showed that co-polymer of compound **11** (2.5 %) had

a better controlled drug release, at pH 2.2, when compared to the other co-polymers. Increasing the percentage of compound **11** (8.8 %) in the co-polymer led to improved control of drug release, at pH 7.4. This result suggests that the amount of  $\beta$ -CD present in the co-polymer might be crucial for the co-polymer performance. Co-polymer **12**, despite the steric hindered cavity, was still capable to impregnate some drug. The results indicate that the  $\beta$ -CD cavity might not be the only factor influencing the interaction between  $\beta$ -CD and the drug.

The materials produced showed some pH-responsiveness, being quite promising in the development of co-polymers for controlled drug administration. The results obtained indicate that co-polymer with 2.5 % of compound **11** would be more suitable for oral administration, while the co-polymer with 8.8 % of compound **11** might be preferred for parenteral administration.

The research area covered in this thesis is quite vast, ranging from organic chemistry to chemical engineering and material's characterization. The co-polymerization using supercritical fluid technology involved a completely different type of experimental approach. In addition, the final characterization of the polymers was complex and difficult, as the co-polymers were crosslinked and built with four monomers, influencing the final properties of the co-polymer. The homogeneity of the assembling during polymerization also affected these properties.

The work developed in this Master thesis is a good starting point for the study of these complex supramacromolecular structured materials. Such materials have huge potential in the pharmaceutical and biomedical areas, where the supercritical fluid technology can have a real impact in the materials purity and in the processes sustainability.



### **3. Experimental Part**

### 3.1 Preamble

The experimental part of this work involves the applications of some general procedures that will be described next:

- Usual work-up implies drying the water- or brine-washed organic extracts over anhydrous sodium sulfate or magnesium sulfate, followed by filtration and evaporation of the solvent from the filtrate under reduced pressure. Anhydrous solvents were dried as described<sup>[72]</sup> and freshly distilled.
- Thin-layer chromatography was performed on Merck silica gel 60 F254 plates and PTLC on 0.5 mm thick plates. Column chromatography was carried out on Merck silica gel 60 (70–230 mesh).
- IR spectra were run on a FT Perkin–Elmer 683 instrument, with absorption frequencies expressed in reciprocal centimeters.
- Ultraviolet-visible (UV-Vis) spectroscopy spectra were traced in spectrophotometer Perkin Elmer, Lambda 25.
- High resolution mass spectra (MS) were recorded on Mass Spectrometry Unit, University of Santiago of Compostela and Analyses Services MALFI-TOF-MS of the Chemistry Department, Faculty of Science and Technology, New University of Lisbon. In the description of the spectra data are presented in the following order: load mass ratio (m/z) assignment of a molecular fragment.
- In nuclear magnetic resonance spectroscopy (NMR) the equipment used to obtain the spectra <sup>1</sup>H-NMR, <sup>13</sup>C-NMR was the Bruker CXP 300 (400 MHz and 100 MHz respectively).
- In high resolution magnetic angle spinning (HR-MAS) the equipment used to obtain spectra <sup>1</sup>H HR-MAS and <sup>13</sup>C HR-MAS was the Bruker Avance III (400 MHz and 100 MHz) respectively, with 4 mm triple resonance HR-MAS probe head at ambient temperature.<sup>2</sup> Samples were spun at the magic angle at a rate of 4.0 kHz in a rotor of 4 mm of zirconium with 50 µl of capacity, and all the spectra acquired under field-frequency locked conditions using that probe channel with the spectrometer's lock hardware. Spectra were processed using Bruker Topspin 2.1. The <sup>1</sup>H HR-MAS

---

<sup>2</sup> The NMR spectrometers are part of the National NMR Network and were purchased in the framework of the National Programme for Scientific Re-equipment, contract REDE/1517/RMN/2005, with funds from POCI 2010 (FEDER) and Fundação para a Ciência e a Tecnologia.



NMR were acquired between 4 and 6 seconds in 16 transients and a spectral width of *ca* between 5300 and 6200 Hz. The  $^{13}\text{C}$  HR-MAS NMR were acquired in 1.36 seconds in 16 transients and spectral width of 24000 Hz. NOESY experiments were acquired with 200 milliseconds mixing time in 16 transients with a relaxation delay of 2.0 seconds and a spectral width of *ca* 4100 Hz, in a total of 2 K data points in *F2* and 256 data point in *F1*. In the description of the spectra data are presented in the following order: deuterated solvent, chemical shift ( $\delta$ , in ppm), multiplicity of the signal (s – singlet, d- duplet, dd- duplet dupleto, m- multiplet), coupling constant (J in Hertz), identification of carbon and number of protons.

- X-Ray Diffraction (XRD): Diffractometers Phillips (2) (PW-1730/10 e X'Pert Pro)

## 3.2 Synthesis

### 3.2.1 Synthesis of compound 10 (6-monoacryloyl- $\beta$ -CD)

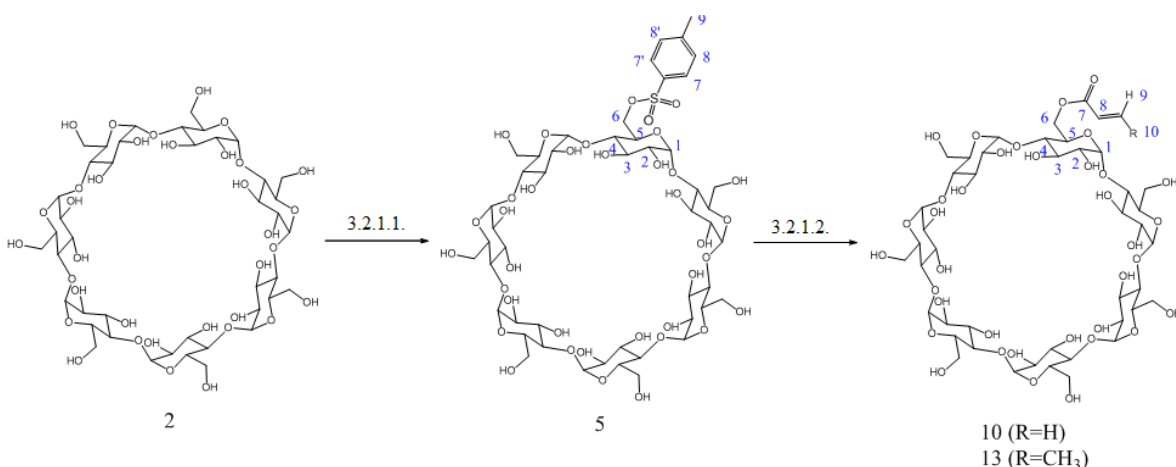


Figure 3.1: Synthetic scheme to obtain products **10** and **13**.

#### 3.2.1.1 Synthesis of 6-Monosyl- $\beta$ -cyclodextrin (5)

##### Method A <sup>[21]</sup>

$\beta$ -CD (2 g, 1.76 mmol) was dissolved in hot water at 80 °C, then cooled down to room temperature under vigorous stirring. *p*-Toluenesulfonyl imidazole (0.78 g, 3.51 mmol, 2 equiv.) was added as finely grounded powder, and the suspension was stirred for 2 hours (h). Sodium hydroxide (0.90 g, 37.5 mmol) was dissolved in water (2.5 mL) and the solution was added to the reaction mixture over a period of 20 minutes (min). After stirring for another 10 min, the mixture was filtered through a frit funnel. The reaction was quenched with ammonium chloride (2.41 g), and the solution was concentrated to about half of its volume. After stirring at 0 °C for 1 h, the precipitate was filtered, washed with water (2.5 mL), acetone (2.5 mL), and then dried in vacuum.  $\eta$ =19%.

##### Method B <sup>[19]</sup>

$\beta$ -CD (2 g, 1.76 mmol) was suspended in water (17 mL), and NaOH (0.22 g, 5.47 mmol) in water (6 mL) was added dropwise. The suspension became homogeneous and slightly yellow before the addition was complete. *p*-Toluenesulfonyl chloride (0.34 g, 1.78 mmol) in acetonitrile

(1 mL) was added dropwise, and a white precipitate was formed. After 2 h stirring at room temperature the precipitate was removed by suction filtration and the filtrate refrigerated overnight at 4 °C. The resulting white precipitate was recovered by suction filtration and dried in vacuum.  $\eta=10\%$ .

### Method C <sup>[20]</sup>

A suspension of  $\beta$ -CD (2 g, 1.81 mmol) and *p*-toluenesulfonic anhydride (0.88 g, 2.70 mmol), in water (44 mL) was stirred at room temperature for 2 h. An aqueous solution of NaOH (0.9 g, 9 mL) was added, and after 10 min unreacted *p*-toluenesulfonic anhydride was removed by filtration in vacuum. NH<sub>4</sub>Cl (1.26 g, 23.6 mmol) was added to the filtrate affording 6-monotosyl- $\beta$ -CD as a precipitate that was cooled at 4 °C overnight. The product was washed with cold water (to remove the salts), then with acetone. The product was obtained as a fine white powder after drying under high vacuum. **Compound 5:**  $\eta=21\%$ . <sup>1</sup>H-NMR ( $\delta_{\text{ppm}}$ , DMSO-d<sub>6</sub>): 7.49 (d, *J*= 8 Hz, H<sub>7,7'</sub>, 2H); 7.13 (d, *J*= 8 Hz, Ar-H, H<sub>8,8'</sub>, 2H); 5.69 (s, OH<sub>2,3</sub>, 14H); 4.84 (d, *J*=4 Hz, H<sub>1</sub>, 7H); 4.48 (s, OH<sub>6</sub>, 5H); 3.67 (m, H<sub>6,3</sub>, 21H); 3.56 (d, *J*=12 Hz, H<sub>5</sub>, 7H); 3.39 (s, H<sub>4</sub>, 7H); 3.29 (s, H<sub>2</sub>, 7H), 2.30 (s, H<sub>9</sub>, 3H). <sup>13</sup>C-NMR ( $\delta_{\text{ppm}}$ , DMSO-d<sub>6</sub>): 128.6 (C<sub>8,8'</sub>), 126.0 (C<sub>7,7'</sub>), 102.4 (C<sub>1</sub>), 82.0 (C<sub>4</sub>), 73.6 (C<sub>3</sub>), 72.9 (C<sub>2</sub>), 72.5 (C<sub>5</sub>), 60.4 (C<sub>6</sub>), 21.3 (C<sub>9</sub>). <sup>[19]</sup> ([Appendix 1](#))

### 3.2.1.2 6-Mono-acryloyl/methacryloyl- $\beta$ -CD (10/13) <sup>[48]</sup>

Methacrylic acid or acrylic acid (4.29 mmol), was added dropwise to an aqueous solution of CsOH (50%, 0.73 mL, 4.29 mmol), at room temperature. The mixture was stirred for 30 min, and concentrated under reduced pressure. The resulting salt was dissolved in dry DMF (5 mL) and 6-monotosyl- $\beta$ -CD (0.56 g, 0.43 mmol) was added. The resulting mixture was heated at 90 °C for 24 h. The reaction evolution was monitored by TLC (silica, MeCN:H<sub>2</sub>O: aqueous ammonia, 6:3:1). The mixture was allowed to cool to room temperature and washed with ethanol (2 x 38 mL) and ethyl ether (38 mL). This washing procedure was repeated twice.

Reaction with acrylic acid. **Compound 10:**  $\eta = 79\%$ . <sup>1</sup>H-NMR ( $\delta_{\text{ppm}}$ , D<sub>2</sub>O): 7.49 (d, *J*= 8 Hz, H<sub>7,7'</sub>, 2H); 7.13 (d, *J*= 8 Hz, Ar-H, H<sub>8,8'</sub>, 2H); 6.07 (dd, *J*= 8-24 Hz, H<sub>10</sub>, 1H); 5.97 (d, *J*= 4 Hz, H<sub>8</sub>, 1H); 5.63 (d, *J*= 8 Hz, H<sub>9</sub>, 1H); 5.06 (s, H<sub>1</sub>, 7H); 3.91 (dd, *J*= 4-20 Hz, H<sub>3</sub>, 7H); 3.82 (s, H<sub>6</sub>, 7H); 3.73 (s, H<sub>5</sub>, 7H); 3.63 (dd, *J*= 4-8 Hz, H<sub>4</sub>, 7H); 3.57 (dd, *J*= 8-20 Hz, H<sub>2</sub>, 7H). <sup>13</sup>C-NMR

( $\delta_{\text{ppm}}$ ,  $\text{D}_2\text{O}$ ): 175.6 ( $\text{C}_7$ ), 133.9 ( $\text{C}_8$ ), 126.5 ( $\text{C}_9$ ), 101.9 ( $\text{C}_1$ ), 81.2 ( $\text{C}_4$ ), 73.1 ( $\text{C}_3$ ), 72.1 ( $\text{C}_2$ ), 71.9 ( $\text{C}_5$ ), 60.3 ( $\text{C}_6$ ). **EM** [ $\text{M}+23$ ]  $m/z$  1242.4 ( $\text{C}_{48}\text{H}_{74}\text{O}_{37}$ ).<sup>[48]</sup> ([Appendix 2](#))

Reaction with methacrylic acid. **Compound 13:**  $\eta=83\%$  (is not complete pure).  **$^1\text{H-NMR}$**  ( $\delta_{\text{ppm}}$ ,  $\text{D}_2\text{O}$ ): 5.65 (s,  $\text{H}_8$ , 1H); 5.32 (s,  $\text{H}_9$ , 1H); 4.96 (s,  $\text{H}_1$ , 7H); 3.83-3.76 (m,  $\text{H}_{3,6}$ , 21H); 3.65 (d,  $J=20$  Hz, 7H); 3.54-3.44 (m,  $\text{H}_{4,2}$ , 14H); 1.77 (s, 3H).<sup>[48]</sup> ([Appendix 3](#))

### 3.2.2 Synthesis of compound 11 (2-monoacryloyl- $\beta$ -CD)<sup>[49]</sup>

To a stirred 0 °C solution of  $\beta$ -CD (2 g, 1.76 mmol) dissolved in freshly distilled pyridine (22 mL) was added dropwise an ice chilled solution of acryloyl chloride (0.32 mL, 3.88 mmol) in THF (1 mL). The solution was slowly warmed to room temperature then stirred for 16 h. Evaporation of solvent under reduced pressure afforded a white solid, which after recrystallization from ethanol. **Compound 11:**  $\eta=94\%$ . **IR** (KBr)  $\nu_{\text{max}}$  ( $\text{cm}^{-1}$ ): 3367.8 (OH), 1726.4 (ROC(O)CHCH<sub>2</sub>).  **$^1\text{H-NMR}$**  ( $\delta_{\text{ppm}}$ ,  $\text{D}_2\text{O}$ ): 6.33 (d,  $J=16$  Hz,  $\text{H}_8$ , 1H); 6.16-6.09 (m,  $\text{H}_9$ , 1H); 5.93 (d,  $J=4$  Hz,  $\text{H}_9$ , 1H); 4.85 (s,  $\text{H}_1$ , 7H); 3.69-3.61 (m,  $\text{H}_{3,6}$ , 21H); 3.58 (d,  $J=8$  Hz,  $\text{H}_5$ , 7H); 3.37-3.32 (m,  $\text{H}_{4,2}$ , 14H).  **$^{13}\text{C-NMR}$**  ( $\delta_{\text{ppm}}$ ,  $\text{D}_2\text{O}$ ): 165.9 ( $\text{C}_7$ ), 132.4 ( $\text{C}_9$ ), 128.7 ( $\text{C}_9$ ), 102.4 ( $\text{C}_1$ ), 82.1 ( $\text{C}_4$ ), 73.6 ( $\text{C}_3$ ), 72.9 ( $\text{C}_2$ ), 72.5 ( $\text{C}_5$ ), 60.4 ( $\text{C}_6$ ).  **$^1\text{H-NMR}$**  ( $\delta_{\text{ppm}}$ , DMSO): 6.33 (d,  $J=4$  Hz,  $\text{H}_9$ , 1H); 6.21-6.14 (m,  $\text{H}_8$ , 1H); 5.97-5.93 (m,  $\text{H}_9$ , 1H); 5.83 (s,  $\text{OH}_{2,3}$ ), 4.85 (s,  $\text{H}_1$ , 7H); 4.45 (s,  $\text{OH}_6$ ) 3.68-3.64 (m,  $\text{H}_{3,6}$ , 21H); 3.59 (d,  $J=8$  Hz,  $\text{H}_5$ , 7H); 3.45-3.16 (m,  $\text{H}_{4,2}$ , 14H).<sup>[49]</sup> **EM** [ $\text{M}+23$ ]  $m/z$  1134.43 ( $\text{C}_{42}\text{H}_{70}\text{O}_{35}$ ), 1242.39 ( $\text{C}_{45}\text{H}_{72}\text{O}_{36}$ ). ([Appendix 4](#))

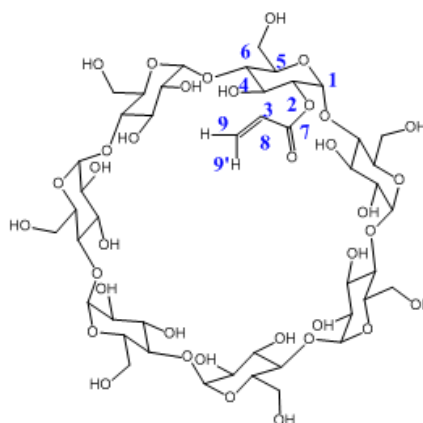


Figure 3.2: Structure of product 11.

### 3.2.3 Synthesis of **12** (6-monoacryloylo-heptakis-(2,3-di-*O*-benzyl)- $\beta$ -CD)

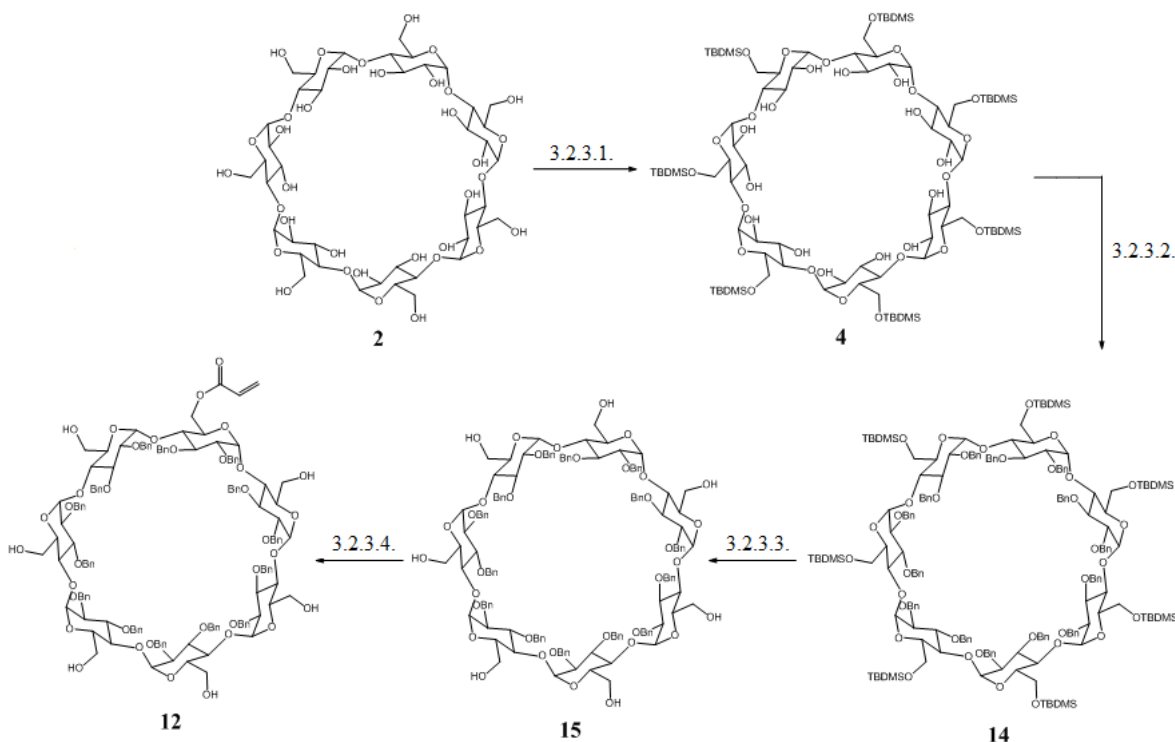


Figure 3.3: Synthetic scheme to obtain compound **12**.

#### 3.2.3.1 Synthesis of persylation- $\beta$ -cyclodextrins (**4**)<sup>[50]</sup>

Dry  $\beta$ -CD (1 g, 0.88 mmol) was dissolved under vigorous stirring in dry pyridine (11 mL). The solution was cooled on an ice bath, producing a thick gel. A solution of TBDMSCl (1.60 g, 10.2 mmol, 12 equiv.) in dry pyridine (16.6 mL) was then added dropwise to the cooled reaction over 3.5 h. During this time, the gel liquefied. Cooling was continued for a further 3 h before the solution was allowed to warm to room temperature. After a further 18 h at room temperature, the solvent was removed under reduced pressure to give a white solid, which was taken up in dichloromethane. The dichloromethane layer was washed with  $\text{KHSO}_4$  to remove any residual pyridine, follow by saturated aqueous NaCl solution. The organic solvent was evaporated. The product was purified by column chromatography with a gradient of solvents dichloromethane /methanol (9:1|8:2). **Compound 4**:  $\eta$  = 81%.  $^1\text{H-NMR}$  ( $\delta_{\text{ppm}}$ ,  $\text{CDCl}_3$ ): 6.73 (s,  $\text{H}_1$ , 7H); 5.27 (s,  $\text{OH}_2$ , 7H); 4.89 (s,  $\text{OH}_3$ , 7H); 4.04 (t,  $J = 9$  Hz,  $\text{H}_3$ , 7H); 3.90 (d,  $J = 9$  Hz,  $\text{H}_6$ , 14H); 3.71 (d,  $J = 11$

Hz, H<sub>5</sub>, 7H); 3.63 (dd, *J*= 4-9 Hz, H<sub>4</sub>, 7H); 3.57 (d, *J*= 8.8 Hz, H<sub>2</sub>, 7H); 0.87 (s, H<sub>10,11,12</sub>, 63H); 0.04 (s, H<sub>7</sub>, 21H); 0.03 (s, H<sub>8</sub>, 21H).<sup>[50]</sup> **EM** [M+23] *m/z* 1933.0 (C<sub>84</sub>H<sub>168</sub>O<sub>35</sub>Si<sub>7</sub>). (Appendix 5)

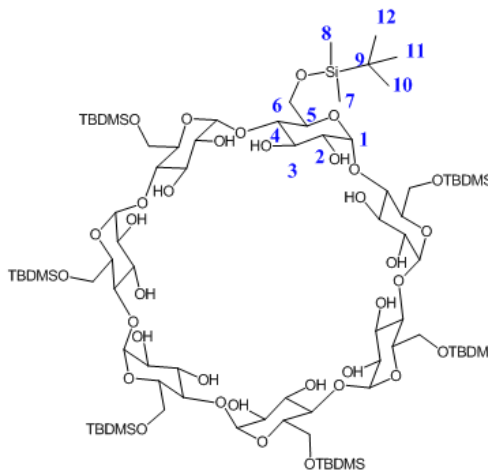


Figure 3.4: Structure of product **4**.

### 3.2.3.2 Synthesis of heptakis-(2,3-di-*O*-benzyl-6-*tert*-butydimethylsilyl)- $\beta$ -CD (**14**)

[51]

To a solution of compound **4** (1 g, 0.512 mmol) in dry DMF (16 mL) was added, at 0 °C, NaH (0.60 g, 0.03 mmol). The suspension was allowed to stir at 0 °C for 2 h, and then benzyl bromide (2.98 mL, 4.29 g, 0.03 mmol) was added. The reaction mixture was stirred for further 2 h at 0 °C and 12 h at room temperature and then quenched with methanol. The organic layer was extracted with pentane, washed with H<sub>2</sub>O, dried (Na<sub>2</sub>SO<sub>4</sub>) and finally the solvent was removed by distillation at reduced pressure. The product was purified by column chromatography with a gradient of solvents hexane/diethyl ether (15:1|10:1|8:2). **Compound 14**:  $\eta$ =43%. **<sup>1</sup>H-NMR** ( $\delta_{\text{ppm}}$ , CDCl<sub>3</sub>): 7.40– 7.05 (m, H<sub>15,16,17,18,19</sub>, 70H); 5.32 (s, H<sub>1</sub>, 7H); 5.09 (d, *J*= 10.8Hz, 14H, CH<sub>2</sub>, Bn-3); 4.71 (m, 14H, CH<sub>2</sub>, Bn-2); 4.51 (m, H<sub>3</sub>, 7H); 4.25 (d, *J*= 10 Hz, H<sub>6</sub>, 14H); 4.04 (dd, *J*= 9 Hz, H<sub>5</sub>, 7H); 3.72 (t, *J*= 10-12 Hz, H<sub>4</sub>, 7H); 3.39 (d; *J*= 6.2 Hz, H<sub>2</sub>, 7H); 0.88 (s, 63H); 0.03 (s, 21H); 0.02 (s, 21H).<sup>[51]</sup> **EM** [M+23] *m/z* 3193.63 (C<sub>182</sub>H<sub>252</sub>O<sub>35</sub>Si<sub>7</sub>). (Appendix 6)

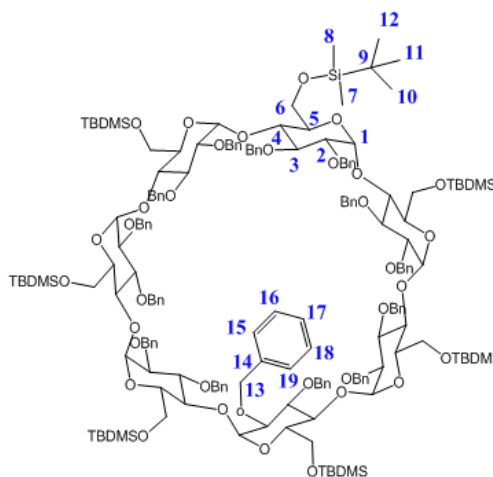


Figure 3.5: Structure of product **14**.

### 3.2.3.3 Synthesis of heptakis-(2,3-di-*O*-benzyl)- $\beta$ -CD (**15**)<sup>[18]</sup>

Compound **14** (0.50 g, 0.16 mmol) was dissolved in dry THF (5 mL) then TBAF (0.57 g, 2.20 mmol, 14 equiv.) was added and the reaction was carried out at room temperature during 24 h. The solvent was evaporated and the final product was obtained after an ethyl acetate/water extraction. **Compound 15**:  $\eta$ = 94 %. <sup>1</sup>H-NMR ( $\delta_{\text{ppm}}$ , CDCl<sub>3</sub>): 7.38– 7.15 (m, H<sub>9,10,11,12,13</sub>, 70H); 5.06 (s, H<sub>1</sub>, 7H); 4.90 (d,  $J$ = 10.8Hz, 14H, CH<sub>2</sub>, Bn-3); 4.67 (m, 14H, CH<sub>2</sub>, Bn-2); 4.52 (m, H<sub>3</sub>, 7H); 3.99 (d,  $J$ = 6.5 Hz, H<sub>6</sub>, 14H); 3.78 (s, H<sub>5</sub>, 7H); 3.65 (d,  $J$ = 7.7 Hz, H<sub>4</sub>, 7H); 3.49 (s, H<sub>2</sub>, 7H).<sup>[18]</sup> ([Appendix 7](#))

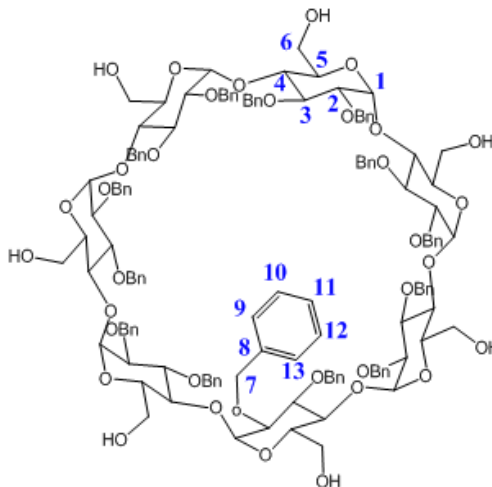


Figure 3.6: Structure of product **15**.

### 3.2.3.4 Synthesis of 6-monoacryloyloxy-heptakis-(2,3-di-*O*-benzyl)- $\beta$ -CD (**12**):<sup>[49]</sup>

The experimental procedure of this last step was the same described in chapter 3.2.2.

Compound **15** (0.50 g, 0.21 mmol) dissolved in distilled pyridine (6 mL). Acryloyl chloride (0.04 mL, 0.46 mmol) dissolved in THF (0.3 mL).

**Compound 12**:  $\eta$ =65%. **IR** (KBr)  $\nu_{\text{max}}$  (cm<sup>-1</sup>): 3390.2 (OH), 1731.6 (ROC(O)CHCH<sub>2</sub>). <sup>1</sup>H-NMR ( $\delta_{\text{ppm}}$ , DMSO-d<sub>6</sub>): 7.07–7.18 (m, H<sub>15,16,17,18,19</sub>, 70H); 5.29 (s, H<sub>1</sub>, 7H); 4.51 and 4.49 (s, H<sub>13</sub>, 28H); 3.76–3.92 (m, H<sub>3,6</sub>, 21H); 3.69 (s, H<sub>5</sub>, 7H); 3.35 (s, H<sub>2,4</sub>, 14H). <sup>13</sup>C-NMR ( $\delta_{\text{ppm}}$ , DMSO-d<sub>6</sub>): 128.9–127.6 (C<sub>14,15,16,17,18,19</sub>), 97.1 (C<sub>1</sub>), 88.0 (C<sub>3</sub>), 79.0 (C<sub>2</sub>), 77.0 (C<sub>4</sub>), 74.0 (C<sub>5</sub>), 69.0 (C<sub>13</sub>), 60.5 (C<sub>6</sub>). **EM** [M+23] m/z 2529.1 (C<sub>143</sub>H<sub>156</sub>O<sub>36</sub> + C<sub>5</sub>H<sub>5</sub>N), 2583.1 (C<sub>151</sub>H<sub>163</sub>O<sub>37</sub> + C<sub>5</sub>H<sub>5</sub>N).<sup>[49]</sup> ([Appendix 8](#))

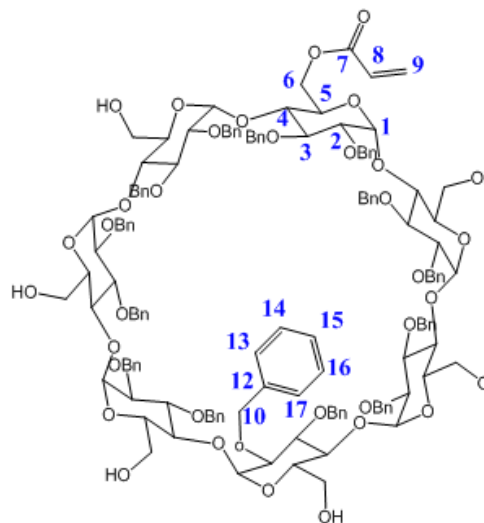


Figure 3.7: Structure of product **12**.

### 3.2.4 Synthesis of acetylation $\beta$ -CD

#### Method A <sup>[52]</sup>

To a solution of  $\beta$ -CD (1 g, 0.88 mmol) in DMF (40 mL) was added ethyldiisopropylamine (6.48 mmol, 1.11 mL, 7 equiv.). A solution of acetyl chloride (0.43 mL, 6.17 mmol, 7 equiv) in DMF (10 mL) was slowly added for 2 h at  $-30\text{ }^{\circ}\text{C}$ . The mixture was left to stand for 14 h at  $20\text{ }^{\circ}\text{C}$ , concentrated in vacuum, and treated with 100 mL of dichloromethane. The precipitate formed was filtered off, washed with dichloromethane and dried in vacuum. **Compound 16**:  $\eta = 89\%$ .  $^1\text{H-NMR}$  ( $\delta_{\text{ppm}}$ , DMSO- $d_6$ ): 4.97 (s,  $\text{H}_1$ , 7H); 3.97-3.77 (m,  $\text{H}_{3,6,5}$ , 28H); 3.64-3.49 (m,  $\text{H}_{4,2}$ , 14H); 2.16 (s,  $\text{H}_8$ , 3H). **EM**  $[\text{M}+23]$   $m/z$  1134.43 ( $\text{C}_{42}\text{H}_{70}\text{O}_{35}$ ), 1176.38 ( $\text{C}_{44}\text{H}_{72}\text{O}_{36}$ ), 1218.39 ( $\text{C}_{46}\text{H}_{74}\text{O}_{37}$ ), 1260.40 ( $\text{C}_{48}\text{H}_{76}\text{O}_{38}$ ), 1302.41 ( $\text{C}_{50}\text{H}_{78}\text{O}_{39}$ ), 1344.42 ( $\text{C}_{52}\text{H}_{80}\text{O}_{40}$ ).

The same procedure was repeated but with 10 equivalents of ethyldiisopropylamine (8.81 mmol, 0.63 mL) and acetyl chloride (0.61 mL, 8.81 mmol).  $\eta = 75\%$ .  $^1\text{H-NMR}$  ( $\delta_{\text{ppm}}$ , DMSO- $d_6$ ): 4.98 (s,  $\text{H}_1$ , 7H); 4.15-3.77 (m,  $\text{H}_{3,6,5}$ , 28H); 3.64-3.49 (m,  $\text{H}_{4,2}$ , 14H); 2.20-2.04 (d,  $J = 7.6$  Hz,  $\text{H}_8$ , 21H). <sup>[52]</sup> **EM**  $[\text{M}+23]$   $m/z$  1157.4 ( $\text{C}_{42}\text{H}_{70}\text{O}_{35}$ ), 1176.3 ( $\text{C}_{44}\text{H}_{72}\text{O}_{36}$ ), 1218.4 ( $\text{C}_{46}\text{H}_{74}\text{O}_{37}$ ), 1260.4 ( $\text{C}_{48}\text{H}_{76}\text{O}_{38}$ ), 1302.4 ( $\text{C}_{50}\text{H}_{78}\text{O}_{39}$ ), 1344.4 ( $\text{C}_{52}\text{H}_{80}\text{O}_{40}$ ), 1386.4 ( $\text{C}_{54}\text{H}_{82}\text{O}_{41}$ ), 1428.4 ( $\text{C}_{54}\text{H}_{82}\text{O}_{42}$ ). ([Appendix 9](#))

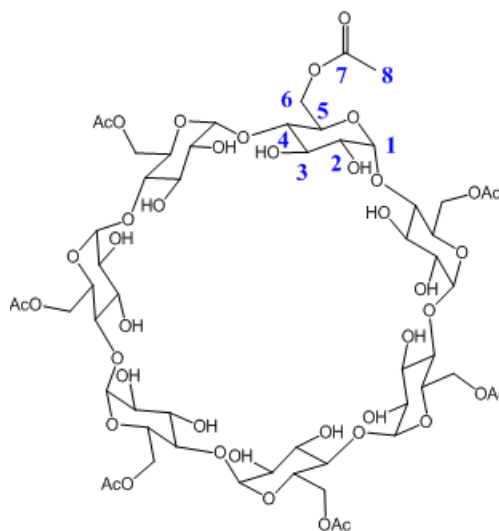


Figure 3.8: Structure of product **16**.

#### Method B <sup>[53]</sup>

**B.1. Procedure for the preparation of compound 22** (1-(1H-1,2,3-Benzotriazol-1-yl)-1-ethanone)

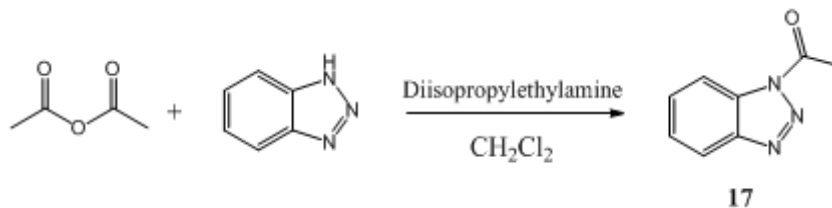


Figure 3.9: Reaction between the acid anhydride and benzotriazole to obtain product **17**.



A solution of the benzotriazole (0.24 g, 2.00 mmol) in dry dichloromethane (10 mL) was treated with diisopropylethylamine (2.50 mmol, 0.43 mL) followed by the dropwise addition of a solution of acetic anhydride (0.21 mL, 0.22 g, 2.20 mmol) in dichloromethane (2 mL) at 0 °C. The resulting mixture was allowed to warm to room temperature and stirred a further 2 h. The reaction mixture was then quenched with H<sub>2</sub>O (20 mL) and extracted with ethyl acetate (2 x 20 mL). The combined organic layers were washed with brine (10 mL) and dried over anhydrous Na<sub>2</sub>SO<sub>4</sub>. The solvent was removed and the obtained product dried in vacuum. **Compound 17**:  $\eta = 72\%$ . <sup>1</sup>H-NMR ( $\delta_{\text{ppm}}$ , D<sub>2</sub>O): 7.79 (d,  $J = 2.5$  Hz, Ar-H, 2H); 7.18 (d,  $J = 1.7$  Hz, Ar-H, 2H); 3.00 (s, CH<sub>3</sub>, 3H).<sup>[53]</sup> ([Appendix 10](#))

### B.2. 6-Peracetylation- $\beta$ -CD (18)<sup>[53]</sup>

To a solution of  $\beta$ -CD (0.25 g, 0.22 mmol), in DMF (10 mL) was added sodium hydride (74.0 mg, 3.08 mmol, 14 equiv). After 2 h 30 min stirring at room temperature a solution of compound **17** (0.50 g, 3.08 mmol, 14 equiv.) in dry DMF (1 mL) was added. After 16 h, the solvent was evaporated and dichloromethane was added. The resulting precipitate was recovered by suction filtration and washed with dichloromethane. **Compound 18**: <sup>1</sup>H-NMR ( $\delta_{\text{ppm}}$ , D<sub>2</sub>O): 7.77 (d,  $J = 2.5$  Hz, Ar-H, 2H); 7.23 (d,  $J = 1.7$  Hz, Ar-H, 2H); 4.92 (s, H<sub>1</sub>, 7H); 3.70 (m, H<sub>3,6,5</sub>, 28H); 3.50 (m, H<sub>4,2</sub>, 14H); 2.00 (s, H<sub>8</sub>, 3H).<sup>[53]</sup> **EM** [M+23] m/z 1283.5 (C<sub>50</sub>H<sub>78</sub>O<sub>39</sub>), 1325.5 (C<sub>50</sub>H<sub>78</sub>O<sub>39</sub>), 1367.5 (C<sub>52</sub>H<sub>80</sub>O<sub>40</sub>), 1409.5 (C<sub>54</sub>H<sub>82</sub>O<sub>41</sub>), 1451.5 (C<sub>56</sub>H<sub>84</sub>O<sub>42</sub>). ([Appendix 11](#))

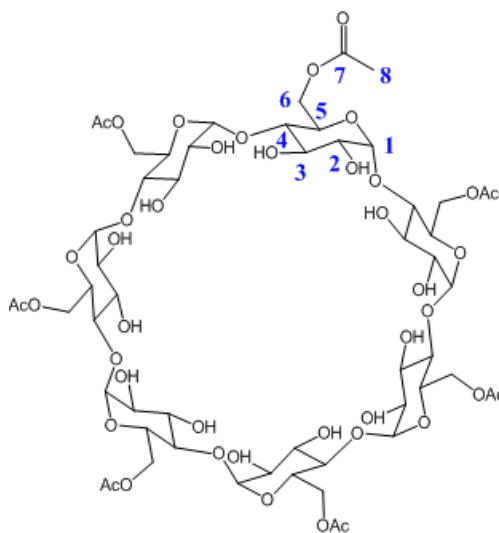


Figure 3.10: Structure of product **18**.

### B.3. 6-Monoacetyly- $\beta$ -CD (19)

To a solution of  $\beta$ -CD (0.25 g, 0.22 mmol), in DMF (10 mL) was added sodium hydride (0.01 g, 0.44 mmol, 2 equiv.). After 2 h 30 minutes under magnetic stirring, at room temperature, a solution of compound **17** (0.07 g, 0.44 mmol, 2 equiv.) in dry DMF (1 mL) was added. After 2 h, the solvent was evaporated and dichloromethane was added. The resulting precipitate was recovered by suction filtration and washed with dichloromethane. **Compound 19**:  $^1\text{H-NMR}$  ( $\delta_{\text{ppm}}$ ,  $\text{D}_2\text{O}$ ): 7.79 (d,  $J=2.5$  Hz, Ar-H, 2H); 7.18 (d,  $J=1.7$  Hz, Ar-H, 2H); 4.93 (s,  $\text{H}_1$ , 7H); 3.86-3.69 (m,  $\text{H}_{3,6,5}$ , 28H); 3.52-3.44 (m,  $\text{H}_{4,2}$ , 14H); 2.05 (s,  $\text{H}_8$ , 3H). **EM** [ $\text{M}+23$ ]  $m/z$  1157.3 ( $\text{C}_{42}\text{H}_{70}\text{O}_{35}$ ), 1199.4 ( $\text{C}_{44}\text{H}_{72}\text{O}_{36}$ ), 1241.2 ( $\text{C}_{46}\text{H}_{74}\text{O}_{37}$ ), 1283.3 ( $\text{C}_{48}\text{H}_{76}\text{O}_{38}$ ). ([Appendix 12](#))

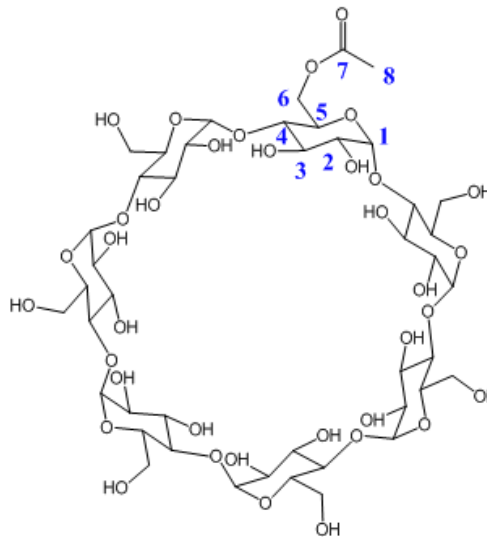


Figure 3.11: Structure of product **19**.

## 3.3 Studies in $\text{scCO}_2$

### 3.3.1 General methods for co-polymer synthesis in $\text{scCO}_2$

Polymerizations reactions were carried out in 33 ml stainless steel high-pressure cell equipped with two aligned sapphire windows, which allow full visualization of the reaction mixture. The cell was loaded with reactants: monomers (MAA and NIPAAm, 1:3), modified  $\beta$ -CD (when used 2.5% and 8.8%), crosslinker (1% EGDMA), initiator (AIBN). The cell is sealed and purged. Liquid carbon dioxide is loaded into the cell using a high-pressure compressor (NWA GmbH). Then the cell was immersed in water bath set to  $65^\circ\text{C}$ , with a stability  $\pm 0.01^\circ\text{C}$ . Temperature control was made through a resistance temperature detector probe contacting the cell, connected to a Hart Scientific PID controller. Stirring was achieved by means of a Teflon coated magnetic bar. Carbon dioxide was added up to 240 bar. Polymerization reactions proceeded for 24 hours under stirring. It could be seen through the sapphire windows that all polymerization started as a completely homogenous phase, with all reactants completely dissolved in  $\text{scCO}_2$ . At the end of the reaction, the polymers were slowly washed with fresh high-pressure  $\text{CO}_2$  in order to clean any unreacted residues. Upon venting a fluffy, dry, white, free-

flowing powder remained in the reaction vessel. The polymer yield was determined gravimetrically.

4.3.1.1. The first test was the co-polymer without  $\beta$ -CD.

4.3.1.2. The second test was made with **10** (2.5%).  $\eta = 77.4\%$ .  **$^1\text{H-HR-MAS-NMR}$**  ( $\delta_{\text{ppm}}$ , DMSO- $d_6$ ): 7.22 (s, polymer); 5.75 (s, polymer); 4.83 (s, H<sub>1</sub>, 7H); 3.86 (s, H<sub>3</sub>, 7H); 3.58 (t,  $J=12$ -24 Hz, H<sub>6</sub>, 14H); 3.44 (s, H<sub>5</sub>, 7H); 3.37-3.19 (m, H<sub>4,2</sub>, 14H); 1.96 (s, polymer); 1.00 (s, polymer). (Appendix 13) **RXD**: Chapter 2, Figure 2.21.

4.3.1.3. The third test was with **11** (2.5%).  $\eta = 78.2\%$ . **RXD**: Chapter 2, Figure 2.22.

4.3.1.4. The fourth test the **12** was used (2.5%).  $\eta = 65.3\%$ .  **$^1\text{H-HR-MAS-NMR}$**  ( $\delta_{\text{ppm}}$ , DMSO- $d_6$ ): 7.13 (m, H<sub>15,16,17,18,19</sub>, 70H); 5.29 (s, H<sub>1</sub>, 7H); 3.83 (m, H<sub>3,6,5</sub>, 28); 2.51 (s, H<sub>4,2</sub>, 14H); 1.06 (m, polymer). (Appendix 14)

4.3.1.4. The last test was with **11** (8.8%).  $\eta = 79.6\%$ .  **$^1\text{H-HR-MAS-NMR}$**  ( $\delta_{\text{ppm}}$ , D<sub>2</sub>O/DMSO- $d_6$ ): 6.21-5.97 (m, H<sub>9,9',8</sub>, 3H); 5.74-5.69 (m, OH<sub>2,3</sub>, 13H); 4.82 (s, H<sub>1</sub>, 7H); 4.50 (s, OH<sub>6</sub>, 7H); 3.92-3.81 (m, polymer); 3.65-3.55 (m, H<sub>3,6,5</sub>, 28); 3.48 (s, H<sub>4</sub>, 7H); 3.35 (d,  $J=9$ Hz, H<sub>2</sub>, 7H); 1.22-1.04 (m, polymer). (Appendix 15)

### 3.3.2 General methods for scCO<sub>2</sub>-assisted impregnation

The impregnation of a model drug, into the co-polymers was performed at 65 °C and 240 bar within 20 h, in a cell similar to that of the polymerization, with a porous support which divides the cell in two compartments. This prevents physical contact between the drug and the samples. The drug was placed in the downer compartment, under the porous support with a magnetic stirrer bar, and in quantity enough to obtain a saturated solution at the p, T impregnation conditions. The polymers were loaded into cellulose membranes (cutoff 3.5 KDa) which were placed in the upper compartment of the cell. At the end of the impregnation period the system was quickly depressurized. Impregnated drug was calculated gravimetrically by weighting the membranes in a Sartorius balance (precision  $\pm 0.00001$  g).

This study was realized with the metronidazole. (Chapter 2, Table 2.3)

### 3.3.3 General methods for *in vitro* drug release experiments

After impregnation, the polymers were transferred to porous membranes and put in buffer solution at pH 2.2 (HCl-Glycine) and at 7.4 (Phosphate Buffered Saline) at controlled temperature 37 °C. 1 ml aliquots were withdrawn at time intervals and the same volume of fresh medium was added to the solution. Quantification was performed by making a calibration curve

in a spectrophotometer at 265 nm and the total mass released was determined considering the aliquots and the dilution produced by addition of fresh buffer solution. The results at different pHs are presented in Tables 3.1 e 3.2.

Table 3.1: Results of metronidazole release of each co-polymer at pH 2.2.

Drug Release (mg/g) at pH 2.2					
Time (h)	Co-polymer without $\beta$ -CD	Co-polymer 10 (2.5%)	Co-polymer 11 (2.5%)	Co-polymer 11 (8.8%)	Co-polymer 12 (2.5%)
0.00	0.62	0.66	0.38	3.61	0.15
0.17	3.20	4.28	1.53	14.41	0.69
0.33	4.39	6.05	4.22	21.15	3.15
0.50	5.11	7.36	5.79	21.24	4.00
0.67	5.62	8.51	6.58	-	4.28
0.83	5.98	9.17	7.74	24.47	4.69
1.08	6.31	9.64	8.90	24.94	4.82
1.33	6.64	10.13	10.07	27.40	5.10
1.62	6.80	10.29	10.85	27.42	4.04
1.93	6.83	10.61	11.25	27.29	5.10
2.27	6.83	10.77	11.64	28.15	5.10
2.60	6.80	10.61	12.02	29.38	5.12
3.10	6.80	10.61	12.41	28.77	5.12
3.60	6.80	10.44	12.42	30.16	4.97
4.43	7.25	10.44	12.80	30.37	4.97
5.43	-	-	-	30.36	-
6.43	-	-	-	31.10	-
7.43	-	-	-	30.61	-
8.43	-	-	-	33.05	-

Table 3.2: Results of metronidazole release of each co-polymer at pH 7.4.

Drug Release (mg/g) at pH 7.4					
Time (h)	Co-polymer without $\beta$ -CD	Co-polymer 10 (2.5%)	Co-polymer 11 (2.5%)	Co-polymer 11 (8.8%)	Co-polymer 12 (2.5%)
0.00	0.00	0.18	0.00	0.00	0.45
0.17	5.76	1.58	5.86	4.74	1.22
0.33	7.12	2.81	11.01	6.90	2.12
0.50	8.93	4.03	-	8.40	2.59
0.67	9.63	4.38	-	10.50	2.89
0.83	10.35	4.73	14.55	11.51	3.04
1.08	11.04	5.26	15.27	11.17	3.20
1.33	11.39	5.26	15.81	13.96	3.33
1.62	11.74	5.44	15.97	14.98	3.33
1.93	11.75	5.61	16.17	15.61	3.65
2.27	12.09	5.61	15.79	16.96	3.65
2.60	11.76	5.61	15.96	18.69	3.49
3.10	12.10	5.61	15.77	19.69	3.49
3.60	12.09	5.79	15.58	21.42	3.49
4.43	11.76	5.44	15.39	22.42	3.65
5.43	-	-	-	23.78	-



## **4. References**

1. Szejtli, J., *Past, present, and future of cyclodextrin research*. Pure and Applied Chemistry, 2004. **76**(10): p. 1825-1845.
2. Loftsson, T. and Duchene, D., *Cyclodextrins and their pharmaceutical applications*. International Journal of Pharmaceutics, 2007. **329**(1-2): p. 1-11.
3. Brewster, M.E. and Loftsson, T., *Cyclodextrins as pharmaceutical solubilizers*. Advanced Drug Delivery Reviews, 2007. **59**(7): p. 645-666.
4. Del Valle, E.M.M., *Cyclodextrins and their uses: a review*. Process Biochemistry, 2004. **39**(9): p. 1033-1046.
5. Dodziuk, H., *Cyclodextrins and Their Complexes: Chemistry, Analytical Methods, Applications*, ed. WILEY-VCH. 2006.
6. Boogaard, M.v.d., *Cyclodextrin-containing Supramolecular Structures From pseudo-polyrotaxanes towards molecular tubes, insulated molecular wires and topological networks*. 2003, University of Groningen: Netherlands. p. 1-154.
7. Astray, G.; Gonzalez-Barreiro, C.; Mejuto, J.C.; Rial-Otero, R. and Simal-Gandara, J., *A review on the use of cyclodextrins in foods*. Food Hydrocolloids, 2009. **23**(7): p. 1631-1640.
8. Van de Manakker, F.; Vermonden, T.; van Nostrum, C.F. and Hennink, W.E., *Cyclodextrin-Based Polymeric Materials: Synthesis, Properties, and Pharmaceutical/Biomedical Applications*. Biomacromolecules, 2009. **10**(12): p. 3157-3175.
9. Szejtli, J., *Introduction and General Overview of Cyclodextrin Chemistry*. Chemical Reviews, 1998. **98**: p. 1743-1753.
10. Connors, K.A., *The stability of cyclodextrin complexes in solution*. Chemical Reviews, 1997. **97**(5): p. 1325-1357.
11. Bambo, M.F., *Synthesis, characterization and application of nanoporous cyclodextrin polymers*, in *Department of Chemical Technology*. 2007, Faculty of Science of the University of Johannesburg: Johannesburg. p. 1-146.
12. Challa, R.; Ahuja, A.; Ali, J. and Khar, R.K., *Cyclodextrins in drug delivery: An updated review*. Aaps Pharmscitech, 2005. **6**(2): p. 29.
13. Shimpi, S.; Chauhan, B. and Shimpi, P., *Cyclodextrins: application in different routes of drug administration*. Acta Pharm, 2005. **55**(2): p. 139-56.
14. Khan, A.R.; Forgo, P.; Stine, K.J. and D'Souza, V.T., *Methods for selective modifications of cyclodextrins*. Chemical Reviews, 1998. **98**(5): p. 1977-1996.
15. Pham, D.T., *Beta-Cyclodextrin Modification and host-guest complexation*, in *Chemistry*. 2007, The University of Adelaide School of Chemistry and Physics: Adelaide, Australia. p. Chapter 1, 1-29.



16. Wang, Z.Z. and Lu, R.H., *Facile direct acylation and acyl migration of beta-cyclodextrin on the secondary hydroxyl face*. Journal of Inclusion Phenomena and Macrocyclic Chemistry, 2009. **63**(3-4): p. 373-378.
17. Ashton, P.R.; Boyd, S.E.; Gattuso, G.; Hartwell, E.Y.; Koniger, R.; Spencer, N. and Stoddart, J.F., *A novel approach to the synthesis of some chemically-modified cyclodextrins*. Journal of Organic Chemistry, 1995. **60**(12): p. 3898-3903.
18. Badi, N.; Jarroux, N. and Guegan, P., *Synthesis of per-2,3-di-O-heptyl-beta and gamma-cyclodextrins: a new kind of amphiphilic molecules bearing hydrophobic parts*. Tetrahedron Letters, 2006. **47**(50): p. 8925-8927.
19. Petter, R.C.; Salek, J.S.; Sikorski, C.T.; Kumaravel, G. and Lin, F.T., *Cooperative Binding by Aggregated Mono-6-(Alkylamino)-Beta-Cyclodextrins*. Journal of the American Chemical Society, 1990. **112**(10): p. 3860-3868.
20. Zhong, N.; Byun, H.-S. and Bittman, R., *An Improved Synthesis of 6-O-Monosyl-6-deoxy-B-cyclodextrins*. Tetrahedron Letters, 1998. **39**: p. 2919-2920.
21. Baugh, S.D.P.; Yang, Z.; Leung, D.K.; Wilson, D.M. and Breslow, R., *Cyclodextrin Dimers as Cleavable Carriers of Photodynamic Sensitizers*. Journal American Chemical Society, 2001. **123**: p. 12488-12494.
22. Schneider, H.J.; Hacket, F.; Rudiger, V. and Ikeda, H., *NMR studies of cyclodextrins and cyclodextrin complexes*. Chemical Reviews, 1998. **98**(5): p. 1755-1785.
23. Oliveira, R.; Santos, D. and Coelho, P., *Ciclodextrinas: formação de complexos e a sua aplicação farmacêutica*. Revista da Faculdade de Ciências da Saúde., 2009: p. 70-83.
24. Takahashi, K., *Organic reactions mediated by cyclodextrins*. Chemical Reviews, 1998. **98**(5): p. 2013-2033.
25. Davis, M.E. and Brewster, M.E., *Cyclodextrin-based pharmaceuticals: Past, present and future*. Nature Reviews Drug Discovery, 2004. **3**(12): p. 1023-1035.
26. Thakkar, F.m.V.T., Doni, T.G., Gohel, M. C. and Gandhi, T.R., *Supercritical fluid technology: A promising approach to enhance the drug solubility*. Journal of Pharmaceutical Sciences and Research, 2009. **1**(4): p. 1-14.
27. Mammucari, R. and Foster, N.R., *Dense gas technology and cyclodextrins: State of the art and potential*. Current Organic Chemistry, 2008. **12**(6): p. 476-491.
28. Casimiro, T.; Banet-Osuna, A.M.; Ramos, A.M.; da Ponte, M.N. and Aguiar-Ricardo, A., *Synthesis of highly cross-linked poly(diethylene glycol dimethacrylate) microparticles in supercritical carbon dioxide*. European Polymer Journal, 2005. **41**(9): p. 1947-1953.

29. Junco, S.; Casimiro, T.; Ribeiro, N.; Da Ponte, M.N. and Marques, H.M.C., *Optimisation of supercritical carbon dioxide systems for complexation of naproxen: Beta-cyclodextrin*. Journal of Inclusion Phenomena and Macrocyclic Chemistry, 2002. **44**(1-4): p. 69-73.
30. Kemmere, M.F. and Meyer, T., *Supercritical Carbon Dioxide: in Polymer Reaction Engineering*. 2005, WILEY-VCH Verlag GmbH & Co. KGaA, Weinheim. p. 1, 5-7.
31. Suleiman, D.; Estévez, L.A.; Pulido, J.C.; García, J.E. and Mojica, C., *Solubility of Anti-Inflammatory, Anti-Cancer, and Anti-HIV Drugs in Supercritical Carbon Dioxide*. Journal of Chemical & Engineering Data, 2005. **50**: p. 1234-1241.
32. Silva, M.S.d.; Romão, J.; Aguiar-Ricardo, A.; Marques, M.M. and Casimiro, T., *Development of Cyclodextrin-Hydrogel Polymeric Systems SCCO<sub>2</sub> for Colon Targeted Drug Delivery*, in *12th European Meeting on Supercritical Fluids*. 2010: Graz, Austria.
33. Abbas, K.A.; Mohamed, A.; Abdulmir, A.S. and H.A., A., *A review on supercritical fluid extraction as new analytical method*. American Journal of Biochemistry and Biotechnology, 2008. **4**(4): p. 345-353.
34. Atkins, P. and Paula, J.d., *Atkins Physical Chemistry*, U.P. Oxford, Editor. 2006: Oxford. p. 119
35. Nair, L.S. and Laurencin, C.T., *Polymers as Biomaterials for Tissue Engineering and Controlled Drug Delivery*. Advances in Biochemical Engineering/Biotechnology, 2005. **102**: p. 47-90.
36. Verma, R.K. and Garg, S., *Current Status of Drug Delivery Technologies and Future Directions*. Pharmaceutical Technology, 2001. **25**: p. 1-14.
37. Bajpai, A.K.; Shukla, S.K.; Bhanu, S. and Kankane, S., *Responsive polymers in controlled drug delivery*. Progress in Polymer Science, 2008. **33**: p. 1088-1118.
38. Becerra-Bracamontes, F.; Sánchez-Díaz, J.C.; González-Álvarez, A.; Ortega-Gudinõ, P.; Michel-Valdivia, E. and Martínez-Ruvalcaba, A., *Design of a Drug Delivery System Based on Poly(acrylamide-co-acrylic acid)/ Chitosan Nanostructured Hydrogels*. Journal of Applied Polymer Science, 2007. **106**: p. 3939-3944.
39. Arun Rasheed; Ashok Kumar C.K. and Sravanthi V.N.S., *Cyclodextrins as Drug Carrier Molecule: A Review*. Scientia Pharmaceutica, 2008. **76**: p. 567-598.
40. Uekama, K., *Recent Aspects of Pharmaceutical Application of Cyclodextrins*. Journal of Inclusion Phenomena and Macrocyclic Chemistry, 2002. **44**: p. 3-7.
41. Loftsson, T. and Brewster, M.E., *Pharmaceutical Applications of Cyclodextrins. 1. Drug Solubilization on Stabilization*. Journal of Pharmaceutical Sciences 1996. **85**(10): p. 1017-1025.

42. Uekama, K.; Hirayama, F. and Irie, T., *Cyclodextrin drug carrier systems*. Chemical Reviews, 1998. **98**(5): p. 2045-2076.
43. Szejtli, J., *Cyclodextrin complexed generic drugs are generally not bio-equivalent with the reference products: Therefore the increase in number of marketed drug/cyclodextrin formulations is so slow*. Journal of Inclusion Phenomena and Macrocyclic Chemistry, 2005. **52**(1-2): p. 1-11.
44. Hirayama, F. and Uekama, K., *Cyclodextrin-based controlled drug release system*. Advanced Drug Delivery Reviews, 1999. **36**(1): p. 125-141.
45. Ivanova, G.I.; Vao, E.R.; Temtem, M.; Aguiar-Ricardo, A.; Casimiro, T. and Cabrita, E.J., *High-pressure NMR characterization of triacetyl-beta-cyclodextrin in supercritical carbon dioxide*. Magnetic Resonance in Chemistry, 2009. **47**(2): p. 133-141.
46. Silverstein, R.M.; Webster, F.X. and Kiemle, D.J., *Spectrometric Identification of Organic Compounds*. 2005, New York: John Wiley & Sons, Inc.
47. Smith, M.B. and March, J., *March's Advanced Organic Chemistry: Reaction, Mechanisms and Structure, Sixth Edition*. 2007, John Wiley & Sons, Inc.: United States of America. p. 426-432.
48. Barr, L.; Lincoln, S.F. and Easton, C.J., *Reversal of regioselectivity and enhancement of rates of nitrile oxide cycloadditions through transient attachment of dipolarophiles to cyclodextrins*. Chemistry-a European Journal, 2006. **12**(33): p. 8571-8580.
49. Piletsky, S.A.; Andersson, H.S. and Nicholls, I.A., *Combined hydrophobic and electrostatic interaction-based recognition in molecularly imprinted polymers*. Macromolecules, 1999. **32**(3): p. 633-636.
50. Ashton, P.R.; Koniger, R.; Stoddart, J.F.; Alker, D. and Harding, V.D., *Amino acid derivatives of beta-cyclodextrin*. Journal of Organic Chemistry, 1996. **61**(3): p. 903-908.
51. Uccello-Barretta, G.; Sicoll, G.; Balzano, F. and Salvadori, P., *NMR spectroscopy: a powerful tool for detecting the conformational features of symmetrical persubstituted mixed cyclornaltoheptaoses (beta-cyclodextrins)*. Carbohydrate Research, 2005. **340**(2): p. 271-281.
52. Sutyagin, A.A.; Glazyrin, A.E.; Kurochkina, G.I.; Grachev, M.K. and Nifant'ev, E.E., *Regioselective acetylation of beta-cyclodextrin*. Russian Journal of General Chemistry, 2002. **72**(1): p. 147-150.
53. Zhang, H.-K.; Shao, Y.; Hong Ding and Hu, L.-H., *Synthesis and Structure-Activity Relationship Studies of Cytotoxic and Ether Anhydrovinblastine Derivatives*. Journal of Natural Product, 2008. **71**: p. 1669-1676.

54. Katritzky, A.R. and Pastor, A., *Synthesis of beta-dicarbonyl compounds using 1-acylbenzotriazoles as regioselective C-acylating reagents*. Journal of Organic Chemistry, 2000. **65**(12): p. 3679-3682.
55. Katritzky, A.R.; He, H.Y. and Suzuki, K., *N-acylbenzotriazoles: Neutral acylating reagents for the preparation of primary, secondary, and tertiary amides*. Journal of Organic Chemistry, 2000. **65**(24): p. 8210-8213.
56. Katritzky, A.R.; Le, K.N.B.; Khelashvili, L. and Mohapatra, P.P., *Alkyl, unsaturated, (hetero)aryl, and N-protected alpha-amino ketones by acylation of organometallic reagents*. Journal of Organic Chemistry, 2006. **71**: p. 9861-9864.
57. Timmer, J.M.K., *Properties of nanofiltration membranes; model development and industrial application*. 2001, Technische Universiteit Eindhoven: Eindhoven. p. 1-154.
58. <http://labvirtual.eq.uc.pt/> (21/04/11).
59. [www.millipore.com/catalogue/module/c3259](http://www.millipore.com/catalogue/module/c3259) (22/04/11). [cited].
60. Zhao, S.P.; Cao, M.J.; Li, L.Y. and Xu, W.L., *Synthesis and properties of biodegradable thermo- and pH-sensitive poly [(N-isopropylacrylamide)-co-(methacrylic acid)] hydrogels*. Polymer Degradation and Stability, 2010. **95**(5): p. 719-724.
61. Silva, M.S.d.; Vao, E.R.; Temtem, M.; Mafra, L.; Caldeira, J.; Aguiar-Ricardo, A. and T.Casimiro, *Clean synthesis of molecular recognition polymeric materials with chiral sensing capability using supercritical fluid technology. Application as HPLC stationary phases*. Biosensors & Bioelectronics, 2010. **25**(7): p. 1742-1747.
62. Brazel, C.S. and Peppas, N.A., *Synthesis and characterization of thermomechanically and chemomechanically and chemomechanically responsive poly(N-isopropylacrylamide-co-methacrylic acid) hydrogels*. Macromolecules, 1995. **28**(24): p. 8016-8020.
63. Timothy, D.W.C., *High-Resolution NMR Techniques in Organic Chemistry*, ed. <sup>n</sup>. Edition. Vol. Volume 27. 2009, Oxford Tetrahedron Organic Chemistry.
64. Sarvothaman, M.K., *Cyclodextrins as Core Molecule in Supramolecular Assemblies and as Molecular Reinforcers in Polymer Coatings*. 2009, Heinrich-Heine-Universität Düsseldorf: Düsseldorf. p. 1-96.
65. Loethen, S.; Kim, J.M. and Thompson, D.H., *Biomedical applications of cyclodextrin based polyrotaxanes*. Polymer Reviews, 2007. **47**(3): p. 383-418.
66. Redigueri, C.F.; Porta, V.; Nunes, D.S.G.; Nunes, T.M.; Junginger, H.E.; Kopp, S.; Midha, K.K.; Shah, V.P.; Stavchansky, S.; Dressman, J.B. and Barends, D.M., *Biowaiver*

*Monographs for Immediate Release Solid Oral Dosage Forms: Metronidazole.* Journal of Pharmaceutical Sciences, 2011. **100**(5): p. 1618-1627.

67. Wu, Y.Q. and Fassihi, R., *Stability of metronidazole, tetracycline HCl and famotidine alone and in combination.* International Journal of Pharmaceutics, 2005. **290**(1-2): p. 1-13.

68. Garmroodi, A.; Hassan, J. and Yamini, Y., *Solubilities of the drugs benzocaine, metronidazole benzoate, and naproxen in supercritical carbon dioxide.* Journal of Chemical and Engineering Data, 2004. **49**(3): p. 709-712.

69. Kazarian, S.G., *Polymer Processing with Supercritical Fluids.* Polymer Science, 2000. **42**(1): p. 78-101.

70. Stella, V.J.B.; Hageman, J.M.; Oliyai, R.; Magg, H. and Tilley, J.W., *Biotechnology: Pharmaceutical Aspects. Prodrugs: Challenges and Rewards. Part 1.* . 2007, United State of America: Springer.

71. Wang, N.; Wu, Q.; Xiao, Y.M.; Chen, C.X. and Lin, M.F., *Regioselective synthesis of cyclodextrin mono-substituted conjugates of non-steroidal anti-inflammatory drugs at C-2 secondary hydroxyl by protease in non-aqueous media.* Bioorganic & Medicinal Chemistry, 2005. **13**(11): p. 3667-3671.

72. Perrin, D.D.; Armarego, W.L.F. and Perrin, D.R., *Purification of Laboratory Chemicals.* Pergamon Press. 1965.

